AN ABSTRACT OF THE THESIS OF

Peter M. Hogan for the degree of Master of Science in Electrical and Computer Engineering presented on June 7, 2007.
Title: A Linear Test Bed for Characterizing the Performance of Ocean Wave Energy Converters.

Abstract approved:_____

Ted Brekken Annette R. von Jouanne

Determining the performance characteristics of various ocean wave energy converters (OWEC) has proven to be difficult due to problems replicating a baseline motion profile in the ocean or wave tank to compare these devices. The linear test bed seeks to mechanically simulate the relative linear motion between the active components experienced by a point absorber OWEC in an ocean environment. A gimbal mount allows the active components of a "float" of a point absorber OWEC to be mounted to the machine's carriage, which is mechanically driven by timing belts. The "spar" portion of the OWEC is mounted to the base of the linear test bed so that as the carriage moves the float vertically, there is relative linear motion between the float and spar. The current control system allows researchers to input a vertical position versus time function to be tracked by the linear test bed.

However, researchers have desired to improve the linear test bed control system by implementing a force control algorithm based on hydrodynamic equations to accurately reproduce the driving force of the ocean wave. With only position control, the linear test bed will use any necessary force to follow that profile, exaggerating the capabilities of the wave especially if the device is electrically loaded. In addition, the hydrodynamic interaction of the OWEC and an ocean wave cannot be reproduced using only a position feedback control system. The linear test bed design, position control system, and a comprehensive presentation of the novel force control system are provided through this thesis work.

A Linear Test Bed for Characterizing the Performance of Ocean Wave Energy Converters

by

Peter M. Hogan

A THESIS

submitted to

Oregon State University

in partial fulfillment of
the requirements for the
degree of

Master of Science

Presented June 7, 2007
Commencement June 2008

Master of Science thesis of Peter M. Hogan presented on June 8, 2007.

APPROVED:

Co-Major Professor, representing Electrical and Computer Engineering

---

Co-Major Professor, representing Electrical and Computer Engineering

---

Director of the School of Electrical Engineering and Computer Science

---

Dean of the Graduate School

I understand that my thesis will become part of the permanent collection of Oregon State University libraries. My signature below authorizes release of my thesis to any reader upon request.

Peter M. Hogan, Author

ACKNOWLEDGEMENTS

I would first like to thank my principle advisor, Dr. Ted Brekken, for all of his support and guidance throughout the writing of this thesis. Truly, without his mentorship this work would not have been completed successfully. Next, I would like to give thanks to Dr. Annette von Jouanne for her help bringing me to Oregon State University. She also provided me with excellent academic guidance and career counseling during my two years in Corvallis. It is through her vision that allowed the study of ocean wave energy to grow at Oregon State University. Next, I would like to thank the late Dr. Alan Wallace as he truly was a pioneer in the study of ocean wave energy. Although I never knew him well, he is an inspiration for me to drive wave energy research forward at OSU. Also from the Energy Systems group, I would like to thank all of the graduate students, especially Alphonse Schacher, Ean Amon, Ken Rhinefrank, David Elwood, Aaron Vander Muelen, and Joseph Prudell. A special acknowledgement should be made to Mundt and Associates, for their excellent design and build efforts toward the linear test bed.

Most importantly I would like to thank my family for their support during six years of college studies. My fiancée, Amy Rosenberger, for all of her support and understanding during the two years spent in Corvallis. My parents, Sue and Greg Hogan for all of their support and guidance they have given me in my life. To my sister, Meredith Hogan, for always reminding me to relax and enjoy life. Also, I would like to give thanks to my Aunt Mary Ellen Pugh and Uncle Richard Pugh, for helping me become the person I am today.

TABLE OF CONTENTS

Page

1. INTRODUCTION ……. 1

1.1 Wave Energy Extraction ……..1

1.2 Oscillating Water Column 2

1.3 Surface Following or Attenuator OWECs……..... 3

1.3.1 Ocean Power Delivery ……3

1.4 Overtopping OWECs …….. 5

1.5 Commercial Point Absorber OWECs 6

1.5.1 Ocean Power Technologies ……..... 6
1.5.2 AWS Ocean Energy..... 7

1.6 Overview of Prototype Direct-drive, Point Absorber OWECs……..9

1.6.1 Linear Air Gap Wound Permanent Magnet Generator …….9
1.6.2 Linear Transverse Flux PM Generator ……..11
1.6.3 Contactless Force Transmission System ……...12

1.7 Motivation for this work ……..14

2. LINEAR TEST BED……16

2.1 Mechanical Design and Safety……16

2.1.1 Frame and Drive Assembly……... 18
2.1.2 Linear Test Bed Base……..24
2.1.3 Carriage Assembly……25
2.1.4 Suspension Arm..... 28

2.2 Control System Overview ……...30

2.3 Equipment Setup in MSRF …… 32

2.3.1 Electrical Interconnection..... 32
2.3.2 DC Bus Regulation…….. 34

3. INPUT/OUTPUT INSTRUMENTATION……43

3.1 Introduction 43

3.2 Data Acquisition Considerations…… 44

3.3 Signal Routing and Wiring Diagrams……47

3.4 LTB Control Inputs and Instrumentation..... 51

3.4.1 DUT Position, Velocity, Acceleration……... 52
3.4.2 Measured Force on DUT…….. 52
3.4.3 Drive Additional I/O Capabilities……... 56

TABLE OF CONTENTS (Continued)

Page

3.5 LTB Control Outputs and Instrumentation 57

3.5.1 Commanded DUT Position 57
3.5.2 Commanded Force on DUT..... 58
3.5.3 Actual Force on DUT 59

3.6 LTB Digital Inputs/Outputs 59

4. CONTROL OF THE LINEAR TEST BED..... 62

4.1 Introduction..... 62

4.2 Pre-Existing Control Methods..... 63

4.3 Motion Control using Delta Tau®..... 64

4.4 Delta Tau® Position Control 66

4.4.1 Turbo PMAC PID Algorithm 69
4.4.2 PID Loop Tuning 72
4.4.3 Turbo PMAC Coordinate System 73

4.5 Programming Motion using Turbo PMAC 74

4.5.1 Motion Programs 74
4.5.2 PLC Programs..... 78

5. NOVEL FORCE CONTROL ALGORITHM FOR LTB 80

5.1 Force Control Introduction..... 80

5.2 Modeling of the Delta Tau Turbo PMAC PCI®..... 82

5.3 CompactRIO® Data Processing 91

5.4 Hydrodynamic and Hydrostatic Modeling..... 92

5.4.1 Generating the Commanded Force 92
5.4.2 Linear Test Bed Implementation of Hydrodynamics..... 95

5.5 Design of Force Controller 96

5.6 Linear Test Bed and Generator Force Modeling..... 101

5.4.1 Linear Test Bed Model 102
5.4.2 Generator Force Modeling of the Device under Test..... 103

5.7 Simulation Results..... 104

4.4.1 Sinusoidal Wave Height Input No Generator Load..... 106
4.4.2 Sinusoidal Wave Height Input, 500W Generator Load..... 108
4.4.3 Sinusoidal Wave Height Input, 1kW Generator Load 112

6. CONCLUSION..... 116

TABLE OF CONTENTS (Continued)

Page

6.1 Benefits of the Linear Test Bed……..….. 116

6.2 Future Work regarding the CompactRIO Interconnection……..…. 117

6.3 Closing the Force Loop with PMAC …….…… 119

6.4 Final MSRF Interconnection Issues and Future Work ……..…… 123

BIBLIOGRAPHY ……..…. 125

APPENDICES ……..……..…. 127

LIST OF FIGURES

Figure		Page
1.1	The Oscillating Water Column	3
1.2	The OPD Palamis WEC	4
1.3	OPD Power Conversion Module	4
1.4	Wave Dragon Overtopping OWEC	5
1.5	The OPT PowerBuoy	6
1.6	The AWS Wave Energy Converter	8
1.7	Linear Air Gap Wound Permanent Magnet Generator	10
1.8	Flux Path of Air Gap Machine	11
1.9	Flux Path of Transverse Flux Machine	12
1.10	Model of CFTS Buoy	13
2.1	Linear Test Bed	17
2.2	Linear Test Bed Frame and Drive Assembly	18
2.3	Torque Requirements, 750 kg DUT, 20kN generator load	20
2.4	Power Requirements, 750 kg DUT, 20kN generator load	20
2.5	Torque Requirements, 300 kg DUT, 10.3kN generator load	21
2.6	Power Requirements, 300 kg DUT, 10.3kN generator load	21
2.7	Bottom Limit Switches and Shock Absorber	22
2.8	Top Limit Switches and Shock Absorber	23
2.9	Linear Test Bed Base	24
2.10	Linear Test Bed Lower Gimbal	25
2.11	Linear Test Bed Carriage Assembly	26
2.12	Linear Test Bed Carriage Attachment Point	27
2.13	Linear Test Bed Suspension Arm	29
2.14	Linear Test Bed Suspension Arm Safety Link	30
2.15	MSRF with Linear Test Bed Additions	33
2.16	Water Rheostat with Electrical Connections shown	35
2.17	CSH Incorporated Float Switch	37
2.18	Float Switch Installation Notes	37

LIST OF FIGURES (Continued)

		Page
2.19	Water Rheostat Controller	38
2.20	No Load Power Chart	40
2.21	Resistance and a Function of Water Level	41
3.1	National Instruments, CompactRIO	46
3.2	CompactRIO Signal Flow	47
3.3	Linear Test Bed Signal Routing	48
3.4	5 Linear Test Bed Signal Routing Alterations	49
3.5	Compact Rio Wiring Diagram	50
3.6	NI 9205 Analog Input Module	51
3.7	Interface Force 1010 Load Cell	53
3.8	Interface Force Signal Conditioner	54
3.9	NI 9203 Analog Current Input	54
3.10	Phoenix Contact Breakout Board	56
3.11	NI 9263 Analog out Board	58
3.12	NI 9401 Digital I/O Board	60
4.1	PMAC Block Diagram	65
4.2	PMAC Closed Loop Servo Control	67
4.3	PMAC Control Block Diagram	69
4.4	PMAC PID Algorithm with Notch Filter	70
4.5	Typical Step Response Errors	73
4.6	Simple Linear Move Code	76
4.7	Simple Linear Move Plot	76
4.8	Example PLC Code	79
5.1	Force Control Scheme	81
5.2	Simulink Model of the Linear Test Bed	82
5.3	Simulink Differentiator	84
5.4	Position Loop with No Compensator	87
5.5	Position Loop with Compensation	88
5.6	Position Loop Simulink Implementation	89

LIST OF FIGURES (Continued)

		Page
5.7	Simulink Model of the CompactRIO ……	92
5.8	Simulink Hydrodynamic Commanded Force Generation……..	95
5.9	Force Controller Response with No Compensator……..…….	99
5.10	Force Controller Response with Compensation……	100
5.11	Force Controller Implementation ……..…	101
5.12	Linear Test Bed Model …….…….……....	102
5.13	Generator Force Modeling …….……...	104
5.14	Wave Height and Actual Vertical Position, Step Input ……..…..	105
5.15	Actual and Commanded Force, Step Input ……..…….	105
5.16	Wave Height and Actual Vertical Position, No Load …….….	107
5.17	Actual and Commanded Vertical Position, No Load ……...	107
5.18	Actual and Commanded Force, No Load …….	108
5.19	Wave Height and Actual Position, 500W Test……..…	109
5.20	Actual and Commanded Vertical Position, 500W Test ……...….	110
5.21	Actual and Commanded Force 500W Test…….…….....	110
5.22	Linear Test Bed Forces, 500W Test ……...…..	111
5.23	Device under Test Power, 500W Test .....…...	111
5.24	Wave Height and Actual Position, 1kW Test ……..…….	113
5.25	Actual and Commanded Vertical Position, 1kW Test……...…	113
5.26	Actual and Commanded Force, 1kW Test…….…....	114
5.27	Linear Test Bed Forces, 1kW Test ……..……...…..	114
5.28	Device under Test Power, 1kW Test…….....…	115
6.1	Closing a Force Loop around a Position Loop …….	120
6.2	Cascading Servo Loops .....…...	121
6.3	Water Rheostat Controller Connection ……...……..…	123

LIST OF TABLES

Table		Page
2.1	MSRF New Conductor Details ……...……....	34
2.2	Water Rheostat Load Testing ……...….	39

LIST OF APPENDICES

		Page
A.	ORIGINAL LINEAR TEST BED SPECICATION ……	127
B.	DC LOAD BANK QUOTATION ……..	131

A LINEAR TEST BED FOR CHARACTERIZING THE PERFORMACE OF OCEAN WAVE ENERGY CONVERTERS

1. INTRODUCTION

1.1 Wave Energy Extraction

Ocean wave energy is only one of five different forms of ocean energy including ocean thermal energy, salinity gradients, marine current energy, and tidal energy. Ocean wave energy strives to use primarily the heave motion of waves to generate electricity, either directly or using some intermediary energy conversation steps in the process. Interest in any form of ocean energy and most renewable energy sources is dependent upon the availability of fossil fuels, which drive traditional forms of electricity generation. Consequently, during the energy crisis of the 1970s, there was significant interest in developing renewable energy sources. After this energy crisis subsided, much of the interest in wave energy also lessened. Today, interest in ocean energy has once again been renewed due to rising cost of traditional types of electricity generation. Other factors for the increased interest are due to environmental considerations and advances in engineering and power electronics that make the technology much more feasible.

Often, ocean energy extraction devices are classified into three major categories that include shoreline, nearshore, and offshore devices. The benefits of shoreline devices include: less equipment maintenance, no expensive mooring systems needed to implement the technology, and less necessary equipment exposed to salt water at all times. Usually, shoreline devices are a form of the oscillating water column technology, which was developed in the 1970s. Nearshore and offshore devices are usually point absorber buoys which more directly convert the heave motion of the waves into electricity. However, these devices are harder to maintain and must be able to stand up to harsh ocean environments for longer periods of time. Also, the point absorber buoys can require complex mooring systems to function correctly.

Presently, researchers all over the world strive to find the optimal prototype ocean wave energy converter (OWEC). In order to select this optimal device, the dynamics of

OWECs must be understood with more confidence. Ocean testing and even wave tank testing of OWECs has led to inconclusive comparison tests due to the inconsistency of the wave profiles used in testing. In order to compare two OWECs, the exact same wave profiles must be used to test each device to ensure efficiencies and thrust capabilities are accurately compared. To achieve this, a device that will mechanically simulate the vertical motion of the ocean waves has been constructed. This device, called the linear test bed (LTB), can replicate real wave profiles, as measured by NOAA data buoys positioned off the coast of the western United States for example, and can reproduce them as often as necessary. It will be used to test and compare OWECs with generation capabilities of up to 10kW. To understand how the LTB will benefit prototype development, it is first vital to understand some of the different technologies and OWEC prototypes that exist today.

1.2 Oscillating Water Column

One of the most studied OWECs is the Oscillating Water Column (OWC). This technology was initially developed in the 1970s and had some success since it was fairly simple to install, being a shoreline device. There are several of these devices installed in the world today, including the first commercial wave generator in the United Kingdom on the coast of the Isle of Islay rated at 250 kW. The basic OWC system contains a partially submerged air chamber that opens to the ocean under the shore's water line and is shown below in Figure 1.1.

As the water level "oscillates" in the air column, there is a pressure difference created associated with the external water level. Basically, as the waves enter the air chamber air is then forced through the turbine, and as the waves retreat, air is sucked back through the same turbine. The turbine spins an electric generator, usually an induction generator, which generates usable electricity. The turbines that are usually used in OWCs are called "Wells Turbines" which are bidirectional. That is, torque is produced in the same direction regardless of air flow direction. There are also more

complicated approaches that use unidirectional turbines that need a valve system to ensure that air only flows in one direction [1].

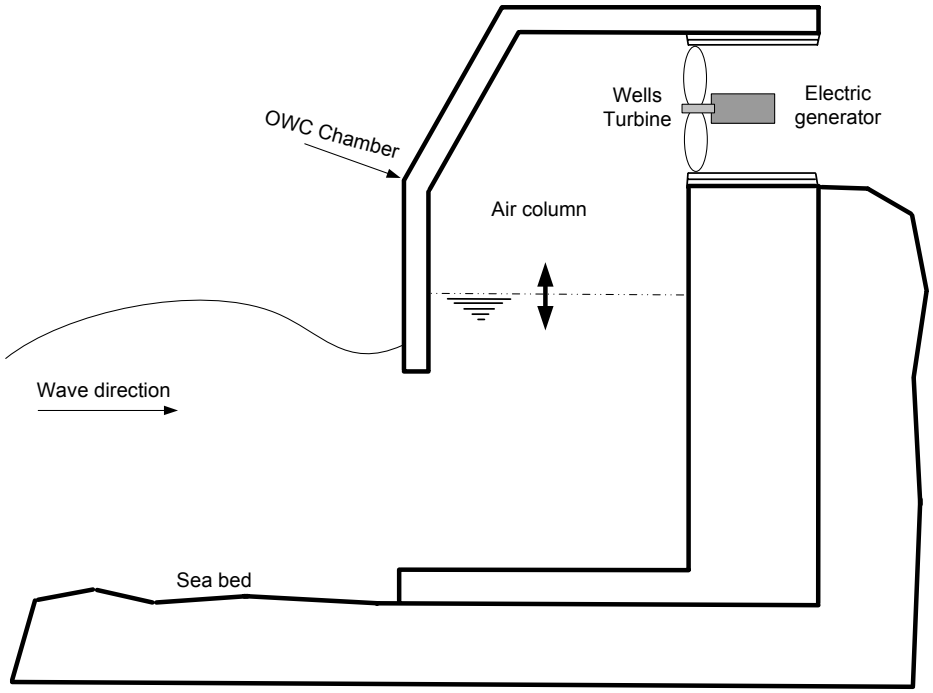

Fig. 1.1 The Oscillating Water Column (OWC) [7]

1.3 Surface Following or Attenuator OWECs

1.3.1 Ocean Power Delivery

One hydraulic device designed by Ocean Power Delivery, LTD (OPD) uses several cylindrical sections linked together by hinged joints. The linear motion of the waves induces motion in the hinged joints which is then resisted by hydraulic rams, which pump high pressure oil through hydraulic motors. These hydraulic motors then drive rotary electric generators. This device is called the Pelamis Wave Energy Converter, and is sometimes referred to as the “wave snake” because of its shape, shown below in Figure 1.2 [2].

Fig. 1.2 The OPD Palamis WEC [2]

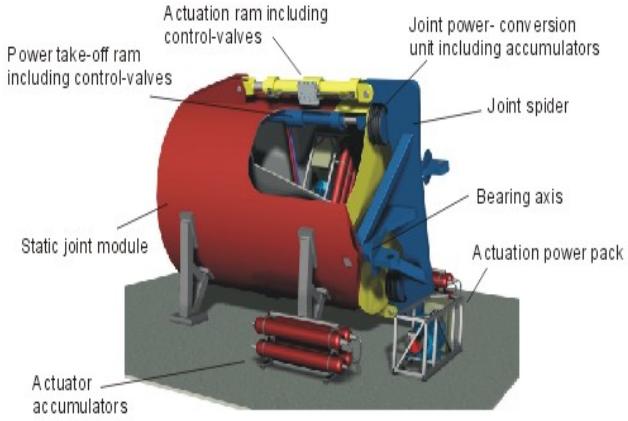

Fig. 1.3 OPD Power Conversion Module [2]

Shown in Figure 1.3 is the power conversion module for the Pelamis. Each device contains three cylindrical sections, each with its own power conversion module. Power take-off cables run from each of these modules to a central junction box on the ocean floor and then transmitted back to shore via undersea transmission cable. The machine is moored using a complex system of floats and weights that prevent the mooring lines from becoming taunt. This allows the mooring system to be strong enough to hold the machine in position but also allow the hinged joints to move with the waves. The Pelamis is designed to operate in 50 to 60 meters of water depth to benefit from large

swells, yet remain close enough to shore to minimize the cost of undersea transmission lines.

The Pelamis has a control system that limits the power generation during storm conditions through design characteristics of the device itself, thus reducing the risk of device damage during storm wave conditions. Also, since power output is varied, the Pelamis stores energy in hydraulic accumulators to steady power output. These features have earned the Pelamis at least one commercial contract off the coast of Portugal, with 2.25 MW installed during the summer of 2006. There are also talks of another Pelamis wave park, 5 MW, which if approved, would be installed off the coast of the United Kingdom near Cornwall. However, since the technology contains the additional energy conversion step with the hydraulic components, some researchers fear efficiency issues as well as continued problems with maintaining hydraulic equipment in ocean environments.

1.4 Overtopping OWECs

Overtopping OWECs seek to use the mature technology of hydroelectric turbines in the ocean environment. An example of this technology is the Wave Dragon Overtopping OWEC shown in Figure 1.4. In this technology, the incoming waves crash into a ramp that elevates the waves into a reservoir above sea level. Then, water is let out through various turbines and electricity and generated. The generation occurs in three steps, namely absorption, storage, and power take off. Absorption occurs as the waves are collected into the reservoir, storage occurs as the water accumulates in the reservoir, and power take off occurs as power is generated using hydroelectric turbines [27].

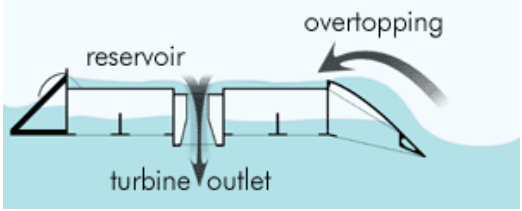

Fig. 1.4 Wave Dragon Overtopping OWEC [27]

1.5 Commercial Point Absorber OWECs

1.5.1 Ocean Power Technologies

Ocean Power Technologies (OPT) produces point absorber buoys that also use a hydraulic energy conversion step in the power take-off (PTO) equipment called PowerBuoy and is discussed in [3]. The PowerBuoy is shown below in Figure 1.5, and currently has a peak power output of 40kW. Plans have been announced for the design of a 500kW PowerBuoy. The 40kW device has a 12 foot diameter, is 52 feet long, with 13 feet extending above the surface of the water. The planned 500kW device has an estimated diameter of 42 feet; a length of 62 feet, with 18 feet extending above the surface of the water. The longest ocean test in company history was a full year and the test environments have included the New Jersey coast and ocean water off of a naval base in Hawaii. The company plans the nation's first commercial wave park off the coast of Reedsport, OR.

Fig. 1.5 The OPT PowerBuoy [3]

The unit is loosely moored to the ocean floor so that it can respond to the heave motion of the ocean wave. Enclosed in the unit includes the PTO system, electrical generator, power electronics system, and the control system. PTO system is a hydraulic system that converter the linear motion of a wave into rotational motion used to drive a traditional electric generator. As discussed, there have been some concerns with the hydraulic system because of an extra energy conversion step that reduces machine efficiency and the numerous maintenance issues of hydraulic systems. The power electronics system conditions the generated power into usable electrical energy. The entire operation of the PowerBuoy is controlled by the control system.

The control system contains an onboard computer that monitors all subsystems in the PowerBuoy. It also has a data acquisition system that monitors wave conditions including wave height, frequency, and shape. The control system uses that data to adjust the PowerBuoy's performance and operation to match the current wave conditions. In effect, the control system is able to adapt and adjust to changing wave conditions on the fly, in real time, on a wave by wave basis. The company believes that this control system is essential to maximize the machine's efficiency. During storm conditions, that is waves greater than 13 feet; the control system automatically locks down the system and does not generate electricity. When the storm ends and the wave climate returns to normal, the control system unlocks the PowerBuoy and normal operation is resumed [3].

1.5.2 Archimedes Wave Swing Ocean Energy

All devices considered up to this point are devices that follow or "ride" the wave with at least part of the device protruding through the water's surface. The Archimedes Wave Swing wave energy converter is fully submerged below the water's surface and consists of two main parts. The "floater" is an air filled cylindrical chamber that can freely move up and down. The "basement" is fixed to the ocean floor and the floater surrounds the basement. Essentially, as the floater moves up and down, there is relative linear motion between the floater and basement. An illustration of this device is shown below in Figure 1.6.

Fig. 1.6 The AWS Wave Energy Converter [4]

The operation of this device is relatively simple. As an incoming wave crest raises the water level above the float, the water pressure above the float increases which causes the air inside the float to compress to balance the pressures. Alternatively, as an incoming wave trough lowers the water level above the float, the water pressure decreases causing the air inside the float to expand. As a result, the float moves down as the air compresses during a wave crest and moves up as the air expands during a wave trough. This creates the relative linear motion between the floater and the basement [4].

This linear motion is converted into electricity using a linear generator. Magnets are placed on the floater and copper wire coils are placed on the basement (or visa versa). As the magnets located in the floater pass through the coils in the basement voltage is directly induced by Faraday's Law. Conversely, if the coils are located in the floater, as the coils pass through the magnetic field created by the magnets in the basement, voltage is also induced. AWS plans rate the first devices at over 1MW, with a capacity factor of near 35%. This means each machine will average 350kW of sustained power over the course of one year.

Some advantages of this technology include the fact that all of the machine parts will be submerged. This means that there will be virtually no visual impact of the implementation of this technology. Also, since the device is submerged, very high storm loading can be avoided, and there is no need for complicated and expensive mooring systems. Finally, the linear generator used will directly convert the motion of the wave into electricity with no intermediate hydraulic step, decreasing maintenance requirements and avoiding possible environmental concerns relating to leaking hydraulic fluid. However, since the device is completely submerged at water depths of 40-100 meters, all maintenance must be performed with a remotely operated vehicle (ROV) and could be characterized as an unseen navigation hazard.

1.6 Overview of Prototype Direct-drive, Point Absorber OWECs

During the last ten years researchers at Oregon State University have been developing novel OWECs. The focus of the research has been on direct-drive OWECs that directly convert the linear motion of the waves into electricity. As shown in previous sections, other OWECs use intermediary energy conversion steps that typical involve hydraulic or pneumatic devices. The intermediary steps can reduce the efficiency of the OWEC and cause a host of maintenance issues. The three direct-drive devices that will be discussed in the following sections are the three that will likely be tested on the linear test bed. The first device to be discussed is the air gap permanent magnet linear generator. The second device will be a permanent magnet linear generator with a slight modification that involves using iron in the air gap. Lastly, the contactless force transmission system OWEC will be overviewed which uses a ball screw to convert linear motion to rotary that drives a rotary generator.

1.6.1 Linear Air Gap Wound Permanent Magnet Generator

The first OWEC developed at Oregon State was the linear air gap wound permanent magnet generator. It was designed with limited funding and the primary design goal was to provide an initial proof of concept. In this design there is a center

section of magnets fixed to the ocean bottom called the translator shaft. Surrounding the magnets is a float that contains the armature coils that heave with the motion of the wave. As the coils move through the magnetic field created by the translator shaft, voltage is directly induced by Faraday's law. This system is shown below in Figure 1.7 [5].

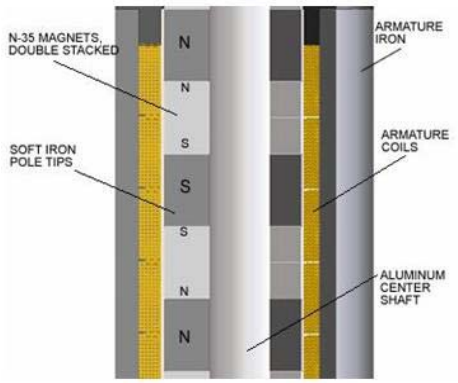

Fig. 1.7 Linear Air Gap Wound Permanent Magnet Generator [5]

The magnet shaft contains neodymium-iron-boron magnets magnetized to 35 MGOs. Figure 1.7 shows how the dark grey pole pieces are magnetized north or south by arranging the magnets in opposing pole orientation. The magnets are arranged in this manner to "squeeze" the flux out of the magnets and pass the flux to the armature coils. To better understand the flux path in this machine let us follow it starting at one of the north pole tips. The flux is squeezed out of the north pole tip, passes through the air gap, and into the copper coils adjacent to the north pole tip. From the copper coils the flux continues into the armature "back iron" and back through the copper coils adjacent to the south pole tip. Finally, the flux passes back across the air gap and back to the south pole tip. Obviously, this is the optimum flux path to induce voltage in the armature coils. However, there will be some flux leakage which occurs in the machine through the aluminum center shaft and air gap. For this design, it was assumed that 50% of the flux would be lost to leakage.

Since this was the first design at Oregon State, several improvements in this design were suggested after this device was tested. The first suggestion was to lower the

center of a mass as it was too high in this design. The high center of mass required unnecessary anchoring tension. The second improvement that was suggested related to the stroke of the generator. In order to extract energy during the entire wave period, the range of water born lift should be equal to or less than the maximum stroke of the generator. In this generator the water born lift was greater than the maximum stroke resulting in no generation during a portion of the wave period.

1.6.2 Linear Transverse Flux Permanent Magnet Generator

The second linear generator developed at Oregon State University is called the transverse flux permanent magnet linear generator. The idea of this machine was to increase the flux density seen in the air gap machine by providing a flux path of lower reluctance. In the air gap machine discussed in the previous section, the flux must pass from the north pole to the back iron and from the back iron to the south pole through air. With this design it is easy to understand that the flux density of magnetic circuit is limited by the low relative permeability of air. Please see Figure 1.8 to understand the limiting factors of the air gap machine.

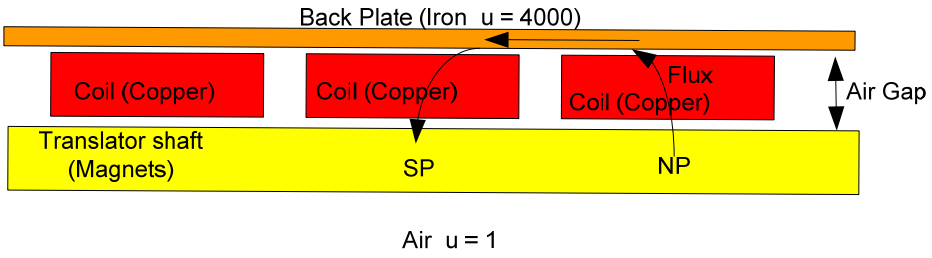

Fig. 1.8 Flux Path of Air Gap Machine [6]

The transverse flux approach seeks to minimize the air gap in the magnetic circuit in order to achieve higher flux density. This is done by using more iron in the armature which has a significantly higher relative permeability and in turn creates a low reluctance flux path between the magnet pole tips. From the north pole, the flux passes through a small air gap to the armature iron. From the armature iron, flux can circulate through the back iron and through another small air gap to the south pole. The air gap in this design

is much smaller than that of the air gap machine. Please see Figure 1.9 which illustrates the flux path in the transverse flux machine.

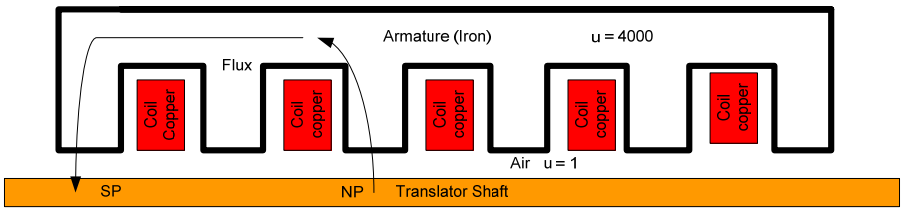

Fig. 1.9 Flux Path of Transverse Flux Machine [6]

In the transverse flux study [6] simulation results showed an increase in flux linkage of nearly 50% compared to the air gap machine. The results also showed an increase by one order of magnitude in cogging force from 2.5% of the change in force to almost 20% of the change in force. Cogging in linear generators causes the higher frequency force components to act on the armature. The research team suggested that more flaring on the tips of the armature teeth would help to reduce the cogging of this machine. However, the overall armature force was greater than that of the air gap machine possibly leading to increased power take-off. Oregon State University is presently developing a 1 kW transverse flux linear generator to further study the performance of this design. The effects of increased cogging force will be looked at during the design of this 1 kW generator. This generator should be ready for ocean testing in the early fall of 2007 [6].

1.6.3 Contactless Force Transmission System OWEC

Of the direct-drive buoys topologies studies so far, all have been linear machines which respond directly to the slow motion of the ocean waves. The next machine discussed was also developed at Oregon State University and uses a linear to rotary power take-off design. In this design, the device indirectly responds to the movement of the waves using a thrust transmission system allowing the use of rotary generators. When designing a thrust conversion system of this type the first concern involves

efficient conversion of slow motion of the waves into high rotary speeds necessary in the power take-off (PTO) system. The second concern involves effectively transmitting the force form the waves onto the PTO system. The contactless force transmission system (CFTS) uses magnetic fields for contactless mechanical thrust transmission. Please see Figure 1.10 which illustrates how the CFTS is utilized in the design of an OWEC [7].

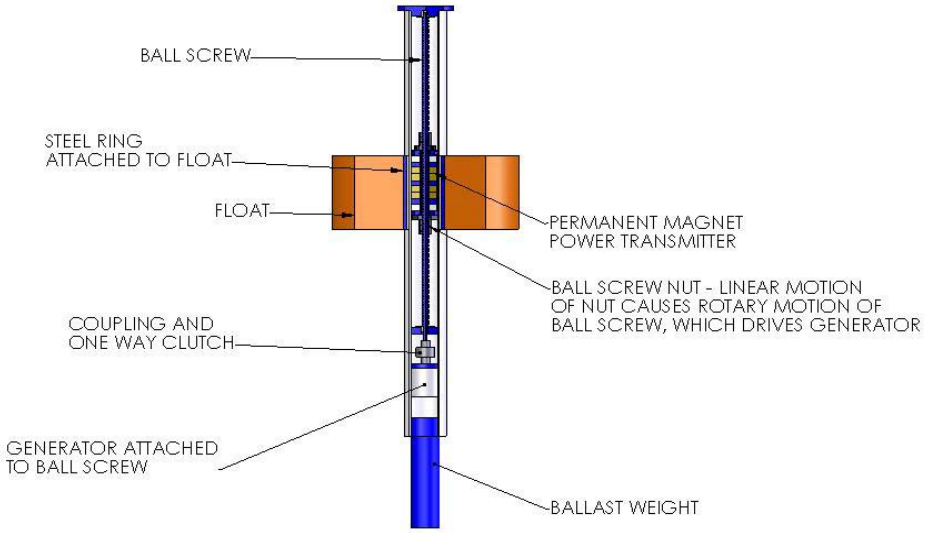

Fig. 1.10 Model of CFTS Buoy [7]

The device consists of an outer buoy float which responses to the excitation force of an ocean wave causing it to move up and down. It contains a ferromagnetic cylinder which moves with respect to the inner modules or spar. The spar contains the PTO components comprising of the permanent magnet piston, ball screw, and the permanent magnet synchronous generator. The spar is completely sealed providing isolation between the PTO equipment and the ocean environment. The force of the wave is transmitted to the PTO equipment by the magnetic field of the CFTS.

To understand how the CFTS system works, the major components of the system must be understood. The piston, or ball nut, which is coupled to the ball screw, is comprised of several magnets which squeeze flux through a central pole piece through the back iron cylinder which is located in the float. This magnetically couples the float

and the spar and means that as the float containing the back iron is moved up and down with the ocean wave, the piston is “pulled” up and down with the float. As the piston moves inside the spar it mechanically couples to the ball screw and causes it to rotate, which drives the permanent magnet synchronous generator.

The benefit of this system is that it is able to use rotary machines that can operate at much higher speeds leading to increased efficiency. Also, the PTO equipment can be sealed inside the spar since the thrust is transferred magnetically through the CFTS which allows isolation from the ocean environment. There is no need for “working” or moving seals with this design leading to increased maintenance. However, the friction between the ball nut and the ball screw can be problematic with this design. The heat that is caused by this friction cannot escape easily since the spar is completely sealed. Currently, researchers at Oregon State University are attempting to design a magnetic screw that would not require direct physical coupling to a nut.

1.7 Motivation for this Work

In the previous sections it was shown that many OWEC technologies exist, some available on a commercial level and others still being researched at the prototype level. At Oregon State University alone, four prototype generators have been developed with plans for a fifth and sixth prototype. For Oregon State, the question becomes which of these prototype generators is most likely to be used at the commercial level. There is a definite advantage to finding an optimum topology for a direct-drive OWEC and focusing the majority of the research efforts on this topology. Oregon State University views the linear test bed as a tool that will determine the optimum topology for a direct-drive OWEC.

The linear test bed will be used to characterize the performance of each of the six prototype generators. Since the linear test bed will be replicating real wave conditions and will be able to repeat any test plan, performance characteristics of each prototype generator, such as generator efficiency, will be able to be compared. Essentially, a motion program of the linear test bed will be based on a wave profile obtained from data

buoys in the ocean. The motion program can be saved and repeated on any device that could be tested in the linear test bed. This means any OWEC under test can be subjected to the exact same wave profile and the performance characteristics of each can be compared. If the testing was done in the ocean, or even a wave tank, there would be no way to ensure that the wave profiles experienced by the different OWECs were identical, making the testing results inconclusive. This problem was first experienced when trying to decide whether the linear air gap permanent magnet generator or the CFTS OWEC was superior.

Also included in determining the optimum topology for a direct-drive OWEC is testing many different topologies, many not yet developed to the prototype stage. The linear test bed allows other direct-drive OWEC ideas to be tested quickly. Since the linear test bed only needs the active components of the OWEC for testing, the prototype design of a new idea can be much simpler. The buoy that will house the active components of the OWEC does not have to be fully designed and built for testing in the linear test bed. This will allow researchers at Oregon State to test ideas briefly discussed in general wave energy meetings such as a roller screw OWEC and a belt drive OWEC with much greater ease. Additionally, the linear test bed can also be used to test other OWECs available on the commercial market. If a company such as Ocean Power Technologies came to Oregon State with a 10kW prototype OWEC and asked for the device to be characterized, researchers at Oregon State will be able to determine generator efficiency. However, the linear test bed will only be able to test point absorber OWECs, such as OPT's PowerBuoy and the AWS OWEC.

Finally, with the force control feature of the linear test bed, the control system of most point absorber buoys will be able to be tested. If the linear test bed is controlled using force feedback, the OWEC response is very close to how it would actually respond in the ocean. OPT already has a control system that strategically positions the PowerBuoy for each incoming wave. Oregon State is also in the process of designing a control system that would possibly back drive a linear generator to optimally position the buoy for the next incoming wave. These types of control systems will be able to be tested on the linear test bed under force control mode.

2. LINEAR TEST BED

Oregon State University's Wave Energy team has recognized that in order to comprehensively research, test, evaluate and advance wave energy conversion devices, they need to upgrade the MSRF with a linear test bed. The linear test bed is designed to create the linear motion between a vertically oriented center "spar" and the active components of a surrounding "float". Thus, the linear test bed will enable the dynamic and controlled testing of wave energy devices, using captured wave profiles from ocean monitoring buoys, while simulating the actual response of ocean waves using various control schemes.

The linear test bed system will be comprised of one vertical axis of servo controlled CNC (computer numerically controlled) motion for moving the OWEC under test. A servomotor, through timing belts, will be used to move the linear test bed carriage to drive the active float up and down. The outer active float will be attached to the carriage using a gimbal mount with linear bearings used provide guidance for the carriage. The base has a gimbal mounting for the center spar and a removable pallet for loading and unloading the device under test.

2.1 Mechanical Design and Safety

Oregon State University's wave energy team developed specifications requirements for the linear test bed, given in Appendix A. Based on these performance requirements, the mechanical design for the linear test bed, shown below in Figure 2.1, was designed by a company located in Phoenix, Arizona called Mundt and Associates and was reviewed by researchers at Oregon State University. Mundt and Associates specializes in one-of machines used for very unique applications and were selected for this area of expertise. Mundt and Associates also designed several safety features that prevent the destruction of the linear test bed if an incorrect motor command is issued. These design considerations should be documented to understand the operation of the linear test bed.

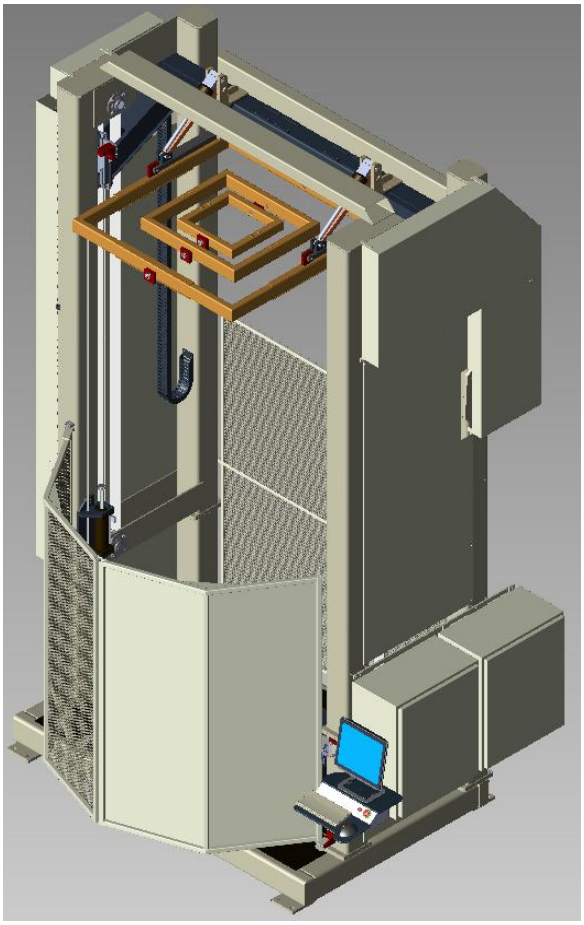

Fig. 2.1 Linear Test Bed

The details of each part of the machine will be discussed in the next few pages. However, there are several general design decisions to review before the details of mechanical design are discussed. In order to ensure that there is no entry to the moving pieces of the operating linear test bed, steel screen doors were installed in the front and a steel screen was bolted to the back of the linear test bed. As we will see later, the drive pulleys are also covered with steel plates as a safety precaution. These covers are removable so that the drive belts can be properly tensioned. The cabinets located behind the host computer are used as the main electrical interconnection point and also to house the necessary motion controllers which will be discussed in detail in chapters 4 and 5. The host computer and emergency stop button are located near the linear test bed as shown. There will also be a remote emergency stop button.

Fig. 2.2 Linear Test Bed Frame and Drive Assembly

2.1.1 Frame and Drive Assembly

The linear test bed frame and drive assembly is shown above in Figure 2.2. The main frame will fit on risers on the base of the linear test bed in order to fit the test bed through the MSRF doorway. Generally speaking, the linear test bed is powered by a 50 HP servo motor, geared down, and motion is translated from rotational to linear motion through the use of several pulleys. The motor shaft is coupled to a timing belt and middle pulley that has a gear ratio of 3:1. The shaft coupled to the middle pulley drives the two top pulleys which have a gear ratio of 3:1 for a total gear reduction of 9:1. This shaft spans the width of the machine and is coupled the opposite upper pulley. There are then two separate shafts attached to the top of the top pulleys. These shafts drive two vertical timing belts which move the linear test bed carriage and OWEC under test up and down. The active components of the OWEC under test are mounted to the carriage, which is

attached to the vertical belts on the left and right sides of the machine. The details of how the carriage attaches to the drive belts are discussed later.

The timing belts are not made of rubber and nylon fibers like traditional timing belts, which would not be able to handle the load of the linear test bed. These timing belts are made of steel and perform more like a chain than a belt. The timing belts are 100mm wide with the belts on each side of linear test bed capable of supporting the driving force at full load. The reason a belt drive system was selected instead of a chain drive or ball screw system is due to the fact the belts are designed for high speed applications, have very high efficiencies, and low noise.

The 50 HP IndraDyn A servo motor is capable of delivering 3278 lb-in of torque continuously or 4513 lb-in maximum and has a useable maximum speed of 2292 RPM. The motor is supplied by a 480 VAC, three phase supply and cooled by a blowing axial fan. The motor brake is electrically released with a capacity of 240 Nm. The motor is controlled in part using an Indradrive variable speed drive made by Rexroth. This drive has a diode rectifier front end with a DC bus at 800VDC which supplies the inverter. A line filter is used to control the harmonic content of the input current. The drive, line filter, and main breaker are housed in the electrical cabinet on the linear test bed.

The motor must be capable of driving a device under test using two different modes of operation. During normal operation mode, the maximum vertical linear velocity is 1 m/s with a maximum acceleration of 1.1 m/s/s, which will simulate the limits of normal wave conditions. During fast mode, the linear test bed must be able to generate 2 m/s of linear velocity at a maximum acceleration of 3.0 m/s/s. A complete table of the linear test bed performance specification can be found in Appendix A. The fast mode of operation is necessary to simulate the effect of back driving the OWEC under test. If a OWEC controller causes that to happen in the ocean, the OWEC will be back driven under water so that during when the next wave front the OWEC will be forced out of the water at a higher velocity due to the higher buoyant force. In most linear electrical machines, higher velocity can mean high efficiency, which is the reason this “hold and release” control method may be utilized in the future and will need to be tested. Based on the linear velocity and acceleration requirements of each mode of

operation, the motor speed and torque requirements can be estimated and are shown in Figures 2.3-2.6.

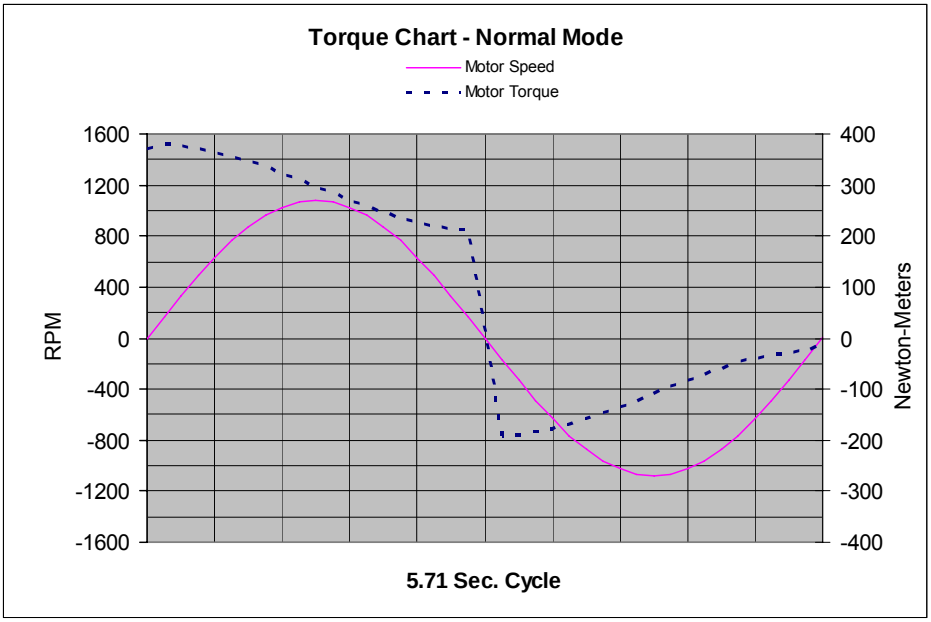

Fig. 2.3 Torque Requirements, 750 kg DUT, 20kN generator load

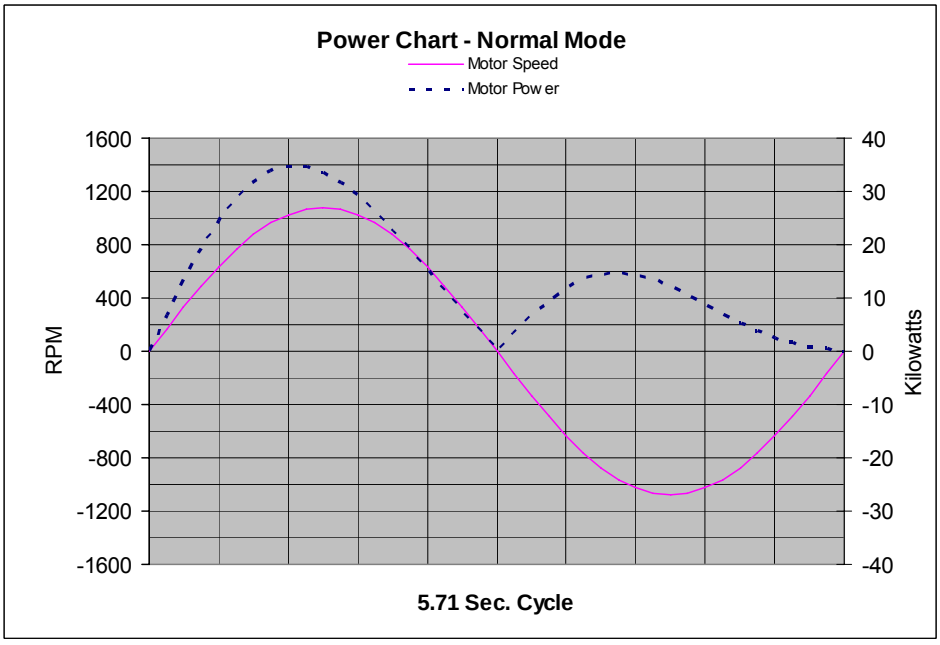

Fig. 2.4 Power Requirements, 750 kg DUT, 20kN generator load

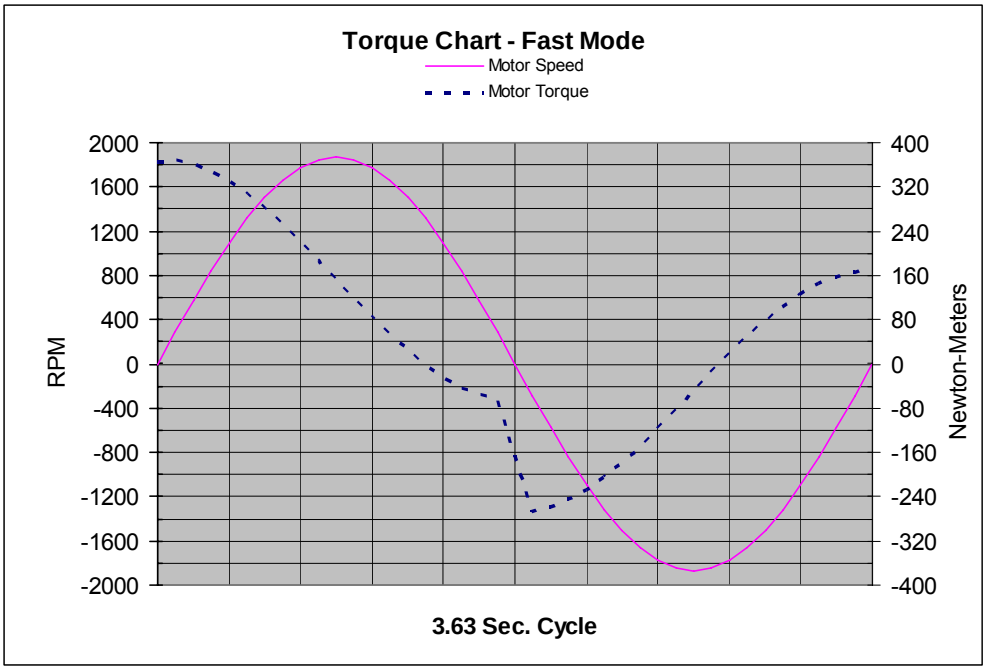

Fig. 2.5 Torque Requirements, 300 kg DUT, 10.3kN generator load

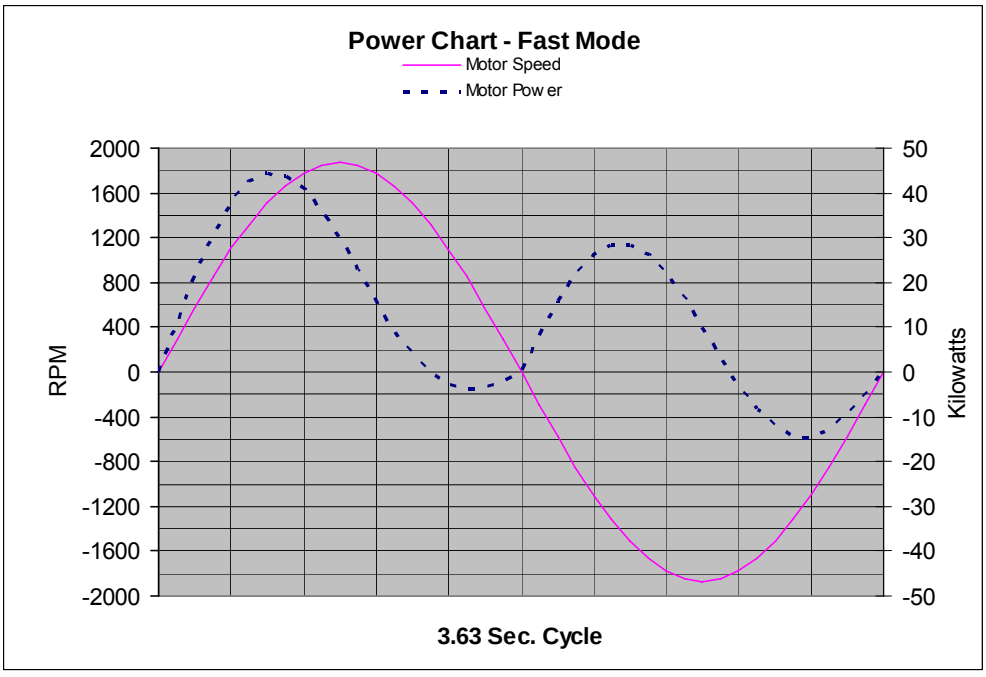

Fig. 2.6 Power Requirements, 300 kg DUT, 10.3kN generator load

The main frame of support structure of the linear test bed is made of steel and is modular in design. Referring back to Figure 2.2, there are two column pieces, one on the right and the other on the left. These pieces are connected by two upper braces, one located above the top pulleys, and the other above the middle connecting drive shaft. Again, the modular design was necessary to fit the linear test bed through the MSRF doorway. There are two cable trays that are attached to the left and right columns used to make electrical connections to the moving components of the linear test bed and device under test. The right tray is reserved for linear test bed use and the left tray for device under test use including power take off cables and data acquisition cables.

Finally, there are several over travel switches which prevent the linear test bed carriage from traveling past the allowable limits of the machine. The over travel limit switches for the bottom range of travel are shown below in Figure 2.7.

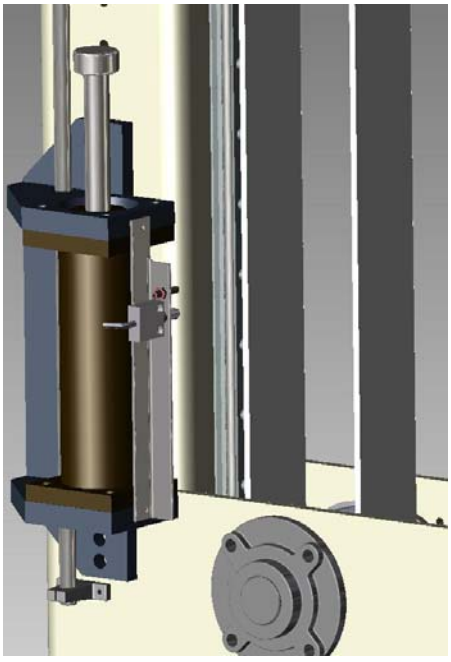

Fig. 2.7 Bottom Limit Switches and Shock Absorber

The top switch, shown in maroon, is a proximity inductive switch that is connected to the main motion controller, made by Delta Tau, so that if it is tripped, will allow the machine to come to a controlled stop. The bottom switch, shown in grey, is a mechanical

microswitch that is connected to the emergency stop circuit so that it is if tripped, power to the machine will be cut off. The shock absorber is also shown and will allow the carriage to stop safely if it is dropped in the event of a belt failure or if the momentum of the machine causes the carriage to move outside the over travel range after a controlled or emergency stop occurs.

The upper over travel limit switches are shown in Figure 2.8. There are a total of two inductive proximity sensors because one is used as a home switch. The home switch allows the motor controller reset the encoder to zero counts when the carriage reaches the middle of the travel range. The upper inductive sensor will trigger a controlled stop and the top mechanical microswitch will trigger an emergency stop as in the case of the bottom over travel limit switches. There is also a shock absorber that slows the motion of the carriage if the momentum of the machine causes it to travel outside the upper range of travel limit.

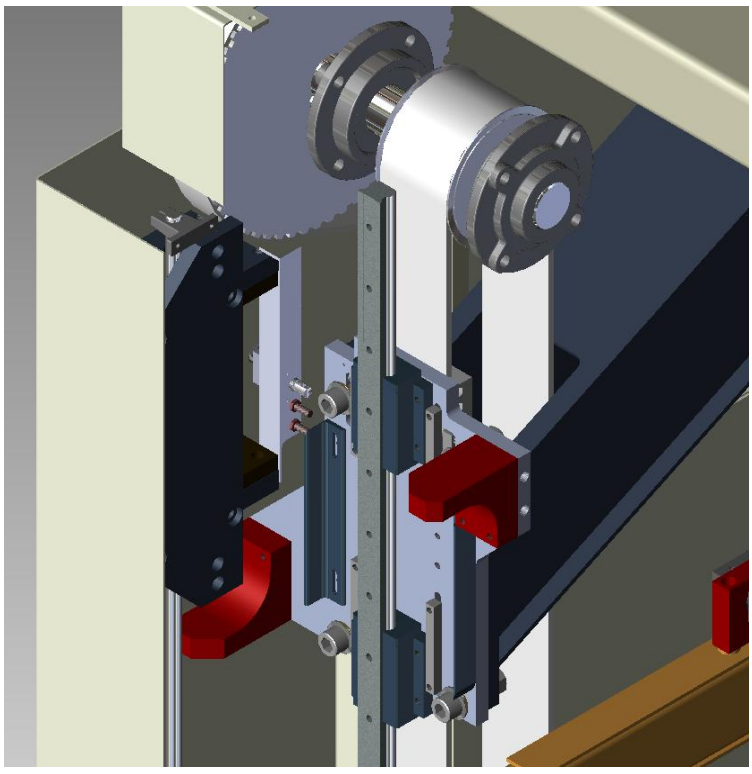

Fig. 2.8 Top Limit Switches and Shock Absorber

2.1.2 Linear Test Bed Base

The base of the linear test bed is shown below in Figure 2.10. There are four column spacers used to ensure that the unit fits through the MSRF doors and still achieve the full vertical displacement required. These column spacers are made of steel to ensure that the base of the support frame is strong enough to support the weight of the moving components of device under test. Also, there is a pallet extension necessary for small devices under test. Since a smaller device under test may have a shorter active spar, the pallet extension allows the smaller active spar to be mounted within the range of motion of the linear test bed.

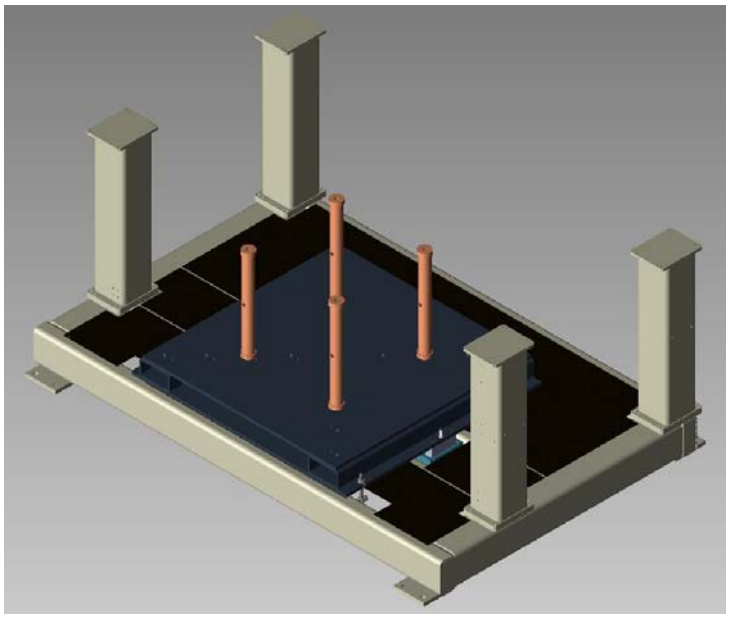

Fig. 2.9 Linear Test Bed Base

The spar pallet is made of two pieces of steel reinforced with two steel supports between the plates and is removable via forklift for loading purposes. The spar pallet must be heavy and strong to accommodate the large weight of the device under test and also all generator loads that will be encountered during testing. The steel supports were necessary because even a single plate of steel would deflect and buckle. Holding the spar pallet is the lower gimbal. The lower gimbal allows the spar pallet to tilt left or right. The lower gimbal effectively places the spar pallet on a “see-saw” which will help

compensate for any side loading present due to imperfects in the spar design or installation of the pallet. For example, if the spar is not mounted exactly vertical up and down, as the active float moves up and down on the spar exactly along the vertical axis, the components of the active float will experience a force from the spar in the horizontal direction.

By allowing the spar pallet to pivot in the center, the spar can slightly move to ensure no side loading is experienced by the active float components due to spar imperfections or improper spar mounting. Essentially, the float and carriage of the linear test bed is able to guide the spar so side loading is eliminated. The lower gimbal assembly is shown in Figure 2.10, with the spar pallet hidden and walking plates shown in black to expose it. As shown, the pivot point of the lower gimbal is in the center with each end supported by springs, which are used to dampen the motion of gimbal if side loading is present. The spar pallet simply fits into the two stainless steel pins in order to allow the whole pallet to pivot. It should be noted that there are bolts used to lock the pallet so the bottom gimbal does not move during loading or unloading of a device under test.

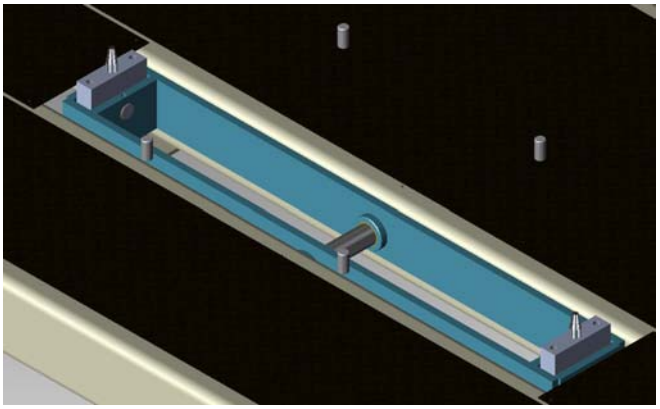

Fig. 2.10 Linear Test Lower Gimbal

2.1.3 Carriage Assembly

The linear test bed carriage attaches to the drive belt and allows for the mounting of the active float components of the OWEC under test, and is shown in Figure 2.11. The

carriage assembly has three bolt patterns which allow the suspension arms to be moved to accommodate different sized yokes. The yokes will attach the active float component of an OWEC under test. Since the design of every OWEC that will be tested in the linear test bed is not known, the mounting of the OWEC to the linear test bed needed to be as flexible as possible. The three yoke sizes will be able to accommodate many sizes of devices to be tested. The load cells which will measure the force exerted by the linear test bed on the DUT are shown in Figure 2.12. It should be pointed out that the force proportional to the suspended mass includes the yoke mass and will need to be subtracted out of the load cell reading. The force is not only dependent on the gravity, but also the acceleration of the carriage. This means this force will be changing constantly as the linear test bed moves, rather than just a constant weight force to be subtracted.

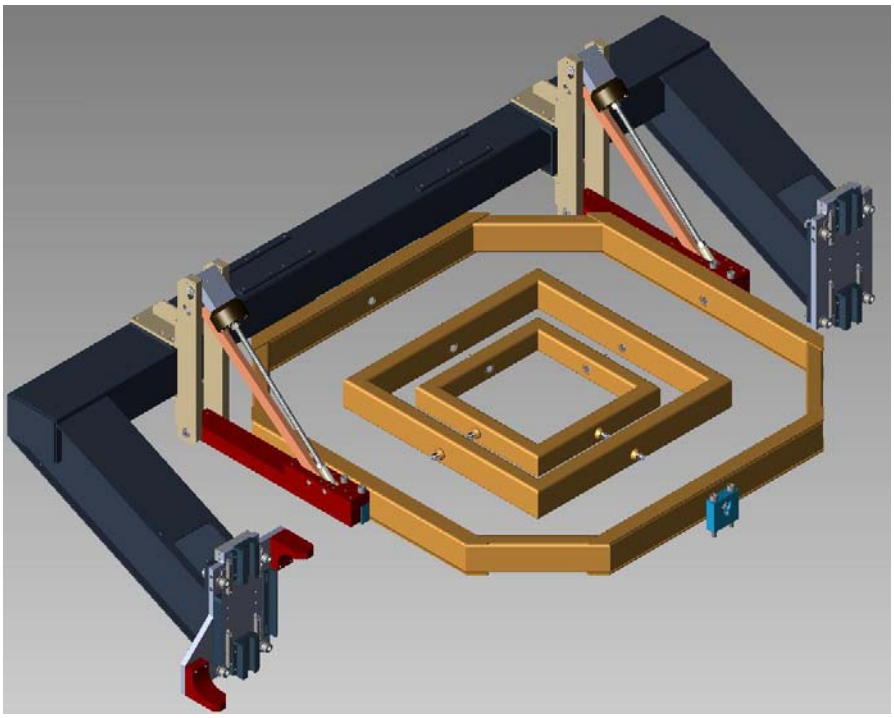

Fig. 2.11 Linear Test Bed Carriage Assembly

When considering the attachment of the carriage assembly to the linear test bed, there are several details that must be mentioned to fully understand how this is accomplished. This carriage attachment point is shown in detail in Figure 2.12. The

shock-stops, shown in corners of Figure 2.12, are made of aluminum and will depress the shock absorbers in the event of a controlled stop or emergency stop. They have a curved impact point so wear and tear is minimized. Thomson stainless steel guide blocks are used to guide the movement of the linear test bed. The two guide bearings are shown in the center of Figure 2.12 and are not fix mounted to the carriage, but mounted with some degree of compliance so that they can move from side to side and up and down to account for any imperfect alignment. The “L shaped” sensor flags are also shown in Figure 2.12 and are used to trigger the over travel proximity switches.

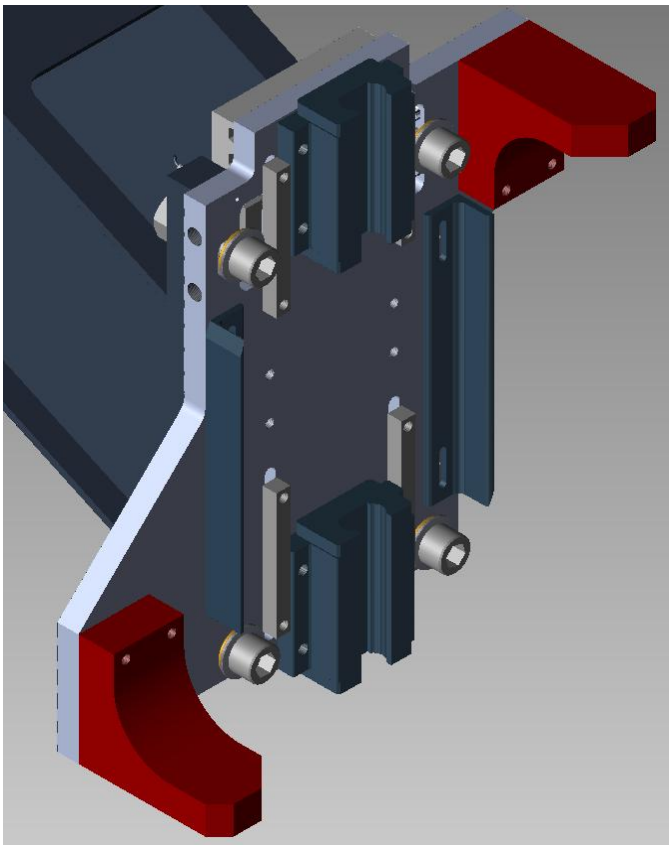

Fig. 2.12 Linear Test Bed Carriage Attachment Point

The carriage assembly attaches to the drive belts on each side of the machine. To better understand how this is accomplished please refer back to Figure 2.9. This figure also shows how the Thomson guide bearings are attached to the rails. The carriage is fixed to the drive belts with a clamping plate equipped with teeth that engage the belt.

These teeth fit into the grooves in the belt much like in the drive pulleys. The clamping plate is then attached to the guide plate on the other side of the belt and bolted together using four steel bolts.

Also on the carriage assembly, there are two gimbals that allow the OWEC under test to pivot both front to back and left to right. The gimbal that allows the OWEC under test to pivot front to back is the attachment point between the suspension towers and the upper yoke. The gimbal that allows pivoting from left to right is the attachment point between the upper yoke and DUT. It is assumed that on the DUT there would be two bearing surfaces, one on the top of the active float components and one on the bottom. These surfaces would allow the float to slide up and down on the spar. Since both gimbals will attach to the top of the active float instead of the middle, any side loading would put all the side loading reactive force on the top bearing surface.

Now, if we assume one gimbal is close to the top bearing surface, and the other is above it, the side loading force acts on each of the gimbals. This causes a reactionary force on the upper bearing from the gimbal close to the top bearing and a torque about the upper bearing proportional to the distance between the top gimbal and upper bearing. Oregon State University researchers determined that the increase in reactionary force is proportional to the distance that separates the gimbals. The initial design had the gimbals spaced far apart which would have put unnecessary force on the upper bearing surface. This is the reason that in the final design the gimbals are spaced vertically as close as possible to each other.

2.1.4 Suspension Arm

The final detail to be discussed is the suspension arms briefly discussed already. The suspension arms attach the carriage to the yoke and can be attached to the carriage in three places to accommodate different yoke sizes. One of the suspension arms is shown below in Figure 2.13. The first point of interested is the mounting and attachment of the load cell to the suspension arm. The load cells are not directly measuring the vertical force applied by the linear test bed to the device under test. Since this force is the force of interest because it is measuring the simulated driving force of a wave, trigonometry

must be used to determine the actual driving force. Additionally, there are two load cells measure the driving force, one per tower, and will need to be summed together to determined the total driving force. The conditioning will be performed with a digital signal processor and will be discussed in chapter three.

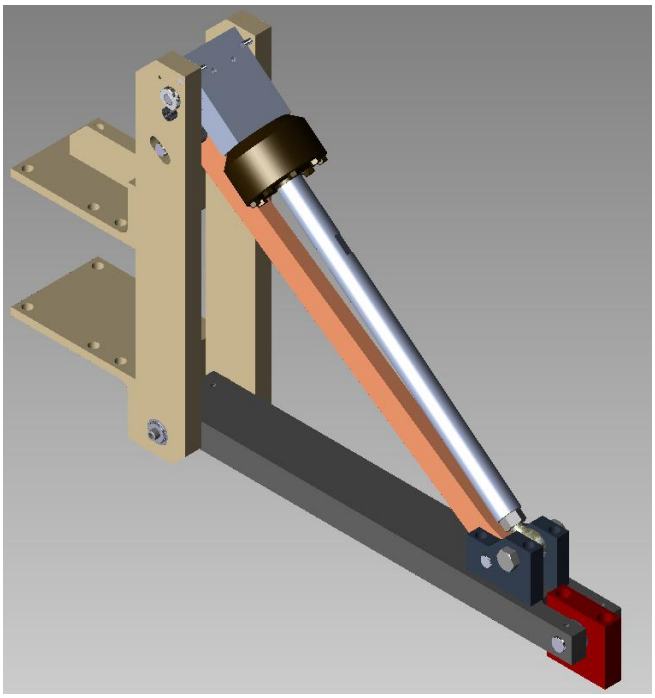

Fig. 2.13 Linear Test Bed Suspension Arm

The suspension tower is made of aluminum because the suspension arms will need to be moved manually when yoke size is changed. The weight of each arm is nearly 55 pounds with the towers made of aluminum and would have been significantly heavier if made of steel, making moving the arms extremely difficult. The suspension arms are attached to the carriage using the suspension brackets, and attach to the yoke with the upper gimbal blocks.

Since the load cells are made to handle are range of forces, if the machine exerts a force beyond the upper limits of the load cells, a safety mechanism has been built into the design. In the event of an overload, a sheer pin located inside the load cell pivot will break causing the safety link, shown below the load cell arm, to support the weight of the

yoke and device under test instead of the load cell arm. This will cause a dowel pin to slide down a groove the suspension tower approximately 1/2 inches. The movement of this pin will be detected by an inductive proximity switch which will alert the controller that this overload has occurred and will bring the machine to a controlled stop. The details of the safety link are shown below in Figure 2.14.

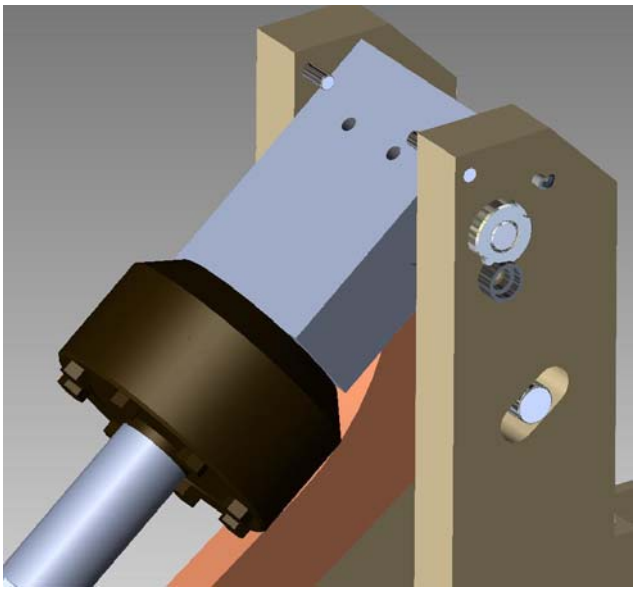

Fig. 2.14 Linear Test Bed Suspension Arm Safety Link

2.2 Control System Overview

The control system that will govern the motion of the linear test bed is a major part of the overall design and will be discussed in great detail in chapters 4 and 5. The intent of this section is to simply introduce the basic function of the control system. The servo motor drives the carriage up and down along the z-axis, if the z-axis is defined vertically. Since the carriage is typically fixed to the active float components of an OWEC and the active spar components are fixed to the stationary base plate, the linear test bed creates relative linear motion between the float and the spar. In the ocean, this relative linear motion is caused by waves. Using two primary modes of control, the control system of the linear test bed attempts to approximate the ocean's relative linear

motion using the first mode, and replicate it with the second mode. The justification for how each control scheme is implemented, including necessary hardware, is provided in chapter 3.

The first mode of control, implemented by Mundt and Associates using the Turbo PMAC PCI, made by Delta Tau, will only approximate the ocean's relative linear motion and is called position control. In this mode of control, the linear test bed will track a predetermined position profile which will move the carriage up and down along the z-axis. The mode of control does not account for the hydrodynamic interaction between the OWEC and the ocean wave including the impact of the wave on the OWEC's position, and the impact of the OWEC extracting energy from the wave itself. Furthermore, this mode of control does not take into consideration the finite driving force of a wave. In this mode, the linear test bed will use any required force to move the carriage from point A to point B along the vertical axis. Obviously, this does not accurately simulate an actual wave profile that the OWEC will experience in the ocean. However, position control can be helpful for simply characterizing OWEC performance characteristics such as efficiency.

The second mode of control, implemented by Oregon State University using the CompactRIO, made by National Instruments, seeks to replicate the relative motion that will be provided by an ocean wave and is called force control. The feedback variable in this mode of control is force on the OWEC under test, not just the position of the OWEC in the linear test bed. In this mode of control, Patel's hydrodynamic equations [8] are used to generate a force command to be applied to the device under test. The force command represents the actual force that the ocean will provide based on the current wave height and the buoy geometry that will house the active float components of the device under test. This mode of control forces the linear test bed to exert only the force that a real wave is capable of supplying. Furthermore, because the commanded force is based on proven hydrodynamic equations, the interaction between the OWEC and the wave is captured in the mode of control. Clearly, this mode of control more accurately replicates a real ocean environment. This mode of control will offer more accurate results and enable the testing of OWEC control systems.

2.3 Equipment Setup in the MSRF

In order for the linear test bed to be installed in the Motor Systems Resource Facility (MSRF) at Oregon State University, several installation issues must be addressed. The first issue will be meeting the input power requirements of the servo motor used to drive the linear test bed. The power cables will need to be sized correctly with regard to motor voltage and current ratings and installed in the lab before the linear test bed arrives at OSU. Also, cable for the remotely located emergency stop will also need to be sized and installed. This will minimize the amount of time that Mundt and Associates will need to spend setting up the LTB in the lab.

Another issue that must be addressed before Mundt and Associates installs the LTB is required DC bus power dissipation. During the upstroke the LTB lifts the DUT and will likely oppose any generator force causing the motor to operate in "motoring" mode. However, during the downstoke, the LTB resists the DUTs tendency to fall due to gravity. This means the motor shaft is rotating the opposite direction forcing the motor into "generating" mode. This generated power must be dissipated after it flows back through the inverter to avoid overcharging the DC bus. All of these installation issues will be discussed in this section.

2.3.1 Electrical Interconnection

The linear test bed will require several new stretches of conductor and a new breaker capable of switching 480V line-to-line at 150 amperes. The new breaker will be mounted in an existing motor control center (MCC1) that is supplied by a dedicated 750 kVA utility supply. The interconnection is shown below in Figure 2.16. The relevant linear test bed additions are shown on the left of Figure 2.15. The installation issues that will be addressed include the new breaker installation and several new cable runs that will be necessary.

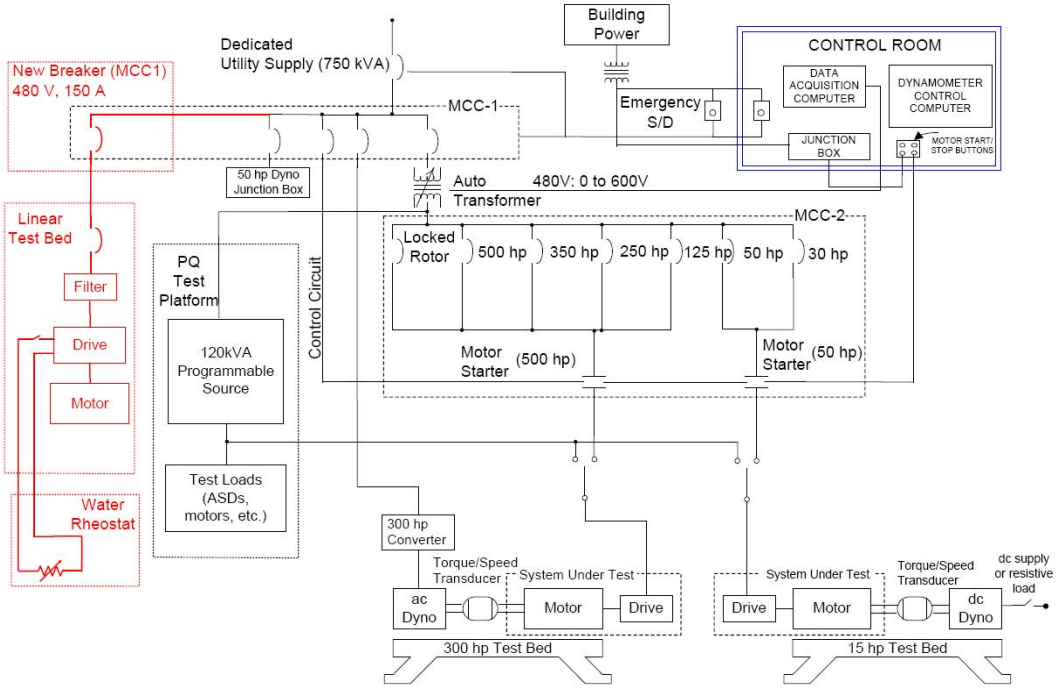

Fig. 2.15 MSRF with Linear Test Bed Additions

Three new conductors will be placed from the new 150 ampere breaker to the linear test bed electrical cabinet and will serve as the main power supply. The linear test bed itself will also have its own breaker which the new cabling will be directly connected to as shown in Figure 2.16. The linear test bed also has an input current filter to control the harmonic content on the line necessary as the drive will produce significant harmonic distortion. Also, new conductors will be installed connecting the drive breaker, accessible form the electrical cabinet, to the water rheostats. This issue will be discussed in detail in section 2.3.1. Finally, a new conductor will be installed that will connect an emergency stop button to the e-stop circuit in the linear test bed.

The details of each of the new cable runs are shown below in Table 2.1. The raw distance is the physical distance between the two points, and the total distance is the total amount of conductor needed based on whether the run is three-phase AC or DC. For example, the run from MCC1 to the linear test bed will require three conductors, one for each phase, requiring a 295.5 feet of conductor. The other two are DC, which require only two conductors to complete each circuit.

Cable Run	Raw Distance	Total Distance	Voltage (Insulation)	Maximum Current	Wire Size (Copper)
MCC1 to LTB	98.5 ft	295.5 ft	480VAC (600V)	150AAC	1/0 Gauge
MCC1 to LTB (Ground)	98.5 ft	98.5 ft	480VAC (600V)	65AAC	6 Gauge
LTB to Water Rheostat	149 ft	298 ft	900VDC (1000V)	127ADC	1/0 Gauge
Emergency Stop	67 ft	134 ft	24VDC	65mADC	16 Gauge

Table 2.1 MSRF New Conductor Details

2.3.2 DC Bus Regulation

As discussed, when the linear test bed is resisting the device under test's tendency to fall due to gravity during the downstroke the motor will be rotating in the opposite direction than that of the upstroke when it is motoring. The means on the downstoke, power will be generated much like it is in a regenerative braking scheme used in hybrid car design. This problem will be exaggerated when a high power device under test is tested with no load since no generation force is present to resist the fall of the device. Also, a high power device will likely be more massive than a small device which will generate more power due to its large downward force due to gravity. This large force will drive the motor in the opposite direction forcing the linear test bed to have a regenerative capability. This generated power will flow back through the inverter as it is bidirectional and cause the DC bus to charge indefinitely if uncontrolled.

To mitigate this problem, Mundt and Associates will design a control system to regulate the power on the DC bus. This means if excessive power forces the DC bus to charge past 820V, a portion of this power must be dissipated to keep the voltage on the

DC bus as close as possible to 800V. The control system is not elaborate, only a single switching motor brake that is controlled by the motor drive. The brake will simply turn on when the DC bus is greater than or equal to 820V and turn off when the bus is pulled back down to 800V. This switching will be either “on” or “off” and will not be controlled through a PWM type waveform. In order to dissipate this power in the MSRF the water rheostats will be used.

The water rheostats essentially behave as variable resistors. In a room near the MSRF, there are a total of eight water rheostats, four of which will be used for the linear test bed application. Each water rheostat consists of a tank with several square plate conductors extended into the tank as shown below in Figure 2.16. As current is conducted into the plates, it is then conducted from plate to plate through the water, dissipating the electricity as heat and also by generating hydrogen through electrolysis. As the water level increases, the overall resistance decreases as there are more parallel current paths through the water. As the water level decreases, the overall resistance increases as there are fewer parallel paths. Thus, by varying the water level, it is possible to vary the electrical load.

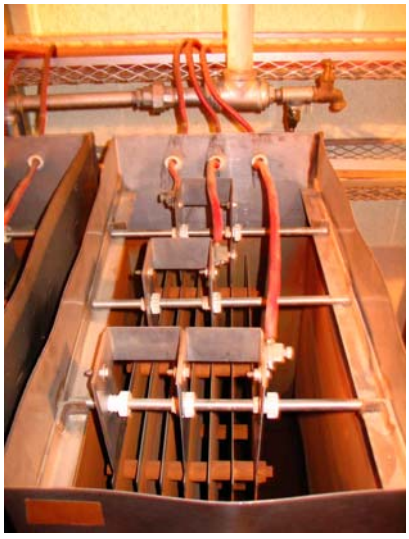

Fig. 2.16 Water Rheostat with Electrical Connections shown

Now that the operation of the water rheostats has been understood, the next step is to understand the challenges of using them in the linear test bed application. The main problem is the water rheostats are typically used as variable loads, used in teaching laboratories to control the load current of a traditional motor-generator sets. In other words, typically the resistance of the water rheostats is not held constant as is necessary in the linear test bed application. The nominal resistance of the resistor that is required by the linear test bed motor drive is six ohms, with an absolute minimum of five ohms. The resistor must be capable of the upper DC bus voltage threshold, or 900VDC. Mundt and Associates has calculated that during an emergency stop, the resistor must be able to handle a maximum power of 97.27 kW from the motor drive in 0.1524 seconds, resulting in a peak current threshold of 127 amps.

The power dissipation requirement causes the second problem of using the water rheostats for this application. Although tests will be required to determine the maximum power dissipation specification per water rheostat, it is clear that one tank will not be able to handle the full 97.27kW. Also, the cabling stretching from the MSRF to the water rheostat room is only rated for 600V and a maximum current of 92 amperes. Consequently, new cabling must be installed and several water rheostats must be connected in parallel to handle the power dissipation requirements.

To address these concerns, new 1/0 cabling with 1000V insulation will be run from the linear test bed located in the MSRF, to another room close by which contains the water rheostats. This length of new cabling has been determined and discussed earlier in this chapter. To ensure that the water rheostats will hold a constant resistance value as required by the linear test bed drive, mechanical float switches will be used to maintain a constant water level. By keeping the water level constant, the resistance will be constant. Since the water temperature inside the water rheostats could be high, thus a high temperature float switch will be used and is shown in Figure 2.17.

Fig. 2.17 CSH Incorporated Float Switch [28]

The float switch is made by CSH Incorporated, Model S-10-UHH, and has a bulb size of 2.5 inches by 3.25 inches and a switch rated for 120V open circuit, and 1A short circuit maximum current. The operation of the float switch is very simple and is purely mechanical which made it desirable for this application. Other approaches use more elaborate methods which use a potential difference between to probes placed in the water. Another option that was considered was an ultrasonic sensor that would be mounted on the top of the tank and would bounce an ultrasonic pulse to the water surface to determine depth. This would output the water depth as an analog signal and would require additional components and a controller to control the water level. The float switch has a weight inside the floating bulb and depending on the bulbs position, the weight moves and opens or closes the switch.

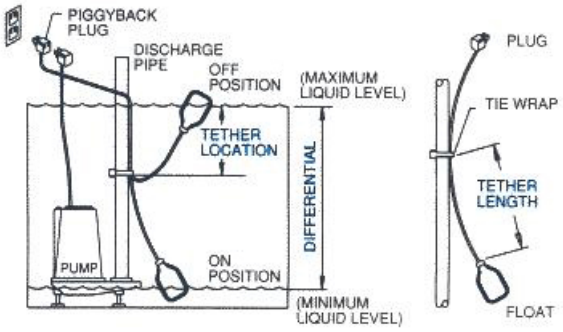

Fig. 2.18 Float Switch Installation Notes [28]

Since these float switches are typically used in large sewer applications, the liquid differential shown in Figure 2.18 is around seven inches to over three feet. Since this large of differential will allow for too much change in resistance, a smaller switch will be used, which will allow for about a two inch differential. This switch can handle one ampere of current maximum, instead of nearly 15 amperes used when direct coupling to the pump is used.

This difference between the water rheostat application and a standard float switch application in the fact that usually the float switch directly connects the pump motor to an electrical supply. This is done using a “piggyback” plug and is shown above in Figure 2.17. However, in the water rheostat application, we need the float switch to only act as a switch. When the water level reaches the “ON” position, the switch closes and shorts the two terminals on the controller and fills the tank. When the water level reaches the “OFF” position, the switch opens and the pump motor no longer receives power to stop the fill. This can be accomplished by simply connecting the switch leads directly to the terminal block, rather than using the “piggyback” plug. Now, the float switch acts the same as the breaker used during testing.

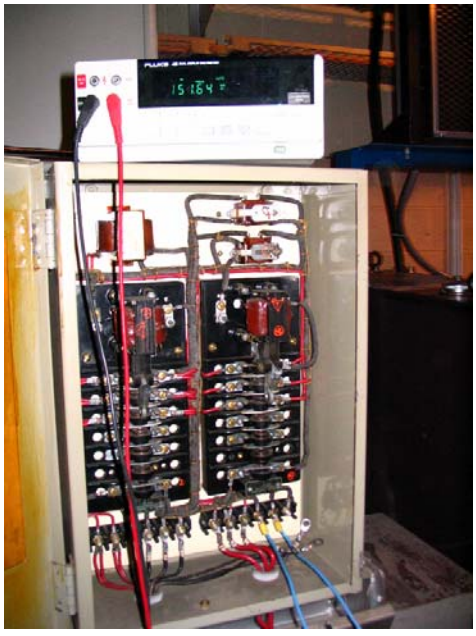

Fig. 2.19 Water Rheostat Controller

In the case of the linear test bed, to fill the tank it is necessary to short two terminals, shown with wire leads connected to them in Figure 2.19, on the water rheostat controller that are normally open. When these terminals are shorted, relays inside the water rheostat controller allow current to be conducted from an external power supply to the pump motor, which fills the tank. Since the float switch will not be used to directly connect the pump to the power supply, the switch current rating can be very low. To verify this, a standard breaker was placed between the two terminals to open and close the contacts. When the switch was opened, there was an open circuit voltage of 120VAC. When the switch was closed, the switch current was only 151mA. Please refer to Figure 2.19 which shows the water rheostat controller, with a breaker connected to the wire leads on the terminal block. Using this information, it was clear the 1A switch in the bulb would work to achieve a smaller differential.

To determine the amount of power that each tank could dissipate, one of the water rheostat tanks was connected to the programmable source located in the MSRF. The programmable source was used to output a variable voltage, variable current, high power waveform. The programmable source outputs AC waveforms, but since only the maximum power limit is desired, we can use the waveforms to dissipate varying power levels in the water tank. The testing results are shown below in Table 2.2, with the voltage, current, and power necessary to boil the water for a given water depth after 15 minutes of testing.

Water Depth (Inches)	Phase Voltage (V)	Current (I)	Total Power (W)
28 (Full)	83	107	26643
18 (Half Full)	100	60	18000
8 (Empty)	300	15	13500

Table 2.2 Water Rheostat Load Testing

From this data it is clear that each tank should be capable of dissipating at least 10kW without boiling water within the first 15 minutes of testing. To add a significant

cushion to ensure that water will not boil after long tests, it will be necessary to determine the amount of power that will need to be dissipated by the water rheostats. To determine the worst case scenario, Mundt and Associates calculated the amount power that the water rheostat would need to dissipate given a device under test with a mass of 1088 kg and no generator load to ease in the power dissipation requirement. The amount of power supplied (and delivered) by the linear test bed motor is shown as a function of time in Figure 2.20 for a 3.63 second period. The points when the motor is regenerating and thus requiring braking resistance is indicated by the negative values for motor power.

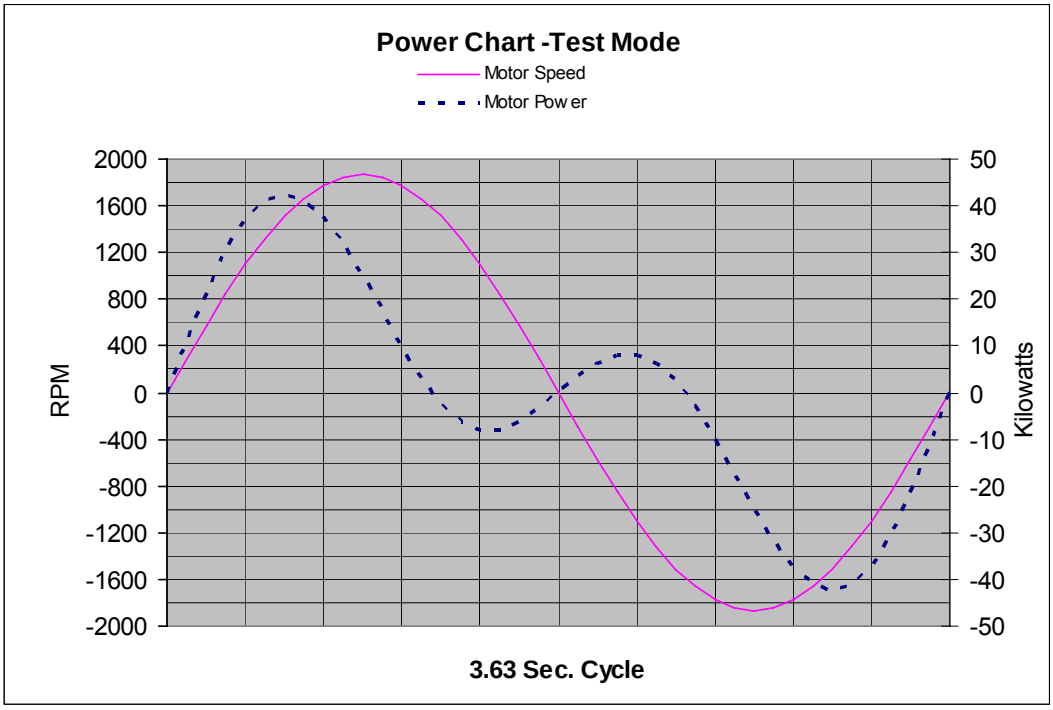

Fig. 2.20 No Load Power Chart

Based on this graph, the peak power dissipation requirement is 45 kW. However, this is only the peak power requirements, and must be converted into average power requirements to properly determine the amount of water tanks needed. Using Maple, a piecewise function was used to integrate only the negative portions of the waveform that indicate power dissipation requirements. Once the integration was performed, the area under the sine wave was known. Consequently, the equivalent average, continuous

power requirement could be determined. This continuous average power dissipation requirement was found to be 10kW. Knowing this, it was decided to use four tanks such that each tank would only need to dissipate 2.5kW, well below the amount of power need to boil water in the tank.

To determine the water level corresponding to a certain resistance, more testing was performed. By using a DC supply to inject a known amount of current into the tank, and measuring the voltage at the tank, the resistance can be computed. By adjusting the water level in the tank this technique produced a relationship between water level and resistance and is shown below in Figure 2.21. The decision was made to use two sets of two tanks set to 6 ohms placed in series, with the two sets at 12 ohms placed in parallel the achieve 6 ohms of braking resistance. This decision was made so that the relationship between resistance and water level was basically linear. As shown in Figure 2.21, at higher resistance values, the relationship is nonlinear.

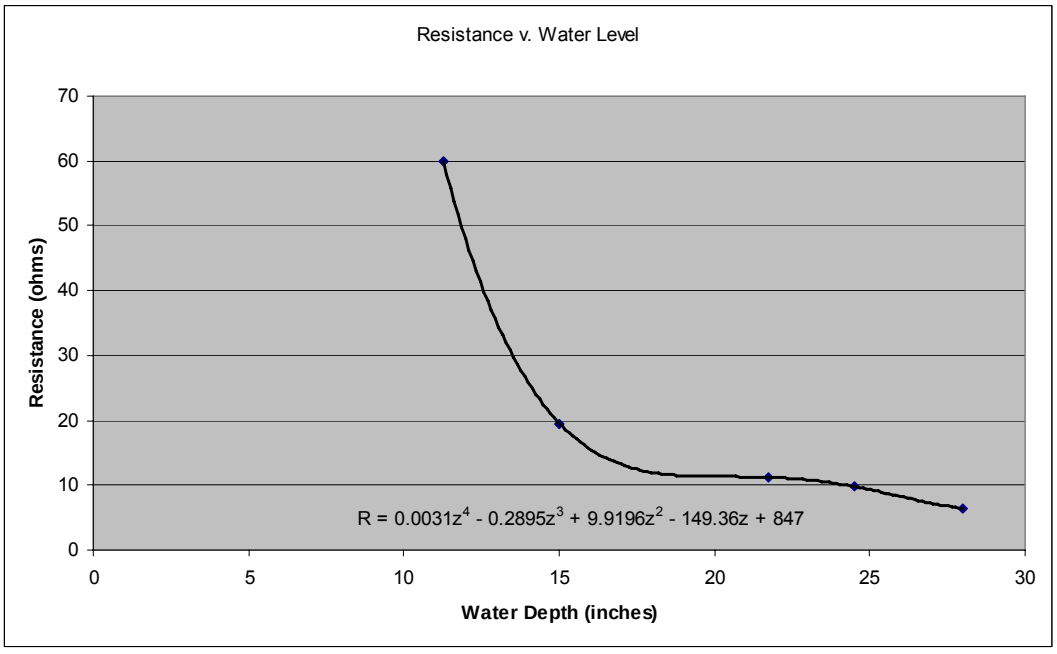

Fig. 2.21 Resistance and a Function of Water Level

Based on this graph, the water level corresponding to 6 ohms can be calculated. This graph is somewhat troubling as it appears the relationship between water depth and

resistance is not linear for all water levels. As a result, it will be necessary to check the resistance of the series and parallel combination of tanks when linear test bed testing is started. However, this graph can still produce a “ballpark” water level that will be close to 6 ohms, especially since the relationship between resistance and water depth at 6 ohms appears to be linear. Based on the equation shown on Figure 2.21, a water level of 26.43 inches should be close to 6 ohms. Again, before testing occurs, the resistance calculations should be checked through experimentation.

3. INPUT/OUTPUT INSTRUMENTATION

3.1 Introduction

The linear test bed will contain a variety of sensors that will be used for data acquisition, safety, and control purposes. This chapter will focus on the routing of signals from these sensors for the purposes of control and data acquisition as the safety features of the linear test bed were discussed in chapter 2. Since the linear test bed is a test device, quantities such as force, position, velocity, and acceleration of the device under test need to be measured to determine performance. Clearly, these quantities will be changing with time and will need to be recorded for analysis during the test and following the test. In the original specification for the linear test bed, Oregon State requested that pertinent data be stored at a rate of one millisecond, or 1000 samples per second. Additionally, some of the sensors will be used for control proposes, specifically for implementing the force control algorithm briefly discussed in chapter 2.

The data acquisition and signal processing necessary for closing the force loop will be performed using a rapid prototyper (RP) digital signal processor (DSP) and/or field programmable gate array (FPGA) board. The selection of this board will be discussed in this chapter. The rapid prototyping system must be capable of recording data at one millisecond as required by the original linear test bed specification. In addition, the rapid prototyper has to have the capability to process and manipulate the load cell signals, required so that force on the device under test can be used as a feedback variable in the force control algorithm. Since the load cells are mounted on the diagonal of the linear test bed suspension, it will be necessary to perform trigonometric calculations on the fly to compute the vertical force applied to the device under test by the linear test bed. Finally, the rapid prototyper will need to have the capability to implement the force control algorithm itself by programming the necessary controller transfer functions into the selected device.

3.2 Data Acquisition Considerations

As a test device, one of the primary considerations when designing the linear test bed was data acquisition or data gathering. In order to properly characterize an OWEC, data must be stored very quickly to capture performance characteristics such as cogging force present in OWECs containing linear generators. As the design of the linear test bed evolved, many different approaches were taken when addressing the issue of data gathering. The Delta Tau Turbo PMAC PCI, which will be used for position control, was first considered the best fit for data acquisition for the linear test bed.

In the Delta Tau, data can be gathered and transferred to a host computer in real time using dual port RAM (DPRAM) located on the Delta Tau. Dual ported RAM can be accessed by both the Delta Tau and the host computer. Another means of data gathering utilizes regular RAM on the Delta Tau and is typically used when creating plots in the Delta Tau software suite. However, regular RAM can only be read by the Delta Tau and therefore has a small usable memory size. Since a linear test bed test could last for several hours or even several days, pertinent data needs to be transferred to the host computer using the DPRAM option in order to not quickly fill up memory on the Delta Tau. By manipulating Delta Tau system variables, the data to be gathered and speed of data gathering can be controlled. The DPRAM data gather buffer must be sized based on the number and length of the data sources. However, the size cannot be greater than 2500 samples for the 8Kx16 of DPRAM available.

This limitation in buffer size was the first problem with using the Delta Tau for data acquisition. Since data will be stored every one millisecond and had a maximum capacity of 2500 samples, this would be filled quickly. However, if the host computer was able to read the values fast enough, a rotary buffer could be used overwrite old values already read by the host with new values. However, another complication with the Delta Tau is Windows is not setup to read DPRAM. It would be necessary to find a Windows programmer to design a piece of software that would read the data values from the DPRAM and store them in a .txt file on the host PC. Additionally, the Delta Tau cannot easily manipulate gathered data so conversion to actual units would happen after a

test was complete. For example, the load cell data is output using a 4-20 mA current that is proportional to the force on the device under test. The Delta Tau would store the 4-20 mA current information and not the data converted to engineering units of force such as Newtons or pounds-force. Because of these complications, it was determined by Oregon State University and Mundt and Associates that the Delta Tau would not be used for data acquisition.

As an alternative, a rapid prototyping (RP) system was suggested as it would be possible to implement the force control algorithm and perform some control operations as well as handle any data acquisition needs. Three RP system companies were considered for the linear test bed application, including Opal-RT, dSpace, and National Instruments. After considering the cost benefit of RP systems made by these three companies it was clear that Opal-RT did not provide enough additional benefits over the other two companies to account for increased cost of an Opal-RT system. The second company, dSpace, had the capability to implement the force control algorithm using a very flexible interface in Matlab Simulink. However, it could not meet our needs when it came to data gathering. The dSpace module is designed to capture data quickly for short amounts of time. It was not capable of recording data for hours, day, and even weeks efficiently. This made National Instruments the most feasible solution for the linear test bed application, as it was able to handle the data acquisition requirement and has a fast enough response time to implement the force algorithm using the on-board FPGA.

The CompactRIO, made by National Instruments, shown below in Figure 3.1, was determined to be the most cost effective, best-fit solution for the linear test bed. With data gathering potentials up to 250 kS/s for the standard analog inputs and 200 kS/s for the current mode analog inputs, the original specification of sampling data at 1 kS/s would be easily met. Using a compatible analog output, the update time for these outputs is between 3 and 9.5 microseconds, depending on the channels in use. The Delta Tau has a default servo cycle speed of 442 microseconds so the output module looks to be able to provide input to the Delta Tau as fast as its servo cycle. The input and output modules of CompactRIO will be discussed in detail in section 3.4, 3.5, and 3.6.

Fig. 3.1 National Instruments, CompactRIO [9]

From a controls perspective, the CompactRIO has an onboard FPGA that has an array of built in functions for analog closed loop PID control, filters, look-up tables, and many others. It is possible to design custom control and acquisition circuitry using the FPGA with a 25 nanosecond triggering resolution. According to National Instruments, it is possible to implement analog PID control systems at loop rates exceeding 100 kS/s. The FPGA can be programmed in a National Instruments development environment called LabVIEW. This is a graphical programming environment, similar to Matlab Simulink, although not quite as flexible. The CompactRIO also features a real time, 200 MHz Pentium processor that can also be programmed in LabVIEW. The real time processor is used for less time critical tasks such as data acquisition. Additionally, all National Instruments software is made available to Oregon State University students and faculty. Overall, the CompactRIO provided the overall best solution to the data acquisition requirements and additional control requirements of the linear test bed [9].

The specific setup for the linear test bed will consist of the CompactRIO cRIO-9012 with a real time processor at 400 MHz, and 64 MB of DRAM. For I/O considerations there will be four accessories connected to the CompactRIO to handle analog and digital I/O for the linear test bed. The CompactRIO and accessory cards will be connected to the linear test bed host computer using Ethernet. Figure 3.2 provides

illustration as to how it will be connected to the host computer and how the CompactRIO handles various tasks.

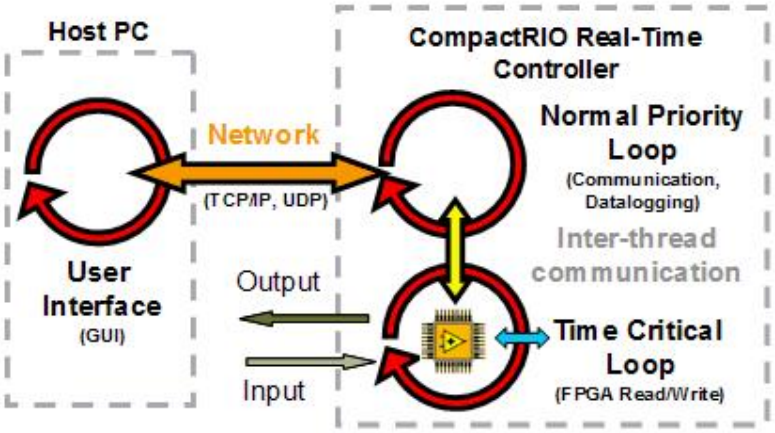

Fig. 3.2 CompactRIO Signal Flow [9]

3.3 Signal Routing and Wiring Diagrams

To better understand how various signals measuring force on the DUT, DUT position, velocity, and acceleration are input to the CompactRIO please refer to the Figure 3.3. This diagram shows how the linear test bed components will be connected in the MSRF and also how the data signals are routed. The velocity and acceleration of the DUT is measured by the motor drive and output via digital to analog converters (DAC). These signals are then read by the CompactRIO using analog to digital converters (ADC). Likewise, the force on the DUT is measured by the load cell and output as an analog signal and read by the CompactRIO. Finally, the position of the DUT in the linear test bed will be output through a DAC in the Delta Tau and read by the CompactRIO.

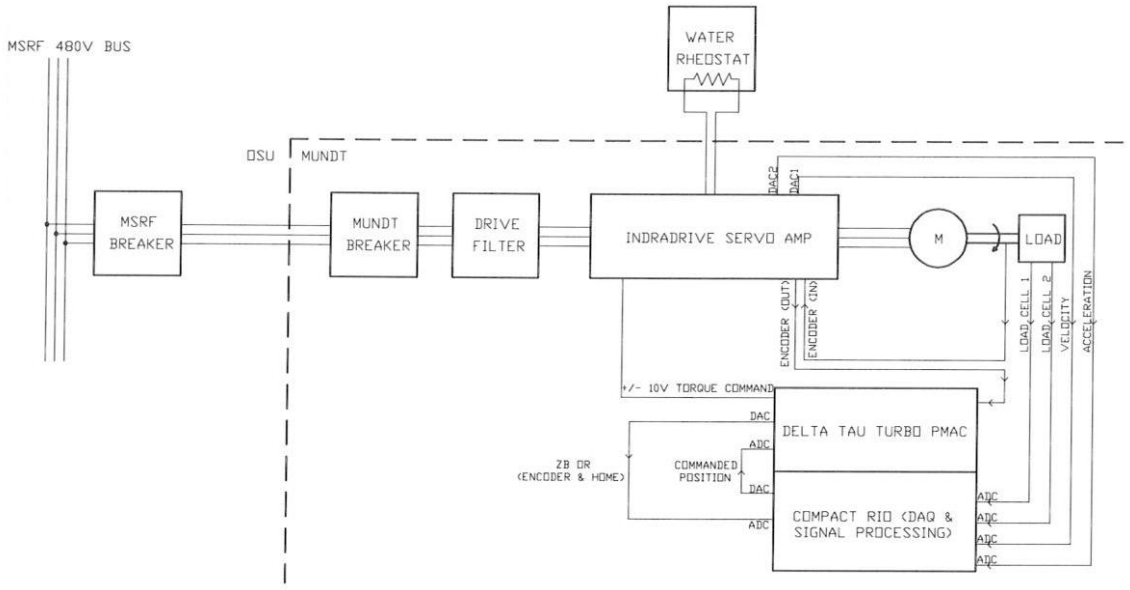

Fig. 3.3 Linear Test Bed Signal Routing

Additionally, the CompactRIO will output either a commanded position or a commanded force via a digital to analog converter. It will depend on whether the force loop is closed using the CompactRIO or the Delta Tau. Initially, the force loop will be closed using the CompactRIO but it will still be possible to allow the Delta Tau controller to close the force loop. The reason for allowing the CompactRIO to close the force loop initially is while the linear test bed is manufactured, it will be possible to simultaneously design the force control loop and the position control loop. Oregon State engineers will be focused on the force loop and will have the CompactRIO to implement the design, and Mundt Engineers will have the Delta Tau to implement position control. Once the linear test bed is installed in the MSRF, the integration between the two systems will be possible.

However, in the future it may be desired to have the Delta Tau controller close the force loop. There are a few changes in the signal routing that will be necessary if the Delta Tau will close the force loop and they are shown below in Figure 3.4. Here, the CompactRIO must output two signals, both the commanded force and the actual force measured by the load cells. The actual force will be measured by the load cells and conditioned by the CompactRIO. The commanded force will be generated using a

program on the CompactRIO based on hydrodynamic equations. In order to achieve the flexibility described in the previous paragraphs, the necessary signals will be routed to a terminal block so wiring changes can be made with ease.

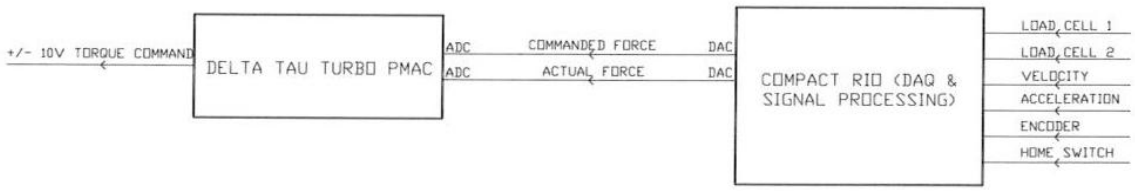

Fig. 3.4 Linear Test Bed Signal Routing Alterations

This terminal block will be located inside the electrical control cabinet relatively close to both the Delta Tau controller and the CompactRIO. As discussed, CompactRIO will contain four modules used to send and receive various signals. The NI9205 will contain ADCs to handle analog inputs, the NI9263 will contain DAC converters to handle analog outputs, and the NI9401 will handle all digital I/O. The NI9203 will be used to handle analog inputs in the form of 4-20mA current signals. This is necessary to input the load cell signals which will be output as a 4-20mA signal proportional to force. A current signal is used to minimize noise on the line as the signal will be transmitted from the loads cells located at the top the machine to the electrical control cabinet at the bottom of the machine. The wiring diagram illustrating the connections from the terminal block to the CompactRIO is shown below in Figure 3.5. The details of each signal will be discussed in detail in sections 3.4, 3.5 and 3.6.

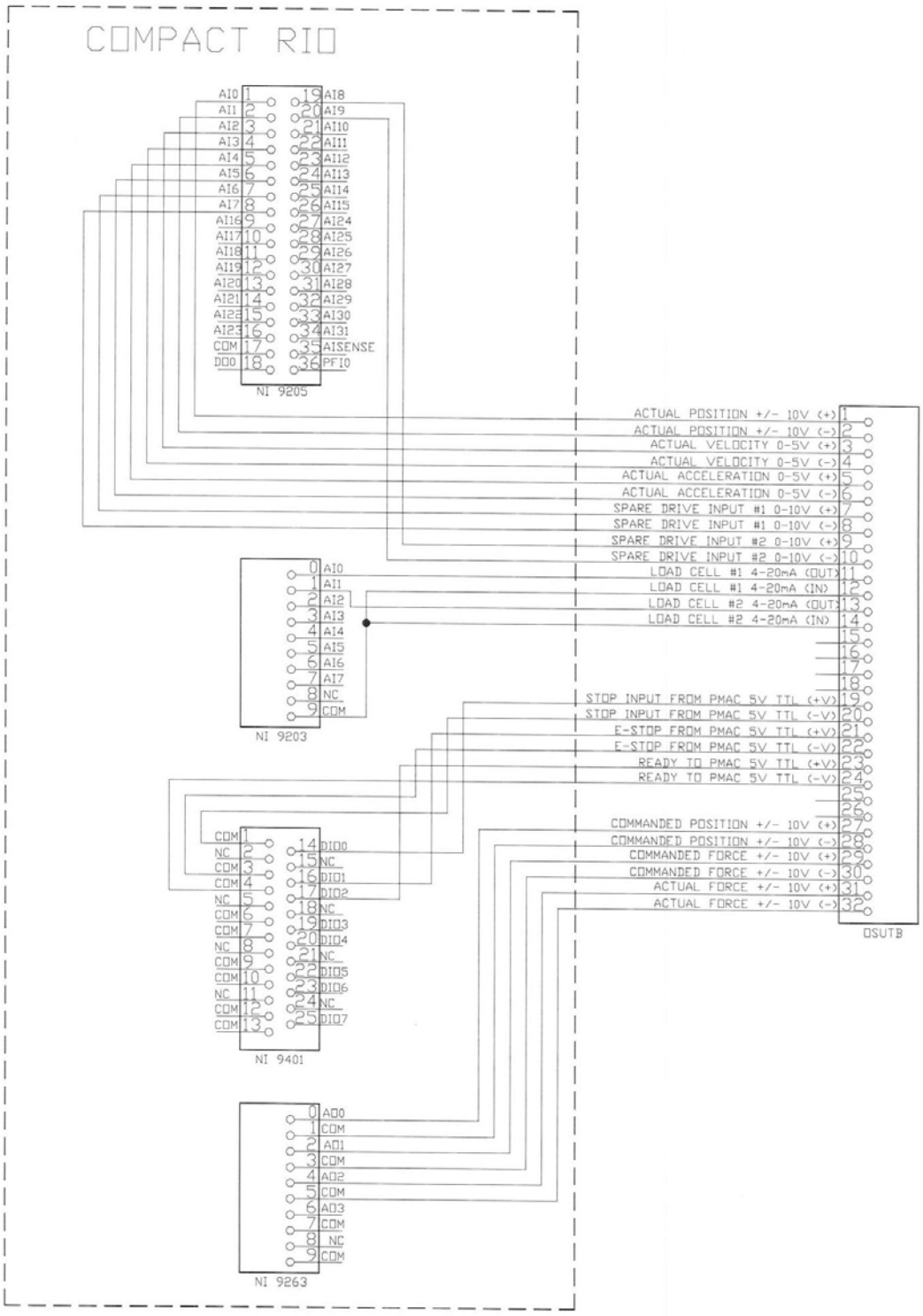

Fig. 3.6 Compact Rio Wiring Diagram

3.4 LTB Control Inputs and Instrumentation

As shown above in Figure 3.4, the CompactRIO will need several inputs to compute the force command and correctly implement the force algorithm. These inputs will be supplied from the linear test bed motor drive, the Delta Tau, and the load cells. The motor drive has the capability to output motor speed and acceleration that through the drive ratio can be converted to linear speed and acceleration. The Delta Tau can output exact position which is necessary to compute the commanded force and close the position control loop which will reside inside the force control loop. The load cells are needed to measure the actual force on the DUT, which is used as reference for the force control loop.

All analog inputs to the CompactRIO will be read by NI 9205 except for the load cell output, which will be read by an input current module. The NI 9205 has a sampling rate of 250 kS/s, with nominal input voltages of +/- 10V at 16 bits of resolution. The NI 9205, shown below in Figure 3.6, is capable of reading 32 single ended inputs or 16 differential inputs. The 9205 with two input connectors; spring terminal, to be used the linear test bed, and a D-sub connector. Each channel also has +/- 30V of overvoltage protection [10].

Fig. 3.6 NI 9205 Analog Input Module [10]

3.4.1 DUT Position, Velocity, and Acceleration

In order for the control system to work properly, position must be fed back to the Delta Tau to close the position loop and to the CompactRIO to close the force loop. In the force loop, position is used to calculate the commanded force based on hydrodynamic equations. Since the Delta Tau will have encoder feedback, absolute position will be known based on the encoder feedback, home switch, and gear ratio. Since the Delta Tau PMAC controller is capable of controlling several motors, and only one motor will be controlled in the linear test bed application, three remaining digital to analog converters will be available. On the Turbo PMAC, there are four DACs on the control board itself with additional DACs available via accessory add-ons. One will be used to send the torque command to the motor drive, leaving three unused. These DACs have output voltage capabilities of +/- 10 volts with 16 bit resolution. One of the three unused DACs on the Delta Tau will be used to output the absolute position as seen by the Delta Tau.

When an OWEC is tested in the linear test bed, the velocity and acceleration of the OWEC under test will be needed to properly characterize the device. Both of these qualities will be measured based on the velocity and acceleration of the motor shaft as measured by the linear test bed motor drive. The motor drive used will be a Rexroth IndraDrive C Drive Controller, which has two DACs standard. These are capable of outputting numerous quantities, but for the linear test bed will be outputting motor speed and acceleration. These DACs have output voltage capabilities of 0-5V, at an output current of 0-1mA at a resolution of 8 bits. They also have short circuit and overload protection. As we will see later in section 3.4.3, additional DACs are available via accessory MA1, and can either replace or supplement the standard DACs.

3.4.2 Measured Force on Device under Test

Two load cells manufactured by Interface Force will be used to measure the force applied to the device under test by the linear test bed. Since the linear test bed will be testing various OWECs capable of generating anywhere from 50 watts to 10 kW, several interchangeable load cells will be used to accurately measure the force applied to the OWEC. This is needed because as the OWEC under test changes, so does the mass of

the OWEC and the generator force. This forces the linear test bed to use more force to lift and oppose generator force of a large OWEC compared to that of a small OWEC. Since force will be used as a feedback variable in the control system, accuracy is paramount. For example, a load cell capable of measuring 25 kN of driving force will not accurately measure 5 kN.

To compensate for this problem, three pairs of load cells will be used to measure the various ranges of driving force. Specifically, the three pairs of load cells that will be used have a maximum readable force of 1.25 kN, 5kN, and 25kN. The Interface Force model number is 1010 and is shown below in Figure 3.7. The output signal from this loads cells is a 1mV/V signal level voltage that is proportional to force. Clearly, this signal cannot be transmitted far with becoming extremely distorted by noise.

Fig. 3.7 Interface Force 1010 Load Cell [29]

The output of the load cell will be input to a signal conditioning module also manufactured by Interface Force as is shown below in Figure 3.8. The signal conditioner will then output a 4-20mA current that can be read by the CompactRIO. The 4-20mA current is proportional to the force measured by each load cell. The reason that the signal will be transmitted as a current rather than a voltage is noise immunity. The signal must be transmitted from the suspension towers to the CompactRIO located in the electrical cabinet. The CompactRIO uses an accessory called NI9203, shown below in Figure 3.9, which is an eight channel, 16 bit, analog input module capable of reading current signals

ranging from either 0-20 mA or +/- 20 mA. The module also includes a double isolation barrier for safety and noise immunity. Additionally, the module has a sampling rate of 200 kS/s. Once the currents have been read by the CompactRIO some conditioning of these signals is necessary to determine the actual force applied to the DUT [11].

Fig. 3.8 Interface Force Signal Conditioner [29]

Fig. 3.9 NI 9203 Analog Current Input [11]

Firstly, the two load cells located in the suspension towers combined measure the total force proportional to both the mass hanging off these load cells and the carriage acceleration. An offset will be used to ensure that the force due to gravity of the hanging mass is not measured by the load cell. As a result, the load cells will read zero when the DUT is centered in the middle of the linear test bed travel range. This accurately simulates the fact that the DUT would be neutrally buoyant in calm water. Now, the load cells will only read the force proportional to the mass hanging off these load cells and the carriage acceleration.

However, since the load cells are not mounted vertically on the suspension arms as shown in Figure 2.13, the measured force will not be only the vertical force. To account for this some trigonometry will be needed to determine the total vertical force applied by the linear test bed. The reason it is critical to measure only the vertical driving force is that this vertical force is the primary driving force in the ocean. Starting with the raw load cell signals coming into the CompactRIO is essential to understand how these signals will be processed to determine the actual vertical force applied to the DUT.

First, the force measured by each load cell must be converted into real units from the 4-20mA current that is proportional to force that is output from the signal conditioner. Second, since the load cells do not measure only vertical force as discussed, the vertical force must be calculated based on the geometry of each suspension arm.

$$F_{vert,1} = F_{LC,1} \cdot \sin\theta \qquad (3.1)$$

$$F_{vert,2} = F_{LC,2} \cdot \sin\theta \qquad (3.2)$$

The angle is determined from the geometry of the suspension arms. Once the vertical forces have been calculated, the two vertical forces measured by each load cell must be summed to calculate the total vertical driving force.

$$F_{Total} = F_{vert,1} + F_{vert,2} \qquad (3.3)$$

Now, it is important to note the vertical force calculated up to this point is exerted on both the DUT and also the mass of the carriage hanging from the load cells. This force that is exerted on the hanging carriage mass must be subtracted to calculate the vertical driving force applied to the DUT.

$$F_{Total} = F_{car} + F_{DUT} = m_{car} \cdot a_{car} + m_{DUT} \cdot a_{car} \quad (3.4)$$

$$F_{DUT} = F_{Total} - (m_{car} \cdot a_{car}) \quad (3.5)$$

From Equation 3.5 it is clear that the force on the carriage that must be subtracted is proportional to carriage acceleration which is always changing. Therefore, the mass of the carriage seen by the load cells is constant and can be determined a priori but the carriage acceleration must be monitored continuously to compute the force on the carriage correctly. This can be done by reading the carriage acceleration from the drive and computing the force on the DUT from Equation 3.5 every update cycle. The force on the DUT will need to be updated continuously as it will always be changing based on load cell readings, generator loading, and carriage acceleration.

3.4.3 Additional Drive I/O Capabilities

Besides the analog input and analog output capabilities of the drive already discussed, it is possible to increase the amount of analog I/O for the drive. This is accomplished by adding analog I/O extension MA1 from Rexroth. With this accessory it is possible to add two analog inputs and two analog outputs. The inputs are dual channel differential analog inputs with a voltage range of +/- 10V with a resolution of 12 bits. The outputs are also dual channel, +/- 10V again with a resolution of 12 bits. The connection point to this accessory is a 15-pin, D-sub connector with a distribution box available from Phoenix Contact shown below in Figure 3.10.

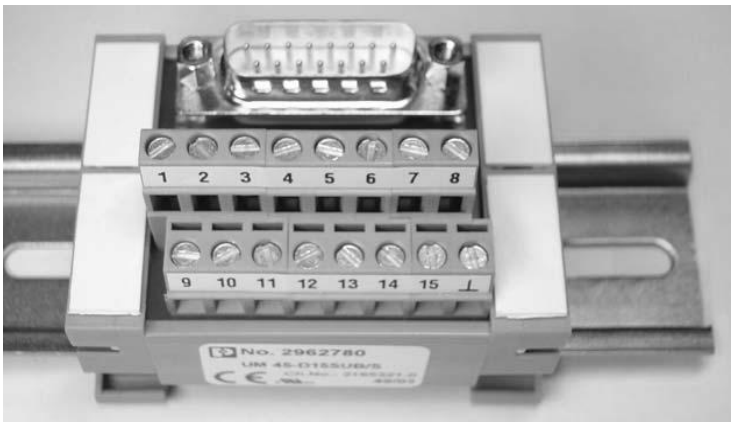

Fig. 3.10 Phoenix Contact Breakout Board

3.5 LTB Control Outputs and Instrumentation

As shown above in Figure 3.4, the CompactRIO must output at least one control signal for the force control algorithm to work properly. Since initially the Delta Tau will close the position loop, the CompactRIO must output a position command from the force algorithm to the Delta Tau. As discussed, in the future the Delta Tau could close the force loop. In this case, the CompactRIO will be used only for signal conditioning and data acquisition. It will output the actual force on the DUT calculated using the steps in section 3.4.2 and the force command based on a Patel's hydrodynamic equations [8] and an input wave profile. These outputs and the instrumentation used will be discussed briefly.

All control outputs discussed above produced by the CompactRIO will need to be read by the Delta Tau to initiate motion of the linear test bed. These outputs will be read by the Delta Tau using Delta Tau accessory ACC-28A. This four channel extension board contains four analog to digital converters (ADC). The ADCs are capable of handling input voltages between +/- 10V. The voltages are then converted to 16 bit signed values at 18 kHz, or in other words have a 55 microsecond conversion time.

3.5.1 Commanded DUT Position

Initially, the commanded DUT position can be read from two locations. If the linear test operates in position control mode, the position command is read directly from a file containing position versus time data. If it is operating in force control mode, the position command will be generated as the output of the force control algorithm implemented on the CompactRIO. This position command will be outputted from the CompactRIO as an analog voltage using the digital to analog converters (DAC) located on a National Instruments accessory board NI 9263. The four channel board is shown below in Figure 3.11 and has output voltage capability of +/- 10V and 16 bit resolution. The update time for the analog out signal is dependent on the number of channels used. If one channel is used, the update time can be as fast as 3 microseconds. If all four are used, the update time slows to 9.5 microseconds. However, in either case this update

time is significantly faster than the Delta Tau servo cycle speed of 442 microseconds. Each DAC on the board is electrically isolated with overvoltage and short circuit protection [12].

Fig. 3.11 NI 9263 Analog out Board [12]

3.5.2 Commanded DUT Force

Initially, the CompactRIO will calculate the commanded force as part of the force control algorithm and will use it directly as the CompactRIO will be used to close the force control loop. In the future, if it is determined that closing the force loop with the Delta Tau could result in a drastic increase in performance; the force command must be output. If this is the case, the force command will still be calculated in the CompactRIO using Patel's hydrodynamic equations and some input wave profile. The exact calculation of this commanded force will be discussed in chapter 5. The force command would then be outputted from the CompactRIO as an analog voltage using the NI 9263. This would allow the Delta Tau to close the force loop and still allow the CompactRIO to perform the hydrodynamic calculations. Additionally, if the Delta Tau was used to close the force loop, the CompactRIO would also have to output the actual force on the DUT.

3.5.3 Commanded DUT Force

As discussed in section 3.4.2, the load cells will be used to determine the actual force on the DUT. Initially, this force will be used directly be the force control algorithm housed in the CompactRIO and will not need to be output to the Delta Tau. However, if the Delta Tau closes the force loop in the future, both the commanded force and actual force will need to be output. If this is the case, the actual force will be calculated using the steps described in section 3.4.2, and output as an analog voltage to the Delta Tau using the NI 9263. To review, initially the only control output from the CompactRIO will be commanded position. However, if in the future a decision is made to use the Delta Tau to close the force loop, both commanded force and actual force will need to be output to the Delta Tau. Obviously in the latter case, the commanded position output is no longer used.

3.6 LTB Digital Input/Output

Digital communication between the CompactRIO and the Delta Tau will be limited to a total of three digital signals, two inputs to the CompactRIO and one output to the Delta Tau. The first input to the CompactRIO is called the stop input and is necessary to tell the CompactRIO that an over-travel limit switch has been tripped and a controlled stop will occur. The second input is called the emergency stop input and is used to tell the CompactRIO an emergency stop has occurred. If the CompactRIO detects either stop condition, either the position or force (depending on control mode) commands to the Delta Tau should be halted immediately. Additionally, the output voltage proportional to either command should be set to zero. This is necessary because if the Delta Tau receives a nonzero input at startup from the CompactRIO corresponding to a position command high in the range of travel, unsafe machine jerk or motor acceleration could occur. A digital output from the CompactRIO to the Delta Tau called ready enable will be used to let the Delta Tau know the CompactRIO is ready to start sending commands.

Fig. 3.12 NI 9401 Digital I/O Board [13]

All digital I/O that will be routed using the CompactRIO is done with an accessory board called the NI 9401, shown in Figure 3.12. This is a 5V TTL, eight channel board grouped into two ports, one port for lines 0-3 and one port for lines 4-7. All four channels in each port are capable of being configured as either digital inputs or digital outputs. However, all four channels in each port must be either inputs or outputs. Port specification of either input or output is done in software. The linear test bed application will use one port as inputs and one port as outputs for a total of 4 digital inputs and 4 digital outputs. The digital inputs have an input high of 2-5.25V max and input low of 0-0.8V. The digital outputs have an output high of 4.3-5.25V and output low of 0.1-0.4V. This card can be connected using a 25-pin D-sub connector if desired [13].

For digital I/O the Delta Tau uses the JOPTO port on the Turbo PMAC itself. The port is not optically isolated but can be connected to the Opto-22 easily as will be done in the linear test bed. The JOPTO port has 8 general purpose digital inputs and 8 general purpose digital outputs. The inputs and outputs are fixed, meaning it is not possible to have 16 inputs and 0 outputs for example. The inputs are described as 24V tolerant 5V logic; with a switching limit around 2-3 volts. The E7 jumper should connect

pins two and three for the inputs to be biased to ground for OFF condition and pulled high for ON. The outputs are set by default to sink current and will be changed to source current by substituting an IC which will be done by Mundt and Associates. The outputs can then be configured individually by removing the internal pull-up resistor and connecting an external pull-up resistor to achieve the desired voltage [14].

4. CONTROL OF THE LINEAR TEST BED

4.1 Introduction

The control of the linear test bed has been an important part of the design dating back to when the first Oregon State University design specifications were written. The control system of the linear test bed governs the motion of the machine and thus how accurately it reproduces the motion of an actual wave profile or a given position profile. The control of the linear test bed can be broken into two main categories, namely position control and force control. When the linear test bed is used in position control, the carriage moves the active float components from point to point along the z-axis. These point to point moves can be implemented in a variety of ways which will be discussed in the following section. Conversely, when the linear test bed is used in force control, a limited and specified force is applied to the carriage. It is this force applied, that accelerates the carriage up and down along the z-axis. This specified force command is calculated using actual wave profile data obtained from observation data buoys and the proposed geometry of the buoy which will hold the active components of the OWEC to be tested.

The control of the linear test bed will be implemented in two stages. Since the machine is being designed by Mundt and Associates, the implementation of the position control will be done at its headquarters in Phoenix, Arizona. Mundt and Associates will exclusively implement the position control system using a Delta Tau Turbo PMAC PCI motion controller. They are very familiar with using the Delta Tau to close position loops and have done so in many previous jobs. The force control system will be almost exclusively implemented by Oregon State University because of its expertise in modeling the interaction between the ocean wave and the OWEC. The force control system will be implemented using a National Instruments CompactRIO and will be discussed in detail in chapter 5. Included in the remainder of this chapter will be an overview of the position control system including all of the preexisting position control modes of operation.

An extensive discussion of position control using Delta Tau is also presented in this chapter. It may become necessary later in the life of the linear test bed to change the PID loop gains of the position loop. This may be necessary when testing various sizes of OWECs since the target device test range encompasses OWECs capable of generating 10kW to less than 50 W. Since position control will be used extensively when testing any OWEC it becomes vital to understand the implementation of position control using a Delta Tau controller.

4.2 Preexisting Position Control Modes

As discussed in the previous section, Oregon State specified several position control modes to command the motion of the carriage along the z-axis. These modes include position versus time input, continuous programmable position control, point to point position control with fixed velocity, and joy stick mode position control. Position versus time control means the data that will govern the z-axis motion of the carriage will be read directly by the Delta Tau controller. The position versus time data points will provide a new commanded vertical position every one millisecond for ten minutes of data. This means that the Delta Tau will be responsible to reading nearly 600,000 data points.

The second means of position control is called continuous programmable position control. In this mode, the linear test bed position will be governed by a trigonometric function. For example, it will allow the motion to be controlled using a sine wave with a specific amplitude and frequency. The reason this mode of position control is desirable is because the simplest approximation of a wave profile is a basic sine wave with a period around eight seconds with amplitude of several meters depending on wave conditions. With this mode of control it would also be simple to simulate naturally occurring higher order harmonics by including additional sine wave components with periods corresponding to the harmonics in question. In this case the equation governing the motion could be in the form of Equation 4.1 below.

$$Z_B = A\sin(wt) + B\sin(2wt) + C\sin(4wt) \qquad (4.1)$$

The third means of position control is called point to point position control with fixed velocity. Under this type of position control the linear test bed would maintain a constant velocity during the up and down strokes after the initial acceleration and before the deceleration. This will be done by establishing a target velocity resulting in velocity ramp commands. When characterizing a device under test, testing the device at constant velocities is often desired. For example, the voltage output of a linear generator is proportional to speed so it could be desired to test the generator at a variety of constant speeds to see how the voltage output behaves.

The fourth means of position control, called joy stick mode, is needed only to correctly place the device under test in the linear test bed. The active float components of the OWEC under test will need to be secured to the linear test bed carriage. Joy stick mode will allow researchers to move the carriage slowly and safely to facilitate the fastening of the device under test to the carriage. When the linear test bed is operated in this mode, the drive will jog the motor slowly to minimize the risk of injury during the setup and installation of the device under test.

4.3 Motion Control using Delta Tau

Delta Tau manufactures a variety of motion controllers capable of controlling many motors simultaneously using a variety of closed loop control methods. The controller used in the linear test bed is called a Turbo PMAC PCI. The controller resides on a single board with a block diagram shown below in Figure 4.1. PMAC stands for programmable multi-axis controller. Turbo is a designation used by Delta Tau which refers to the extended capability of the Motorola digital signal processor (DSP) used in the controller. The standard PMAC uses a slower DSP which can handle fewer motors, coordinate systems, and axes of control. PCI refers to the way the controller can communicate with a host computer, in this case the PCI bus. The host computer can be used to interface to the PMAC for the purposes of downloading motion programs, capturing data, and other purposes. However, the entire Delta Tau family can be used as a stand alone controller once a motion program is downloaded to the DSP [15].

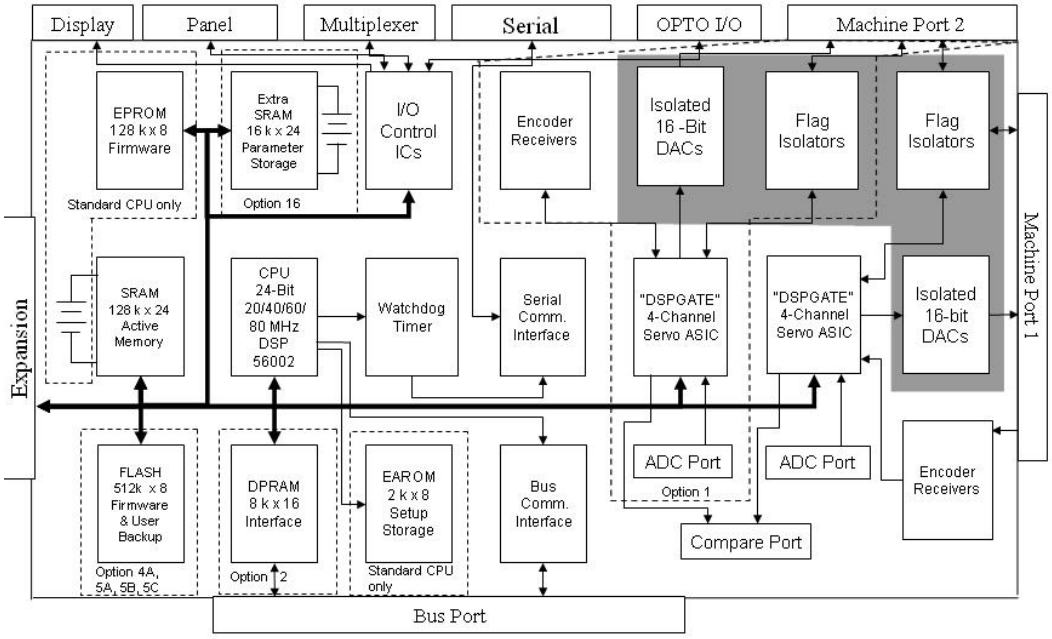

Fig. 4.1 PMAC Block Diagram [15]

Any Delta Tau controller includes a software package called the PMAC Executive Pro2 Suite. The host computer uses the software included in this package to communicate with the controller, either by Ethernet, USB, or PCI bus. Using the editor in the Pro2 Suite allows the user to develop motion programs and PLC programs, which will be discussed in detail. PMAC Plot2 allows the user to create motion trajectory plots or plot any memory registry information including motor speed and acceleration. PMAC Tuning Pro2 can be used to optimize gain parameters for maximum allowable system bandwidth and settling time for the PID algorithm. Setup Pro2 is a tool that can be used to configure any Delta Tau motion controller with any kind of motor. These tools will become important when understanding how to program the Delta Tau to handle force feedback if desired.

There are many benefits of using a Delta Tau controller in motion control applications and understanding them will illustrate why this controller was selected for use in the linear test bed. The built in capability of the PID algorithm allows the user to quickly implement a closed loop position control system by using the Tuning Pro2

software. Several advanced features are also convenient for the linear test bed such as backlash compensation, acceleration and jerk control, and cascaded servo loops. Cascaded servo loops enable the implementation of a force control loop and will be discussed in chapter 5. To understand how the Turbo PMAC will be used in the linear test bed as designed by Mundt and Associates, we will first look at how variables are defined in the Turbo PMAC, consider how the position feedback system functions, and how the servo PID algorithm is tuned to enable accurate position feedback. Next, an overview of coordinate system definition, motion programs, and PLC programs will be presented.

Delta Tau defined four different types of variables based on how they are used by the controller. I-Variables are defined by Delta Tau and are used for general setup and editing motor specific variables such as jog speed. They can be used to activate different motors; set position, speed, and acceleration limits on each motor. P-Variables are global, user defined variables that are typically used in motion programs and PLC programs. Q-variables are not global and are coordinate system specific, and are also user defined for use in motion control programs and PLC programs. M-variables are used to access PMAC memory and I/O ports. Delta Tau has a listed of suggested M-variable definitions that are used by most end users as a starting point of how to assign these variables. Understanding variable definitions will be important when designing motion programs, reading input and output, setting up feedback loops and other tasks necessary to control the linear test bed.

4.4 Position Control

In order to understand how the PMAC controller will be used in the linear test bed application, please refer to Figure 4.2 below, which describes the evolution of the controller/motor drive interface. This figure only describes the position control method that will be implemented by Mundt and Associates. The input to this system is a commanded position, which is usually a linear position command defined by encoder counts and the mechanical system. This is compared to actual position based on the

encoder count measurement and then converted to linear position using the mechanical design of the machine. This position error is controlled and forced to be as close to zero as possible by a PID loop. From here, there are multiple ways to achieve a closed loop system based on the type of motor drive used in the system.

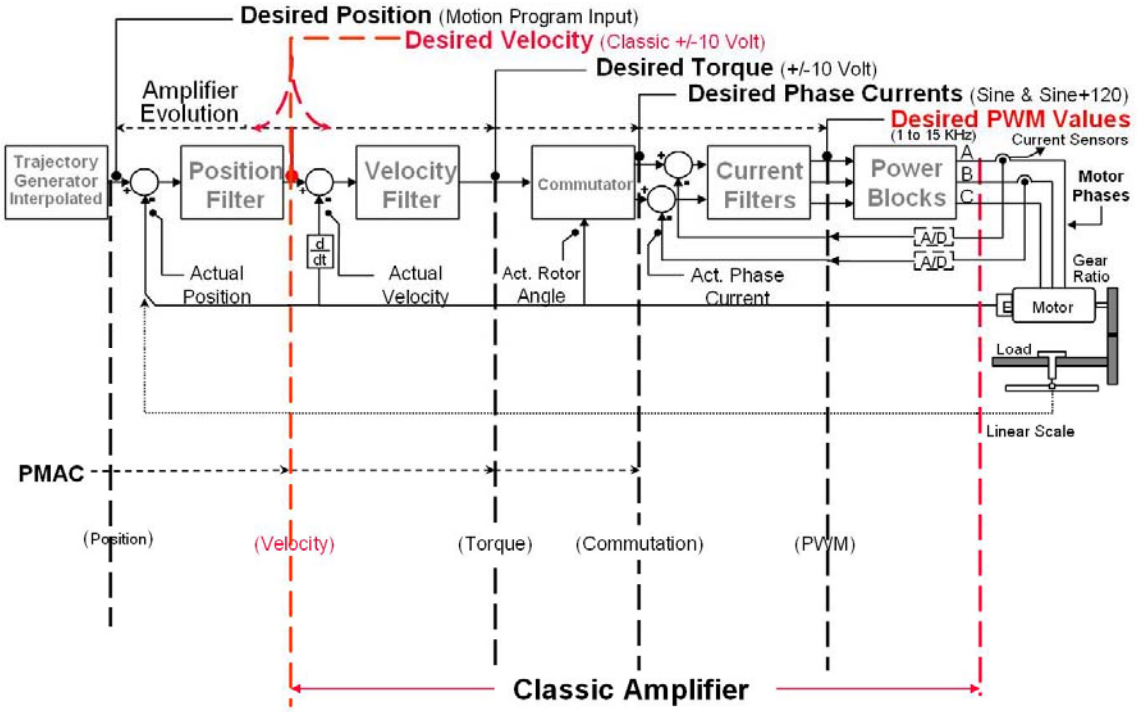

Fig. 4.2 PMAC Closed Loop Servo Control [15]

First, based on the position error, the position PID controller outputs a +/- 10 volt control signal proportional to necessary motor torque to drive this error to zero. The control signal is output through a DAC to the motor drive. The drive then takes this torque command and generates necessary phase current commands to achieve this torque. Then, based on the difference between the actual motor currents and the commanded motor currents, the drive switches the power transistors on and off to drive this current error to zero. In this case the Delta Tau closes the position and speed loops and the motor drive closes the current loop.

In the second method, the PMAC controller closes all loops including the velocity and current loops and commutates the current, making the drive basically an amplifier that only converts the power and has no part in the control scheme. In this case, the PMAC controller outputs the on/off signals that are needed by the power transistors in the drive. Deciding which loops the PMAC will close is left to the end user depending on individual needs and/or capability of the drive used in the system. In classic applications, the drive is used to close the velocity loop, commutate the current, and close the current loop as shown in Figure 4.2. Again, the PMAC has the capability to perform all control operations.

As stated, the decision regarding which loops the drive will close depends on the type of drive used and the application. There are four basic types of motor drives (amplifiers) including velocity-mode amplifiers, torque-mode amplifiers, sinewave-input amplifiers, and power-block amplifiers. Velocity-mode amplifiers are used to close the velocity and the current loops as well as performing the current commutation. Since velocity loop parameters are load dependent they must be set by the machine builder. Torque-mode amplifiers are used to close the current loop and commutate the current. The velocity loop is then closed in the PMAC controller. Since the velocity loop is closed in the PMAC, it is subject to digital limitations stemming from the encoder feedback. Since the encoder only measures position, and thus velocity, incrementally, absolute position and velocity are not known at all times. However, since the velocity loop is closed in the PMAC, the amplifier tasks are not load dependant, and can be set by the amplifier manufacturer. Sinewave-Input Amplifiers are used to close phase current loops. The velocity loop and commutation is performed in the controller. The PMAC outputs two analog voltage commands for the phase currents. The third is then calculated based on Kirchoff's current law. In this case the current loop is still closed in the drive. Finally, power block amplifiers receive only the actually on/off commands for the power transistors. The PMAC is in charge of the entire control scheme including closing the current loop and commutation.

However, in the case of the linear test bed the current commutation will be done with the drive. The PMAC will use a DAC to output a +/- 10 V signal to the drive

representing a desired torque (current) command, the first approach described in the previous paragraphs. The position and velocity loops will be closed by the Turbo PMAC controller as shown below in Figure 4.3 and will be discussed in detail in the following section.

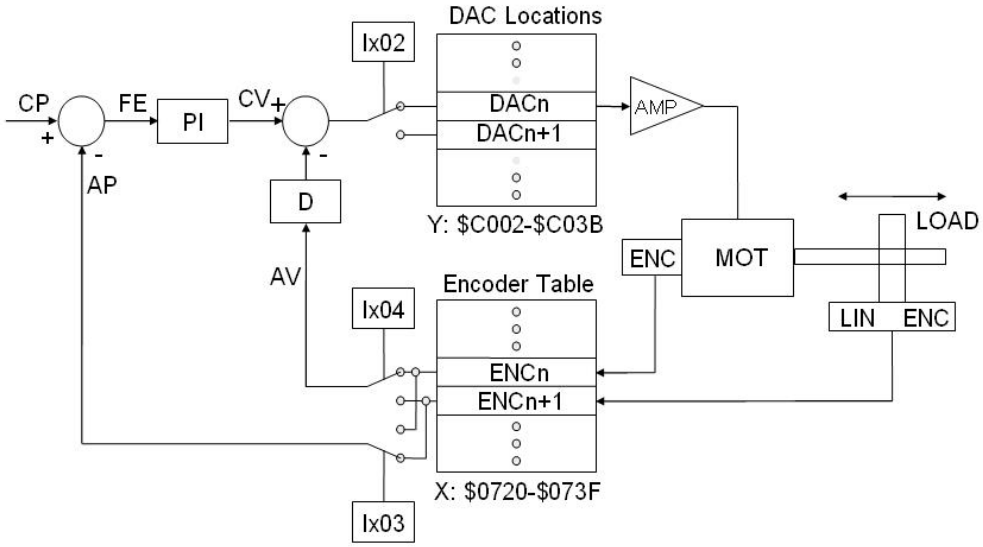

Fig. 4.3 PMAC Control Block Diagram [15]

4.4.1 Turbo PMAC PID Algorithm

The Delta Tau Turbo PMAC uses a PID Algorithm to close the position and velocity loops when outputting a torque command to the motor drive. From control theory we know that a PD controller adds damping to a system without affecting the steady-state response. A PI controller improves the relative stability and improves the steady-state error at the same time, but the rise time increases. To capitalize on the benefits of each controller, the Turbo PMAC uses a PID controller, with the details shown below in Figure 4.4. The gains of the PID controller are modified by using either the TuningPRO2 software or can be directly modified by changing the I-variables shown below on the Figure 4.4.

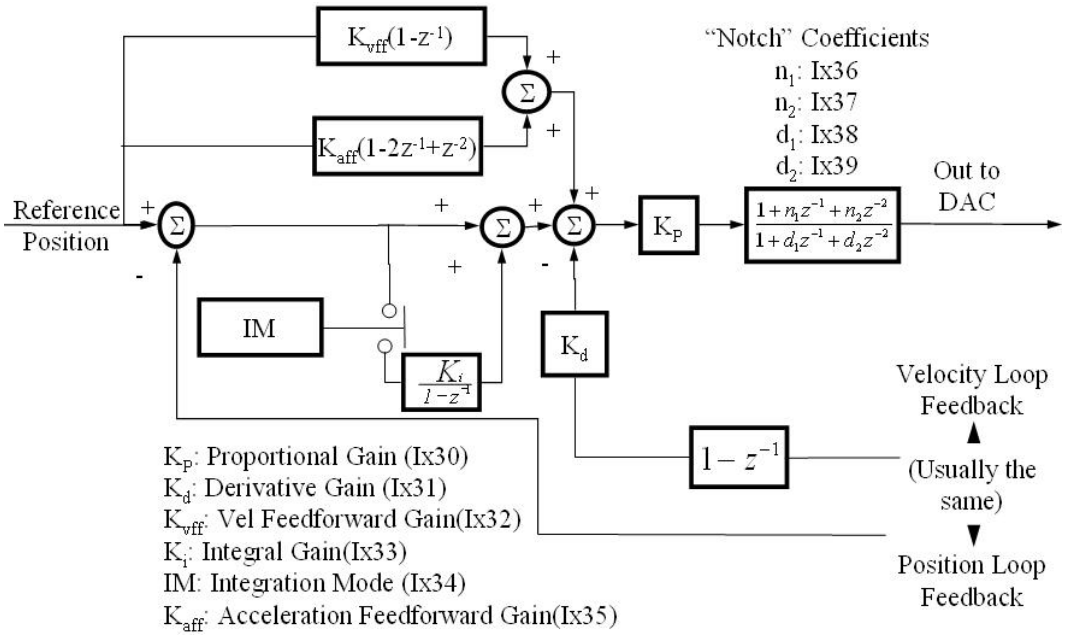

Fig. 4.4 PMAC PID Algorithm with Notch Filter [15]

To better understand this algorithm, let us carefully consider each parameter of the system. The proportional gain term provides the basic corrective action for position errors, providing a control effort proportional to the size of the error in an attempt to minimize the error. This term acts like a spring, the higher the gain term, the stiffer the spring response. In the Turbo PMAC, this proportional gain is an overall loop gain term in which the other gain terms are postmultiplied, not simply a proportional gain. The derivative gain term provides a dampening effect, similar to a shock absorber, by providing a control effort proportional to the actual velocity acting against that velocity. The higher the derivative gain, the more dampening action. This derivative gain, effectively a velocity loop, is necessary for a stable position loop. As discussed previously, this velocity loop can either be closed in the Turbo PMAC, or in the motor drive. If it is closed in the motor drive, the I-variable Ixx31 must be set to 0. The integral gain term provides correction against steady state errors, usually caused by friction. This term controls how fast the position error integrator term discharges and charges. These three gain terms, proportional, derivative, and integral compose the gains represented in a traditional PID controller. The Turbo PMAC uses several other gain

terms to make the response even better including velocity feedforward, acceleration feedforward, and a notch filter built into the PID algorithm.

In order for feedback terms to work, there must be error in the system. Turbo PMAC feedforward terms do not rely on error in the system, only a commanded input value. Basically, feedforward terms are the "best guess" estimate of the control effort that will be required to achieve the next move, the next commanded input. This can happen before any error builds up in the system resulting in a quicker response. Delta Tau estimates that up to 95% of the control effort can come from feedforward terms if the system is well tuned; the feedback terms are needed only to compensate for discrete disturbances in the system. Delta Tau uses two feedforward terms, acceleration feedforward and velocity feedforward.

Velocity feedforward adds to the control effort a gain proportional to commanded velocity. It is used to compensate for position errors caused by the velocity feedback term, the derivative gain term that provides the dampening required for stability. Acceleration feedforward adds to the control effort a gain proportional to commanded acceleration. It is used to compensate for position errors proportional to acceleration caused by the fundamental fact that inertia resists acceleration. Essentially, the acceleration feedforward gain term is an estimate of the inertia in the system. If the velocity and acceleration feedforward terms are set correctly, following error proportional to velocity and acceleration will be eliminated.

The last aspect of the PID algorithm is the notch filter that acts on the output of the PID section of the servo loop. The purpose of this filter is to counteract a known physical resonant frequency in the system. Delta Tau states that there are many ways to design a notch filter but recommends that a lightly damped band-reject filter at 90 percent of the resonant frequency and a heavily damped band-pass filter at a frequency greater than the resonant frequency. The end user can either manually calculate the filter coefficients or simply allow the Executive program calculate them. Using the software, the end user can enter a resonant frequency that he wishes to control and the program will automatically calculate the filter coefficients and downloads them to PMAC. In other

words, the notch filter can be created for a certain frequency without the end user really understanding how it functions.

4.4.2 PID Loop Tuning

Now that the PID position loop parameters and gain terms have been discussed and understood, the next step to understanding position control is how these parameters can be edited and changed such that the performance of the loop is acceptable. This process of adjusting the response of the loop by determining the proper values of the PID gain terms is called tuning. In the PMAC software package, Executive Pro2, there is a program used to tune the PID loop used in position feedback control automatically.

Turbo PMAC autotuning automatically figures out the dynamics of the system based on some quick movements of the motor and calculates the PID gains. Since quick motor movements are required, the load attached on the motor must be decoupled if it is not able to handle quick motor movements. The first step when using the autotuning program is to setup to DAC that will be used to output a torque command or velocity command to the drive. Calibration of the DAC is needed to ensure there is no movement at zero percent command output. Essentially, the motor shaft should not be moving if there is no output from the DAC. The second step in autotuning is to select “auto-select system bandwidth” without computing integral gain, velocity feedforward, and acceleration feedforward gain terms. This will compute proportional gain, derivative gain, and give a conservative system bandwidth estimate.

The third step of autotuning is to multiply the very conservative bandwidth estimate by 2 or 3 to make it a more “real world” estimate, enter the desired damping ratio and have the program recalculate the gains. Again, this will only more accurately calculate the proportional and derivative gain terms. The forth step is to add in integral, velocity feedforward, and acceleration feedforward gain terms and have the program again recalculate the gains. This will accurately set these last terms. The final step is to open a tool in the software suite called “motor interactive tuning” to check the response of the system now that it has been calibrated. Using this tool it is possible to implement a step response, a parabolic velocity response, and several other responses to see how the

system responses. Please refer to Figure 4.5, which illustrates some common problems that can occur when gain terms are set to improper values.

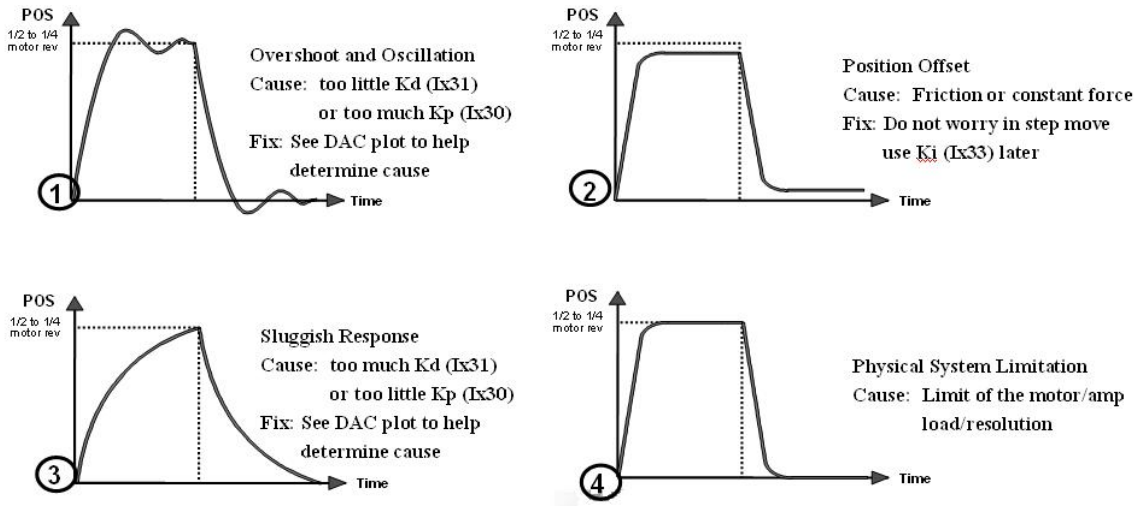

Fig. 4.5 Typical Step Response Errors [15]

If necessary, the gain terms can be manually adjusted to compensate for any error observed during a step or parabolic velocity response test. The next step is to write a motion program that will control the desired motion of the load. However, before any motion program can be written, a coordinate system needs to be defined so the Turbo PMAC knows where to run the desired profile.

4.4.3 Turbo PMAC Coordinate System

A coordinate system in the Turbo PMAC is a grouping of one or more motors for the purpose of synchronizing motion along several axes. It is significant to understand that it is a coordinate system that is capable of running a motion control program, a motor by itself cannot. Usually, depending on the desired action, motors are grouped into the same or different coordinate systems. Basically, if different motors are grouped into different coordinate systems, the motion of each is completely independent from each other. However, if the motors are grouped in the same coordinate system it is possible to coordinate motion along any axes on the coordinate system. This creates the possibility

of achieving more complex moves such as arcs and other circular trajectories. The Turbo PMAC is capable of 16 different coordinate systems.

The axes defined by the Turbo PMAC are (X, Y, Z), (U, V, W), and (A, B, C). XYZ is defined as the primary Cartesian axis, UVW the secondary Cartesian axis, and ABC a rotary axis controlling yaw, pitch, and roll. A single motor can be assigned to a single axis and several motors can even be assigned to the same axis. However, it is not permissible to assign a single motor to two axes or assign a single motor to more than one coordinate system. A coordinate system is defined by addressing it and assigning motors to axes within it (XYZ, UVW, ABC). Motors are mapped to axes letters with a scale factor and offset if desired. The scale factor represents how many encoder counts there are per user unit along that axis. This allows motion programs to be written using engineering units, not just encoder counts. The syntax below represents the correct way to define a coordinate system and assign motors to that system.

```
&1              ; define use of coordinate system 1
#1 -> 10000z    ; assign motor 1 to the z-axis of CS 1, with 10,000 counts/user unit
```

4.5 Programming Motion using Turbo PMAC

As shown in previous sections, it is possible to control the motion of the linear test bed using the Turbo PMAC. It is now necessary to understand how to control this motion. The two main ways of programming motion in the Turbo PMAC is to either write a so-called “motion program” or a “PLC program.” Motion programs are used to automatically execute a sequence of motions. PLC programs are primarily used monitor inputs and to set outputs but they can also be used to call motion programs. Each type of program will be discussed in the following sections.

4.5.1 Motion Programs

Motion programs are used to compute the sequence of commanded positions for all motors in the coordinate system. In a motion program the Turbo PMAC must be working ahead of the actual motion to keep the trajectory generator fed with data. As

discussed in the coordinate system section, only a coordinate system, not a motor, is capable of running a motion program. Furthermore, a coordinate system can only run motion program at a time, but a motion program can call other motion programs as subprograms to get around this limitation. Motion programs can be written in any text editor but must be downloaded using the Delta Tau Pro2Executive Suite. Motion programs can also be written or edited using the editor included in the Pro2Executive Suite.

To run a motion program, the coordinate system in which it will run must be addressed using an "online" command. Online commands can be executed at anytime, regardless of the state of the machine. Then, it is necessary to point to the program buffer where the motion program resides. Finally, the online command "R" will run the program after the previous steps have been completed. These commands can be executed all at the same time, entered in the host computer as "&1B10R." This will run motion program 10 in coordinate system 1. There are a variety of commands that are used in motion programs including modal, move, logic statements, logic comparators, and functions.

Modal commands describe the general motion characteristics of the move and include LINEAR, CIRCLE, RAPID, and SPLINE. LINEAR mode is used for trapezoidal or triangular velocity profiles. Usually, the motion will be a straight line path traced in a standard Cartesian coordinate system. When using this move mode it is possible to specify the absolute endpoint of the move (ABS) or the total distance of the move (INC). It is also possible to specify the speed of the move (F) or the total move time (TM). TA is used to specify the acceleration time to achieve desired speed or how much of the move time should be spent in acceleration or deceleration. TS can be used to smooth the machine acceleration so that jerk is minimized. TS is the amount of time needed to achieve the specified acceleration so that acceleration is not changed immediately. This is done by exponentially increasing acceleration or exponentially decreasing deceleration, resulting in less jerk. An example of a simple linear move is shown in Figure 4.6 and plotted in Figure 4.7.

```
********************* Set-up and Definitions *********************

DEL GAT  ; Erase any defined gather buffer
&1       ; Coordinate System 1
CLOSE    ; Make sure all buffers are closed
#1->X    ; Assign motor 1 to the X-axis - 1 program unit
         ; of X is 1 encoder count of motor #1

********************* Motion Program Text ************************

OPEN PROG 1       ; Open buffer for program entry, Program #1
CLEAR             ; Erase existing contents of buffer
LINEAR            ; Blended linear interpolation move mode
ABS               ; Absolute mode - moves specified by position
TA500             ; Set 1/2 sec (500 msec) acceleration time
TS0               ; Set no S-curve acceleration time
F5000             ; Set feedrate (speed) of 5000 units(cts)/sec
X10000            ; Move X-axis to position 10000
DWELL500          ; Stay in position for 1/2 sec (500 msec)
X0                ; Move X-axis to position 0
CLOSE             ; Close buffer - end of program
```

To run this program:

```
&1 B1 R  ; Coord. System 1, point to Beginning of Program 1, Run
```

Fig. 4.6 Simple Linear Move Code [15]

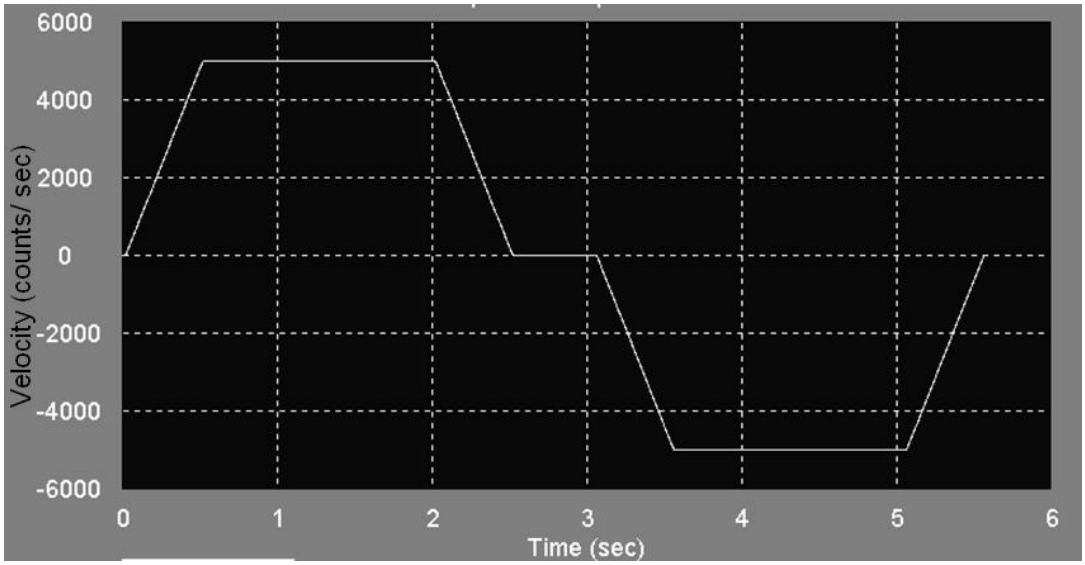

Fig. 4.7 Simple Linear Move Plot [15]

The CIRCLE move mode is used to implement sinusoidal velocity profiles. This is usually used to create arc moves in the Cartesian coordinate system and requires multiple motors to control the axes needed for the arc move. For the linear test bed application,

this move mode will not be used as all motion will be along one axis. The RAPID move mode is very much like the LINEAR mode but is used to command the minimum time needed for point to point moves. The SPLINE move mode is used to implement parabolic velocity profiles and is used for circular paths. The list below describes various logic operators, comparators, and functions that can be implemented inside a motion program.

1. Logic Control Statements
   N, O, GOTO, GOSUB, CALL, RETURN
   G, M, T, D (Special CALL statements)
   IF, ELSE, ENDIF, WHILE, ENDWHILE
2. Logic Operators
   & (bit by bit AND)
   | (bit by bit OR)
   ^ (bit by bit Exclusive OR)
3. Comparators
   = (equal to)
   != (not equal to)
   > (greater than)
   !> (not greater than)
   < (less than)
4. Functions
   SIN, COS, TAN, ASIN, ACOS, ATAN, ATAN2,
   SQRT, LN, EXP, ABS, INT

The detail of each of these operators that can be used in motion programs will not be discussed in detail, however, can be found in the PMAC User Manual. The next feature that is standard in all Turbo PMACs applicable to motion programs is called “lookahead.” This feature looks ahead in motion programs to check for possible errors and problems that the motion program could cause. Lookahead checks for problems

associated with over travel software limit switches, motor velocity limits, and acceleration limits. All of these limits are set through I-variables in the Turbo PMAC. Lookahead checks for possible violations that would occur if the motion program ran in its entirety. If violations are found that would cause the machine to travel too far, too fast, or accelerate too quickly, the lookahead feature will slow the program down and not allow it to travel outside the software limit switches.

4.5.2 PLC Programs

PLC programs run independently of motion programs and perform similar tasks of standard hardware PLCs. PLC programs cycle through calculations repeatedly and quickly regardless of the current state of any motion program. In PMAC applications PLC programs are helpful for monitoring inputs, setting outputs, changing gains, monitoring PMAC card status, commanding actions, and sending messages to the host computer. Monitoring inputs with a PLC works well because the program is scanned over and over so if the state of an input changes, the PLC will immediately recognize it. There are three major types of PLC programs including foreground PLCs, background PLCs, and compiled PLCs.

Foreground PLCs are used only for time critical tasks and the Turbo PMAC can only run one foreground PLC. It is possible to change the repetition rate of a foreground PLC by changing an I-variable. Background PLCs are used the majority of the time and the repetition rate is dependant on length, calculation requirements, and the number of motors associated with the PLC. Background PLCs are run between each servo cycle. Compiled PLCs also known as PLCCs are PLCs that are compiled into executable code and downloaded to the PMAC. This allows the PMAC to execute them much faster because there is no “interpretation time.” Interpretation time is the amount of time that PMAC requires to convert a standard PLC code into executable code. Since PLCCs are already executable, this step is not necessary. Floating point operations are about 2 or 3 times faster while integer operations are 20 to 30 faster in a PLCC. PLCCs are also scanned after every standard PLC. A standard PLC is only scanned again after all other PLCs have been scanned once and all PLCCs have been scanned multiple times.

The I-variable, I5, controls which type of PLCs are allowed. Changing this variable allows the user to allow background PLCs and compiled PLCs but not allow foreground PLCs for example. To run a PLC program simply enter an online command entitled ENABLE PLC(C) n, where n refers to the PLC program number. To stop a PLC program either enter DISABLE PLC(C) n or type control-d. As discussed, PLCs have the capability of action statements such as command, send, and display. COMMAND will execute an online command such as running a motion program or jogging the motor. SEND and DISPLAY send messages to the host computer or the PMAC display respectively. PLCs are also capable of the same conditional statements as motion programs.

In order to better understand how PLCs are used in the Turbo PMAC, consider the following example. This example creates a jogging switch specific to motor 1 by reading the input state of a thumbwheel. As the PLC scans each time the input lines are checked and commands are given as necessary. In this program a latching flag is used so that the command only changes when the state of the input changes. If this flag was not used and the switch was turned from off to on and subsequently issued the jog command, since the PLC scans so quickly, the jog command would be issued many times. This would eventually compromise the performance of the PMAC. The code for this example is shown in Figure 4.8.

```
;********************* Set-up and Definitions*****************
CLOSE
M50->Y:$FFC1,0          ; Thumbwheel port input bit 0
M60->*                  ; Latching bit for M50
;****************** PLC Program Text **********************
OPEN PLC 16
CLEAR
IF (M50=1)                          ; Motor 1 jog plus switch on
        IF (M60=0)                  ; But not on last time
           COMMAND"#1J+"            ; Issue command
           M60=1                    ; Set latching flag
        ENDIF
ELSE                                ; Motor 1 jog plus switch off
        IF (M60=1)                  ; But not off last time
          COMMAND"#1J/"             ; Issue stop command
          M60=0                     ; Set latching flag
        ENDIF
ENDIF
CLOSE
```

Fig. 4.8 Example PLC Code [15]

5. NOVEL FORCE CONTROL ALGORITHM FOR THE LTB

5.1 Force Control Introduction

The linear test bed as designed will be position-controlled using feedback from the motor encoder. When the linear test bed idea was envisioned, engineers at Oregon State University felt that position control would not be accurate for all tests necessary to characterize the performance of an ocean wave energy converter. First of all, using position control to test OWECs would force the linear test bed to use any necessary force to move the OWEC from one point to the next on the z-axis. The force exerted by the linear test bed may far exceed the capabilities of a real ocean wave. Thus, the input parameter to the linear test bed must be a commanded force, not a commanded position. Beyond this, using a preprogrammed motion profile would neglect the fluid dynamics associated with the OWEC heaving and interacting with ocean waves. More simply, it is significant to understand what happens to an ocean wave profile when energy is extracted from it.

Since the linear test bed will be primarily testing OWECs it is necessary to create a test platform that will simulate not only the impact of the wave profile on the OWEC but also the impact of the OWEC on the wave profile. Thus, the commanded force that will become the input parameter to the linear test bed will be dependent on the position, velocity, and acceleration of both the incoming wave and the OWEC. Engineers at OSU have developed a linear hydrodynamic model that models this interaction of OWEC and wave profile based on the Patel equations [8]. The inputs of this model are the position of both the wave profile and the OWEC, with velocity and acceleration computed through differentiation. The output of this model is the driving force that the wave produces. In the linear test bed, the position of the wave profiles will be determined from NOAA data acquisition buoys in the ocean. The position of the OWEC will be determined by the motor encoder and translated into engineering units based on the mechanical design.

The first step to achieving this type of control is to close a force loop around the existing position loop. This involves taking a commanded driving force, comparing it to the actual driving force measured by dual load cells on the linear test bed, and feeding that error signal to a force controller that adjusts the actual driving force to make the error close to zero. Since the commanded driving force cannot be known ahead of time, it must be generated using Patel's hydrodynamic equations. The details of each of these steps will be explained in the following sections. A general block diagram of this control scheme is shown below as Figure 5.1.

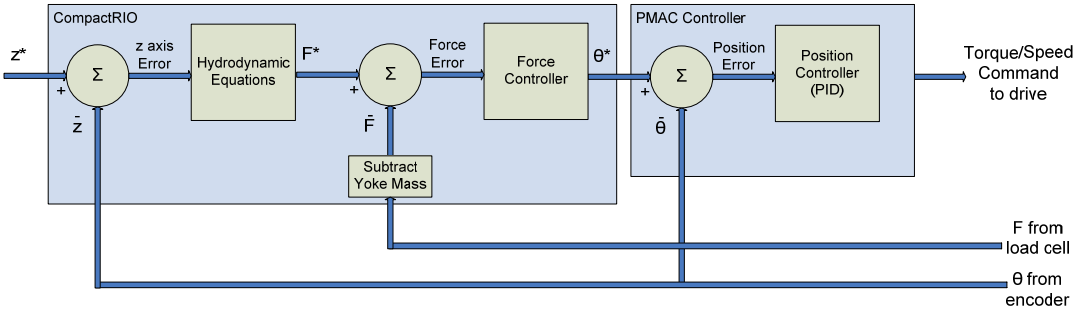

Fig. 5.1 Force Control Scheme

This diagram is helpful in understanding the basics of the overall control system. Generally, a force command is generated using the position of the OWEC under test in the linear test bed and the incoming desired wave height. This force command is compared to the actual force being applied by the linear test bed as measured by the load cells. Any error is then fed into the force controller and converted to a position command, which is fed into the Delta Tau PMAC controller. Next, any error in the commanded position and actual position is fed into the PMAC PID position controller and outputs a control signal to the motor drive. The signal is a motor torque command, which causes the motor torque to change, resulting in new carriage acceleration. This new linear acceleration value will drive the position error to zero. Understanding how the CompactRIO, Delta Tau, and drive interface with each other is paramount to the understanding of the overall control design. Since the linear test bed was not designed initially for force control, it is prudent to simulate the performance of the new control

system using Matlab Simulink. In addition, the design of the force controller transfer function will be done using the SISO (Single Input, Single Output) tool in Matlab. To model the system accurately, there are five specific aspects of the linear test bed that must be simulated. Specifically the generation of the force command using the Patel's hydrodynamic equations [8], the force controller, the PMAC PID position controller, the linear test bed itself, and any electric loading of the OWEC under test. The overall Simulink block diagram is shown below in Figure 5.2 and broken into subsystems that represent the five aspects of the linear test bed model. The hydrodynamic calculations and force controller design are included in the CompactRIO subsystem. The modeling and design steps that were necessary to accurately simulate the performance of these specific subsystems in the linear test bed system will be discussed in detail in this chapter.

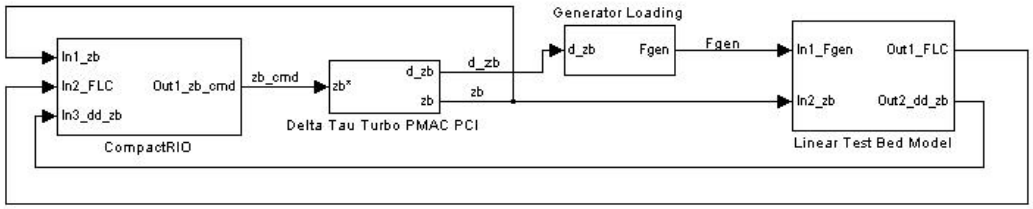

Fig. 5.2 Simulink Model of the Linear Test Bed

5.2 Modeling of the Delta Tau Turbo PMAC PCI

In order to accurately simulate the force controller it is important to understand how it will interact with the inner loop position controller. In order to do this, an accurate model of the Delta Tau controller must be generated in Simulink before any force control work is completed. The purpose of the position controller is to ensure the actual linear position of the OWEC under test in the linear test bed carriage, z_b, is as close to the commanded position, z_b* as possible. Thus, the input to the Delta Tau will always be a commanded vertical position of the OWEC under test. The output will be the actual position of the system under test.

The Delta Tau has a PID control structure so it must be modeled as such. The basic function of the Delta Tau PID loop has been previously discussed in chapter 4. For modeling purposes, the feedforward terms that are specific to Delta Tau PID loops have been ignored. This means that the model is a "worst case" response since the feedforward terms in the Delta Tau will only improve the response. The transfer function of a PID controller, $C_P(s)$, is shown below in Equation 5.1, with the equivalent proper transfer function shown in Figure 5.2. A high frequency pole is used to ensure the transfer function in Equation 5.2 is proper for Simulink use.

$$C_P(s) = K_P + \frac{K_I}{s} + K_D \cdot s \qquad (5.1)$$

$$C_P(s) = K_P + \frac{K_I}{s} + \frac{K_D \cdot s}{s \cdot T_D + 1} \qquad (5.2)$$

In Simulink, it is necessary that all transfer functions are proper, that is, the numerator must not be of a higher order than the denominator. This is problematic for implementing a differentiator in the Laplace domain shown below in Equation 5.3 where the numerator of the required transfer function would have a higher order than the denominator. To compensate for this, a higher frequency pole placed at ω_D is used to ensure the transfer function as shown in Equation 5.4 is proper.

$$\frac{dz_B}{dt} = s \cdot z_B \qquad (5.3)$$

$$sz_B = \frac{s}{1 + \frac{s}{\omega_D}} \cdot z_B \qquad (5.4)$$

Often it is desired to use integrators as much as possible to implement transfer functions so that limits can be set on the integrators. This is desired to implement anti-windup control which will be used in elsewhere in the linear test bed system model and discussed later. The Simulink implementation of Equation 5.4 is shown below in Figure 5.3, with the transfer function shown in Equation 5.5.

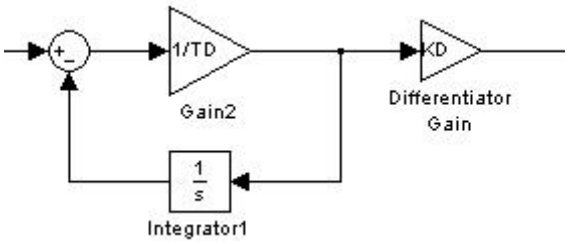

Fig. 5.3 Simulink Differentiator

$$\frac{sz_B}{z_B} = \frac{\frac{1}{T_D}}{1 + \frac{1}{T_D} \cdot \left(\frac{1}{s}\right)} \qquad (5.5)$$

Equation 5.5 can be simplified into Equation 5.6 by multiplying the numerator and denominator by $s*T_D$. Equation 5.6 is exactly the same the transfer function implementation of a differentiator shown above in Equation 5.4 where T_D is the inverse of ω_D.

$$\frac{sz_B}{z_B} = \frac{s}{1 + T_D \cdot s} \qquad (5.6)$$

From the form of Equation 5.2 it is possible to understand the how the controller must be designed. For example, it is clear that the controller must contain a constant gain term, an integrator, two zeros, and a higher frequency pole. When designing this controller, this is all the flexibility that is available. However, before we can start to understand the design of the controller, we must establish the "plant" which is the process that will be controlled by the PID controller. To review, the Delta Tau controller will be used to send a motor torque command to the motor drive to achieve a certain linear position. Thus, the plant transfer function is the relationship between motor torque and actual linear position. To simplify this transfer function, it was assumed that motor torque is proportional to the mass of the device under test, generator loading, and linear acceleration. If we assume a worst case generator loading force, proportional to a known maximum rated generator load and a known mass of the device under test, torque is only proportional to linear acceleration. This means that the plant function is effectively only

the relationship between linear acceleration and linear position. This equation is the frequency domain is stated below in Equation 5.7.

$$G_P(s) = \frac{1}{s^2} \qquad (5.7)$$

The model of the Delta Tau controller will only be an approximation and the true response of the system will not be known until the linear test bed is built and installed in the MSRF. The approximation of the response of the controller is based on the sampling rate of the Delta Tau (442 microseconds). From this, a control system designer can estimate a crossover frequency of the Delta Tau. One "rule of thumb," is if there is a sine wave input to the controller, it is necessary to have at least 10 samples per period to accurately reproduce this sine wave. For a sampling frequency of near 2kHz (about 442 μs), it would be possible to track signals at 200 Hz, or about a tenth of 2 kHz. This means that the gain crossover frequency should be at 200 Hz since the controller will not be able to track higher frequency commands.

To properly design a stable controller, the designer must be conscious of numerous factors. It is not the intent to of this thesis to give an in depth procedure about how to properly design a control system. However, when the controllers were designed for the linear test bed, several indicators of relative stability in the frequency domain were used. The first that was used is called gain margin (GM) and is defined as the amount of gain that can be added to the control loop before it becomes unstable. Gain margin is measured at the phase crossover frequency, the point when the phase becomes less than -180 degrees. Gain margin is calculated using Equation 5.8 below.

$$GM = -20 \cdot \log\left|L(j\omega_P)\right| \qquad (5.8)$$

If the plot of $L(j\omega_P)$ never crosses the negative real axis on the root locus plot the gain margin is infinite. This means that theoretically the loop gain can be increased indefinitely and instability will never be reached. In general, a system with a large gain margin will be more stable than that of one with a small gain margin. However, gain margin is not the only factor to consider when designing a controller in the frequency domain.

The other factor, phase margin, is the amount of pure phase delay that can be added before the system becomes unstable. The phase margin is measured at the gain crossover frequency, or where |L(jω)| is equal to 1 (0 dB). Phase margin is calculated using Equation 5.9.

$$PM = < L(j\omega) - 180° \qquad (5.9)$$

To easily view the crossover frequencies, phase margin, and gain margin, the open-loop bode editor in Matlab was used. This tool facilitates the visualization of the effects of adding different controllers and changing parameters of the controllers. This open-loop bode editor is called SISO tool, and is used by entering a known plant function and guessing at the controller function, perhaps setting it to 1. Then, using the SISO tool it is possible to add integrators, zeros, poles at all frequencies and view the gain and phase margin. To recap, for the Delta Tau we estimated a required crossover frequency of 200 Hz, or about 1250 rad/s. The design criterion was a controller that crossed over at 1250 rad/s, had a phase margin of at least 60 degrees and a gain margin of -30 dB. Using a plant function of $G(s) = 1 / s^2$, and a controller function of $C(s) = 1$, the SISO tool opens the open loop bode editor and shown the unstable response shown in Figure 5.4.

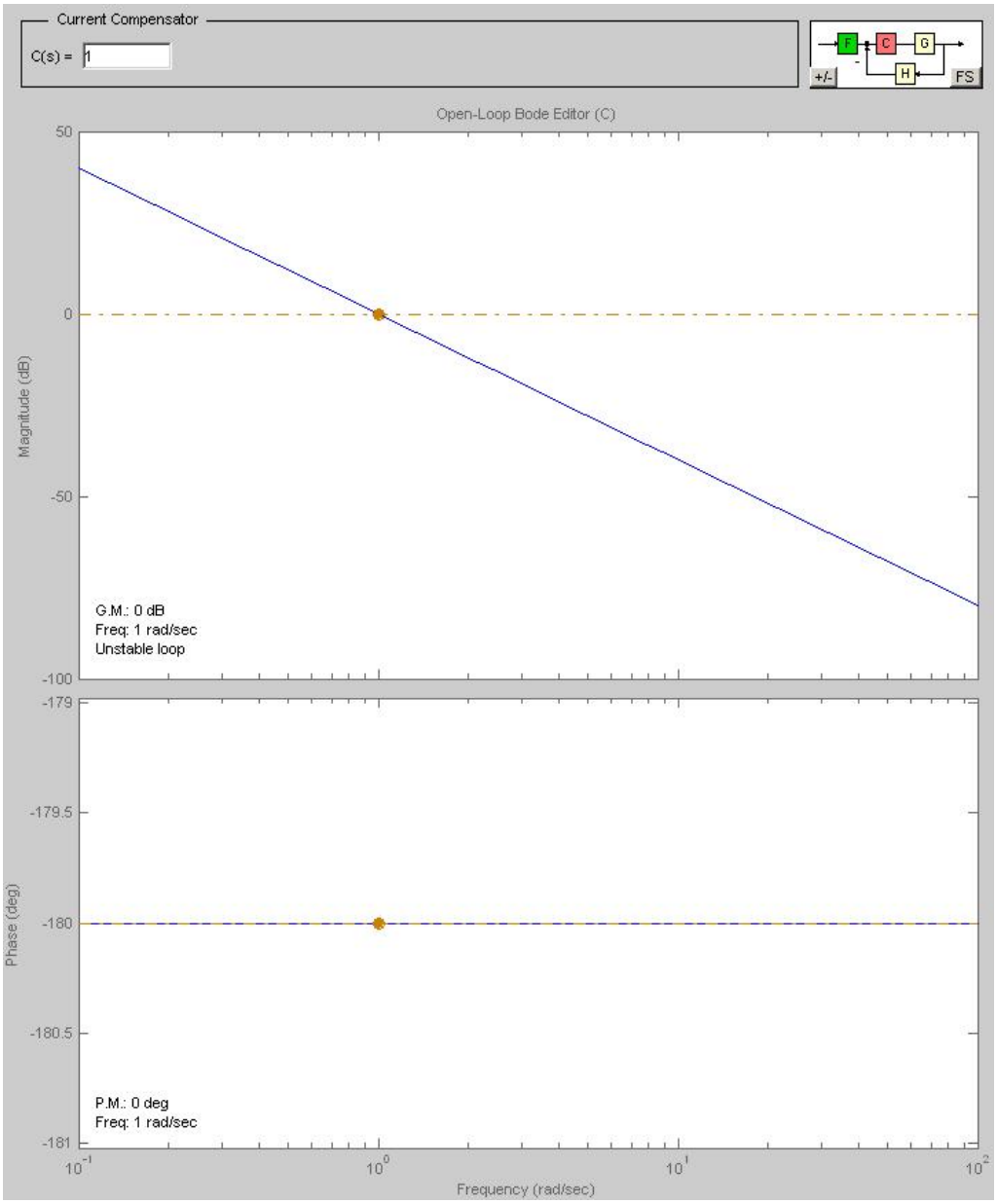

Fig. 5.4 Position Loop with No Compensator

Clearly, some controller function was needed to stabilize this system. As discussed before, using a PID control approach we had the flexibility to add constant gain, an integrator, two zeros, and a pole at some higher frequency. After some

experimentation to achieve the required gain margin and phase margin, the controller had a response shown below in Figure 5.5.

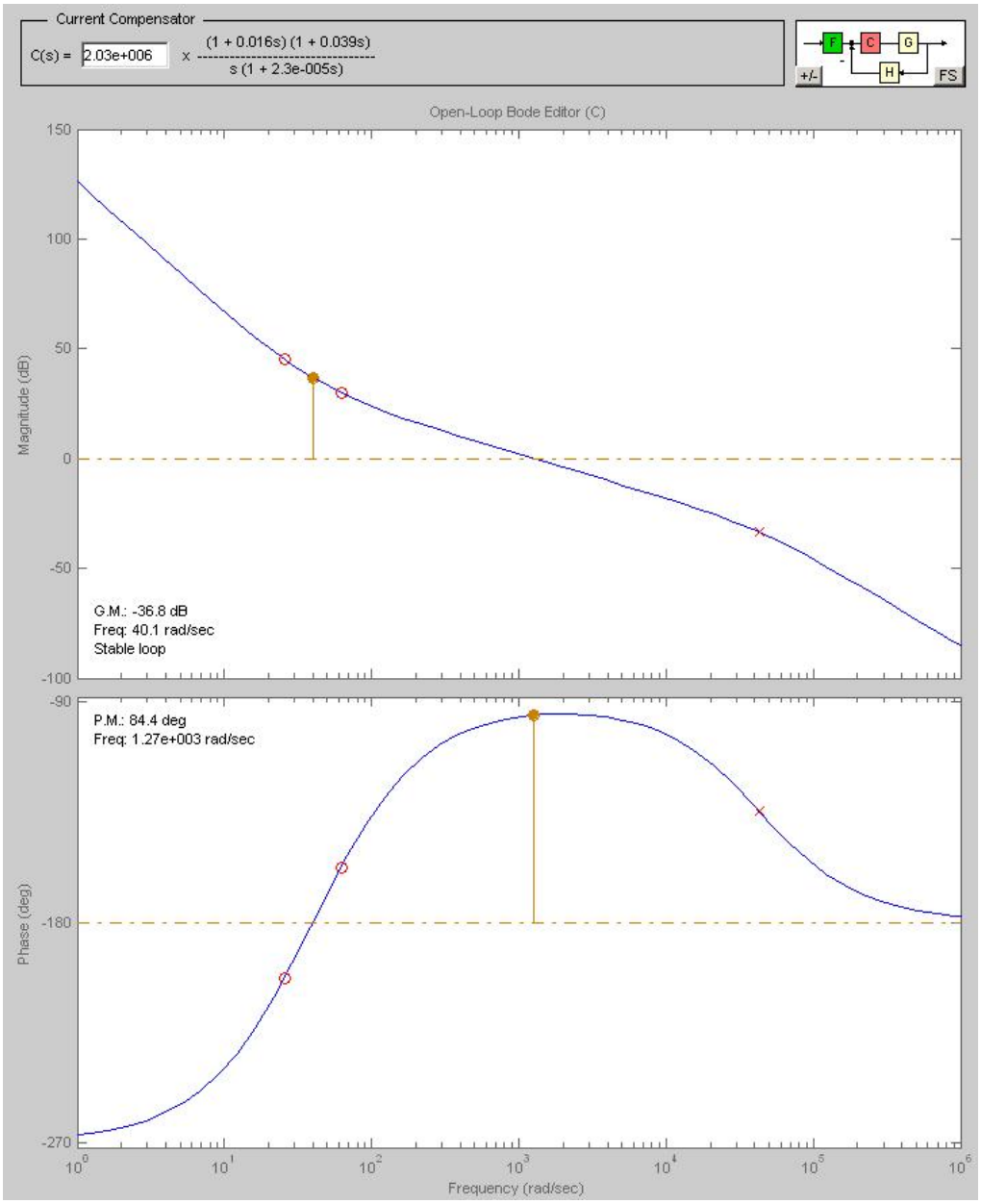

Fig. 5.5 Position Loop with Compensation

The controller transfer function C(s), shown at the top of Figure 5.5 can be simplified to the form of Equation 5.10. The simplification of the transfer function is necessary to determine the PID values.

$$C_P(s) = \frac{1267s^2 + 111650s + 2.06 \cdot 10^6}{2.3 \cdot 10^{-5} s^2 + s} \qquad (5.10)$$

Consider the transfer function for a PID controller described above in Equation 5.2. After simplification the equation takes on the form shown below in Equation 5.11.

$$C_P(s) = \frac{(T_D K_P + K_D)s^2 + (K_P + K_I T_D)s + K_I}{T_D s^2 + s} \qquad (5.11)$$

After comparing the form of Equations 5.10 and 5.11 it is clear that K_I must be equal to $2.06 \cdot 10^6$ and T_D must be equal to $2.3 \cdot 10^{-5}$. By knowing the values of K_I and T_D and equating coefficients, it is possible to calculate $K_P = 1.1160 \cdot 10^5$ and $K_D = 1.2644 \cdot 10^3$. After the PID values have been calculated they must be implemented in Simulink. The implementation is shown below in Figure 5.5 and will be fully explained in the following pages.

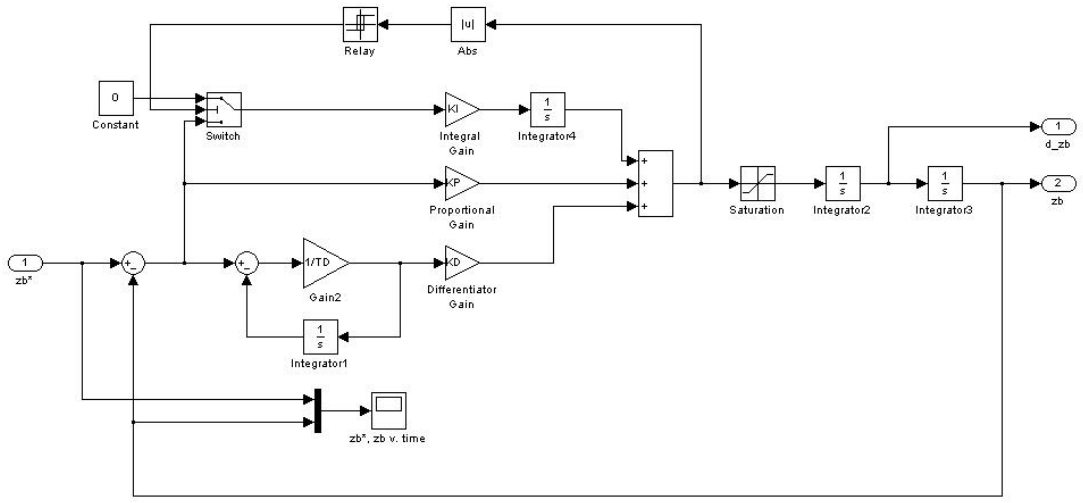

Fig. 5.6 Position Loop Simulink Implementation

The Simulink implementation of the Delta Tau PID loop is very straightforward. The inputs to the system are the commanded OWEC under test position and the actual position effectively measured by the motor encoder. The error of these two signals is calculated, which is fed into the PID controller. The components of the PID controller are visible in the integrator with gain, proportional gain, and Simulink differentiator model with gain, all summed together. The PID controller outputs the linear acceleration (motor torque) that is required to correct the position error. The plant model discussed earlier is implemented using two integrators used to calculate the actual position. There are two aspects of the model which are more complicated and necessary to ensure the controller operates safely.

The first is the saturation block shown connected to the output of the PID controller. The saturation block limits the output of the controller such that maximum acceleration (maximum motor torque) is not exceeded. The acceleration limits are computed based on the generator force, mass of the device under test, and the maximum short term duration torque specification provided by the motor manufacturer. The only aspect of the PID implementation that requires additional understanding is the implementation of what is known as anti-windup control. Anti-windup control is necessary to control the behavior of the integrator minimize overshoot and limit the output of the integrator.

The PID controller output is limited by the torque limits of the motor driving the linear test bed. For the sake of discussion, let us assume the limits of the motor torque correspond to linear acceleration limits of +/- 2 meters per second per second. Now, for the linear test bed there is obviously limits to the actual position of the device under test. If the commanded position is outside the range of these limits, there will effectively be a constant error between the commanded and actual position. The error causes the output of the controller to increase very quickly as the integrator will be integrating a constant value causing the output to increase well outside the range of operation. Then, once the commanded input is changed back to something reasonable, the integrator output takes a long time to decrease from the higher output back to expected output. This problem is solved by limiting the output of the integrator.

In the case of the Delta Tau position loop, anti-windup control was implemented using a relay and a switch controlled by digital logic. Referring back to Figure 5.5, the absolute value of the output of the controller is computed using the ABS block. This is necessary as linear acceleration can either be positive or negative and must be limited in either case. Then, the signal is passed into the relay, which outputs a "1" if the controller output is greater than or equal to the maximum acceleration allowed by the system. If it is lower, the relay outputs a 0. This control signal is then passed into a conditional switch. The switch will pass the first input, 0, when the second input is greater than or equal to the threshold of 0.5 (limit reached). Otherwise, the switch passes the third input, the error signal. Basically, if the maximum acceleration has been reached, the integrator turns off. If not, it will continue to work and pass the position error signal as originally designed. This approach limits the output of the integrator and thus prevents the integrator from "winding up."

5.3 CompactRIO Data Processing

Before the details of each specific component of the CompactRIO subsystem model are presented, there is some basic signal processing that will be performed using the CompactRIO subsystem, in addition to the implementation of the hydrodynamics and the force controller. For example, the mass of the yoke must be multiplied by the linear acceleration of the system to properly determine the force supplied by the linear test bed. Additionally, since the first action taken by the hydrodynamic model is differentiation, a ramp function has been used to limit the amount of simulation startup transients. The details of the CompactRIO subsystem are shown below in Figure 5.7 and should be understood before the discussing the hydrodynamic model and force controller.

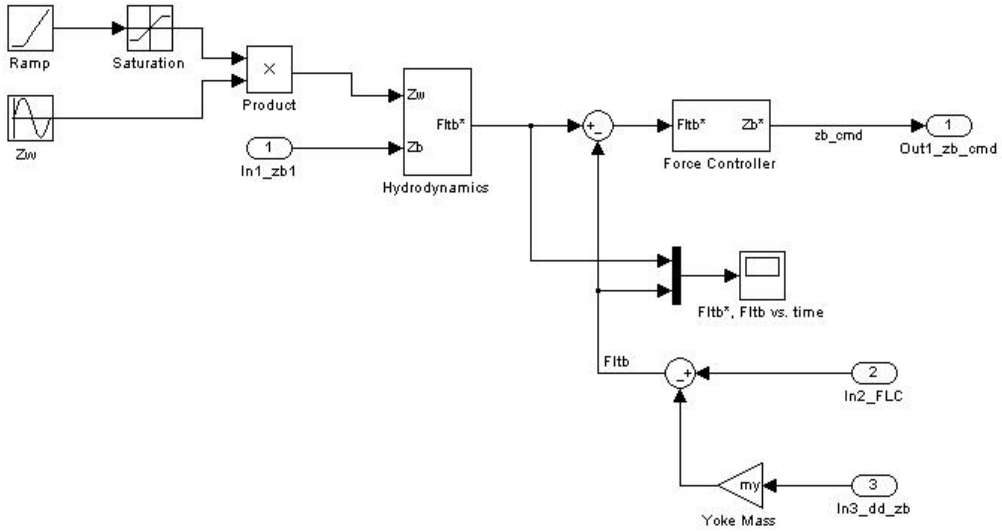

Fig. 5.7 Simulink Model of the CompactRIO

From Figure 5.7, the signals measured by the load cells that represent the total force applied by the linear test bed to the system under test, including the yoke mass force, and the linear acceleration measured by the drive are all inputs to the CompactRIO model. The linear acceleration of the system under test and multiplied by the yoke mass and subtracted from the load cell measurements to determine the force applied the system under test. A sine wave with amplitude and frequency corresponding to an ocean wave is used as wave height input. This is the most basic approximation of an ocean wave but will be used initially when testing a device in the linear test bed. A ramp function is used to slowly increase the amplitude of the sine wave to minimize the startup transients caused by the initial differentiation of the sinusoidal error between the wave height and actual buoy position.

5.4 Hydrodynamic and Hydrostatic Modeling

5.4.1 Generating the Commanded Force

Before the force loop can be closed, there must be a means for calculating the commanded force to be applied to the system under test by the linear test bed, F_{LTB}. The

force will not be known ahead of time, we will show how it will depend on the position, velocity, and acceleration of both the wave and the OWEC as governed by the Patel equations [8]. The first step in order to properly calculate F_{LTB} is to first calculate the excitation force, F_e, where the wave elevation z_w exerts an excitation force on the buoy. F_e is calculated using Equation 5.12 below.

$$F_e = k_w z_w + C_w \dot{z}_w + A_w \ddot{z}_w \qquad (5.12)$$

The coefficients A_w, C_w, and k_w represent the added mass, damping, and hydrostatic stiffness induced forces on the buoy. Added mass is an inertia force associated with a heaving buoy often thought of as an induced force caused by the buoy accelerating some additional fluid with it. Damping occurs due to energy lost in the system from hydrodynamic friction between the fluid and the buoy. Damping also occurs when energy is lost due to radiation waves created by the heaving buoy. Hydrostatic stiffness is the buoyant force proportional to displacement and is analogous to a spring force. These three forces are induced forces due to the differential motion between the buoy and the surrounding fluid. However, this only represents the first step in determining F_{LTB}, which is relating wave elevation to force.

The second step involves relating wave force to actual motion and is necessary for properly deriving a body motion response from wave elevation. Now that the excitation force is known, it is possible to calculate the buoy's motion response using Equation 5.13. Equation 5.13 includes all forces that will be acting on the OWEC and thus F_{LTB} can be calculated using this equation. This equation includes a generator force that is proportional to the electrical loading of the OWEC. The generator force will be proportional to velocity and opposite in direction. In other words, the force will be in phase with velocity but will oppose the OWEC velocity effectively adding more damping to the system.

$$F_e + F_{gen} = z_B k_w + \dot{z}_B C_w + \ddot{z}_B (m + A_w) \qquad (5.13)$$

The linear test bed must provide the excitation force plus all forces that would be present in the ocean that will not be present in the linear test bed. A careful analysis of Equation 5.13 will show which forces will not be present in the linear test bed. Any forces that are

exerted on the buoy by the water will not be accounted for in the linear test bed. $F_{HS} = z_B k_w$ represents the hydrostatic stiffness force on the buoy. $F_D = \dot{z}_B C_w$ represents the damping force of the water, and $F_A = \ddot{z}_B A_w$ represents the inertial force. Since these forces will not be present in the linear test bed, they must be subtracted from the excitation force in order to determine F_{LTB}.

If Equation 5.13 is solved for $\ddot{z}_B m$, the force required to accelerate the OWEC, the result will yield Equation 5.14.

$$\ddot{z}_B m = F_e - z_B k_w - \dot{z}_B C_w - \ddot{z}_B A_w + F_{gen} \qquad (5.14)$$

Let us now define $F_{DUT} = \ddot{z}_B m$ and $F_{LTB} = F_e - z_B k_w - \dot{z}_B C_w - \ddot{z}_B A_w$. F_{DUT} is the force that present as a result of the acceleration of the device under test and F_{gen} is the force that will be present due to generator loading. The reminder of the forces must be supplied by the linear test bed and are thus grouped together and defined F_{LTB}. Using the new definitions and rearranging 5.14 it is possible to state a much simper equation, shown below at 5.15.

$$F_{LTB} = F_{DUT} - F_{gen} \qquad (5.15)$$

This equation makes sense on an intuitive level because the linear test bed will accelerate the DUT which is opposed by any loading force.

Now that we have established which forces must be supplied by the linear test bed, let us verify that we have enough information to calculate F_{LTB}. From above, $F_{LTB} = F_e - z_B k_w - \dot{z}_B C_w - \ddot{z}_B A_w$. The coefficients k, C, and A are constants that are dependant on the geometry of the buoy and are known ahead of time through experiments. F_e was calculated above and is dependant on the same coefficients and the wave motion elevation. Finally, z_B the position of the buoy will be determined from the motor encoder and converted to linear position using the mechanical design of the machine.

5.4.2 Linear Test Bed Implementation of Hydrodynamics

Now that F_{LTB}, the commanded force has been determined it must be implemented using the CompactRIO controller. To explicitly see all the terms present in F_{LTB}, let us substitute F_e into to $F_{LTB} = F_e - z_B k_w - \dot{z}_B C_w - \ddot{z}_B A_w$. This equation is shown below as Equation 5.16, simplified in Equation 5.17, and converted into the Laplace domain in Equation 5.18. The difference in the position of the incoming wave height and the buoy position is defined as z_{wB}.

$$F_{LTB} = k_w z_w + C_w \dot{z}_w + A_w \ddot{z}_w - z_B k_w - \dot{z}_B C_w - \ddot{z}_B A_w \qquad (5.16)$$

$$F_{LTB} = k_w (z_w - z_B) + C_w (\dot{z}_w - \dot{z}_B) + A_w (\ddot{z}_w - \ddot{z}_B) \qquad (5.17)$$

$$F_{LTB} = k_w (z_{wB}) + sC_w (z_{wB}) + s^2 A_w (z_{wB}) \qquad (5.18)$$

Now that the generation of the commanded force has been determined we can now show a Simulink block diagram which shows how Equation 5.18 will be implemented in the Simulink model of the linear test bed system.

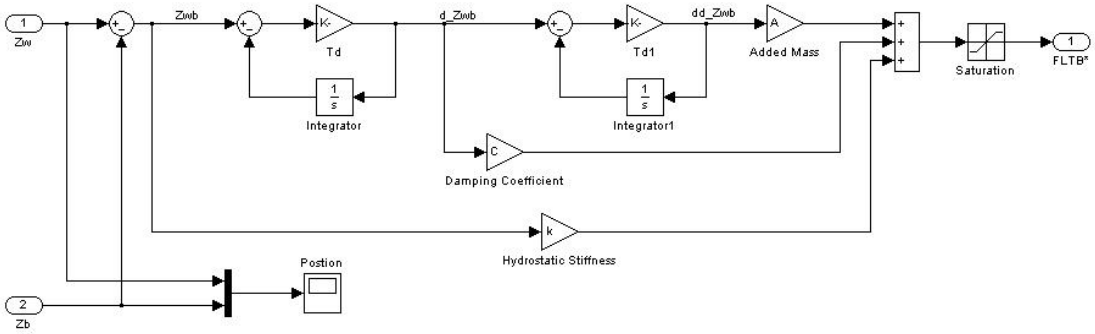

Fig. 5.8 Simulink Hydrodynamic Commanded Force Generation

This Simulink implementation of Equation 5.18 is very straightforward. The signal that represents the difference between wave height and buoy position, z_{wb}, is differentiated twice, with $z_{wb}, \dot{z}_{wB}$ and $\ddot{z}_{wB}$ multiplied by the constants in Equation 5.18 representing hydrostatic stiffness, damping, and added mass respectively. Summing these together will produce F_{LTB}. A saturation block is used only to limit the output of this force

command generation subsystem. This will prevent the hydrodynamics asking for a force that cannot be handled by the linear test bed and is only used as a safety measure.

5.5 Design of the Force Controller

Now that the force command can be generated using the hydrodynamic model, a force controller is needed to ensure that the commanded force is applied. This force controller will have two inputs, the first being commanded force, F_{LTB}*, which is generated using the hydrodynamic model. The second input is the actual force applied by the linear test bed to the system under test, F_{LTB}. This force is used to accelerate the device under test and also to drive the opposing generator force. As stated, F_{LTB} is computed by reading the load cells and subtracting the force necessary to accelerate the yoke mass. By subtracting these inputs a force error is computed and fed into the force controller. The force controller then outputs a position command that will cause the force error to be driven to zero by effectively changing the linear acceleration of the system.

The design of the force controller was approached much like the modeling of the Delta Tau PID controller. However, as was the case in the position control loop, the plant, or process to be controlled, must be understood first. For the purposes of designing the force controller, generator force was ignored because generator force is an independent variable and cannot be known ahead of time. Additionally, this will likely cause additional damping in the system that will only make the system more stable. By not including generator force, the controller was designed for a “worst case” scenario when there would be less system damping. The force controller must output a position command to be fed into the Delta Tau controller. Therefore, the plant transfer function is the relationship between commanded position and actual force applied by the linear test bed.

Since the modeling of the Delta Tau position controller has already been discussed, we can use our understanding of that system to help us begin to understand the plant model for the force controller. The closed loop gain of the Delta Tau model is included in the force controller plant since it encompasses the relationship between

commanded linear position and actual linear position. The calculation of the closed loop transfer function, $T_P(s)$, is shown below in Equation 5.19 and Equation 5.20 with $G_p(s)$ and $C_p(s)$ shown earlier in Equations 5.7 and 5.10.

$$T_P(s) = \frac{G_P(s)C_P(s)}{1 + G_P(s)C_P(s)} \qquad (5.19)$$

$$G_{F1}(s) = \frac{0.02914\,s^3 + 1270\,s^2 + 1.117e5\,s + 2.03e6}{5.3e-10\,s^5 + 4.6e-5\,s^4 + 1.03\,s^3 + 1270\,s^2 + 1.12e5\,s + 2.03e6} \qquad (5.20)$$

Now that the relationship between commanded linear position and actual linear position is known it is only necessary to find the relationship between actual position and force applied by the linear test bed. Since we assume the generator force is zero, the force applied by the linear test bed to the system under test, F_{LTB}, is used only to accelerate the device under test. The force on the device under test is simply the mass of the device under test multiplied by linear acceleration. The mass is known ahead of time and the acceleration can be computed by taking the second derivative of the actual linear position. This calculation is done using Equation 5.21. Finally, by multiplying Equations 5.20 and 5.21, there entire plant function for the force controller can be realized. This represents the relationship between commanded position and force applied by the linear test bed to the system under test. The final plant function is shown in Equation 5.22 and is used to design the force controller.

$$G_{F2}(s) = \frac{m\,s^2}{\left(1 + \frac{s}{200 \cdot \pi}\right) \cdot \left(1 + \frac{s}{200 \cdot \pi}\right)} \qquad (5.21)$$

$$G_F(s) = \frac{38.96\,s^5 + 1.697e6\,s^4 + 1.493e8\,s^3 + 2.714e9\,s^2}{1.3e-15\,s^7 + 1.2e-10\,s^6 + 2.8e-6\,s^5 + 0.007\,s^4 + 5.4\,s^3 + 1630\,s^2 + 1.2e5\,s + 2.03e6} \qquad (5.22)$$

Now that the plant function has been defined, the design of the controller will be performed using the SISO tool in Matlab. The process will be very similar to the way the position controller design was estimated. However, in this case, we are not limited to a PID controller. It is possible to implement any controller design, not only a PID controller using the CompactRIO. Any controller transfer function that will be designed

using the SISO tool can be implemented in the CompactRIO using a z-transform. The z-transform is used to convert continuous time transfer functions in the s-domain to discrete time transfer functions is the z-domain. This makes for much flexibility in the design of the force controller.

Based the output of the hydrodynamic model the force controller must be able to track sinusoidal force inputs in the frequency range of 0.6-1.0 radians per second. These are typical wave frequencies. To track these frequencies well, a good rule of thumb would be to design the controller to crossover at ten times this range. Thus, the design specification for the force control is a gain crossover frequency of 6 radians per second. Additionally, the controller must have a phase margin of 60 degrees with as much gain margin as possible. These design specifications are estimates. Simulations are needed to see how the entire system responds to various inputs, which will be present in the simulation results section later in this thesis.

Using a plant function of $G_F(s)$, and a controller function of $C(s) = 1$, the SISO tool opens the open loop bode editor and displays the unstable response shown in Figure 5.9.

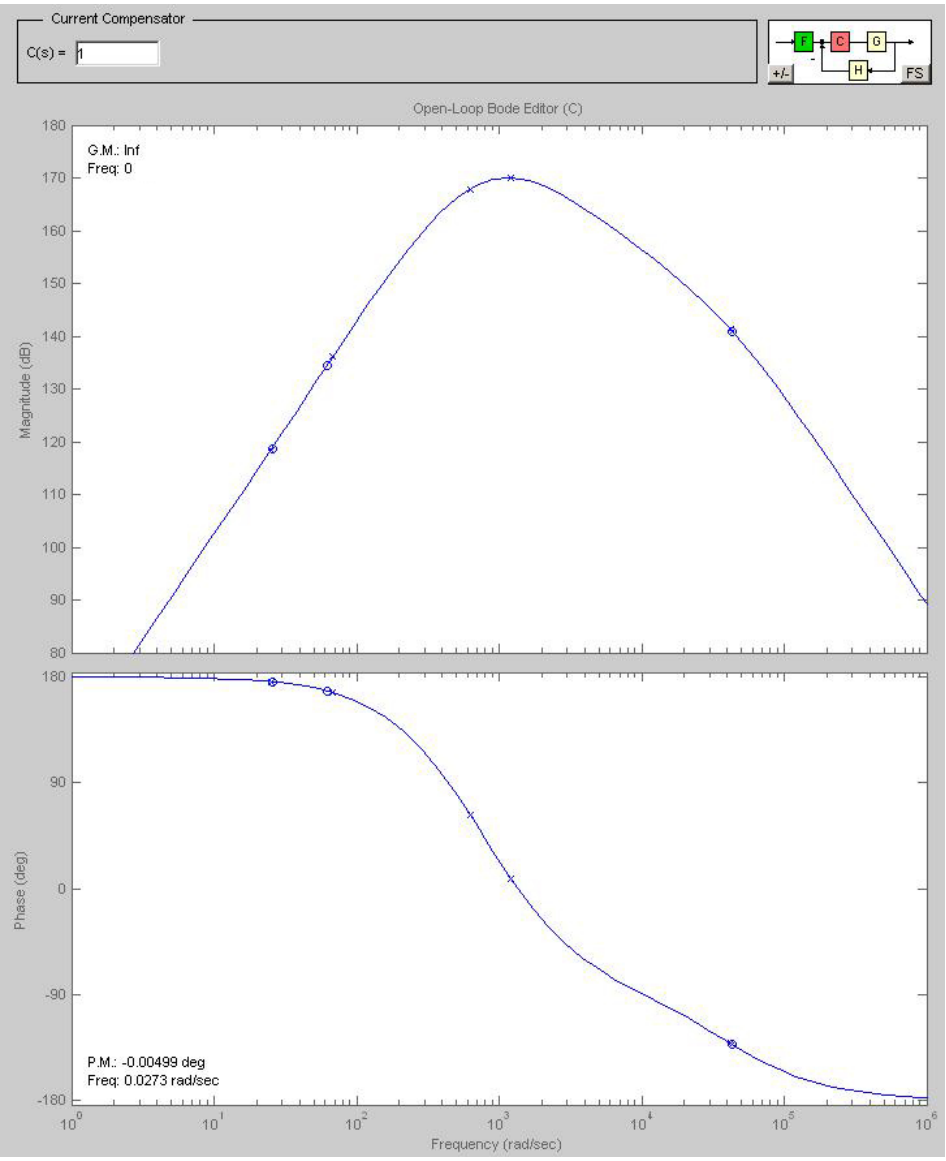

Fig. 5.9 Force Controller Response with No Compensator

It is clear that the system with a force controller with a gain of 1 will not be sufficient to stabilize the system, which is to be expected. SISO tool allows the designer to implement and change the controller's transfer function on the fly. From intuition it seems reasonable that three integrators could be a decent start to designing this controller. Two are needed to compensate for the differentiation needed to compute the force in the plant function, and an additional integrator for integrator action. After some experimentation with the addition of the integrators and the gain, the controller was able

to achieve the required gain margin and phase margin. The response of the controller is shown below in Figure 5.10.

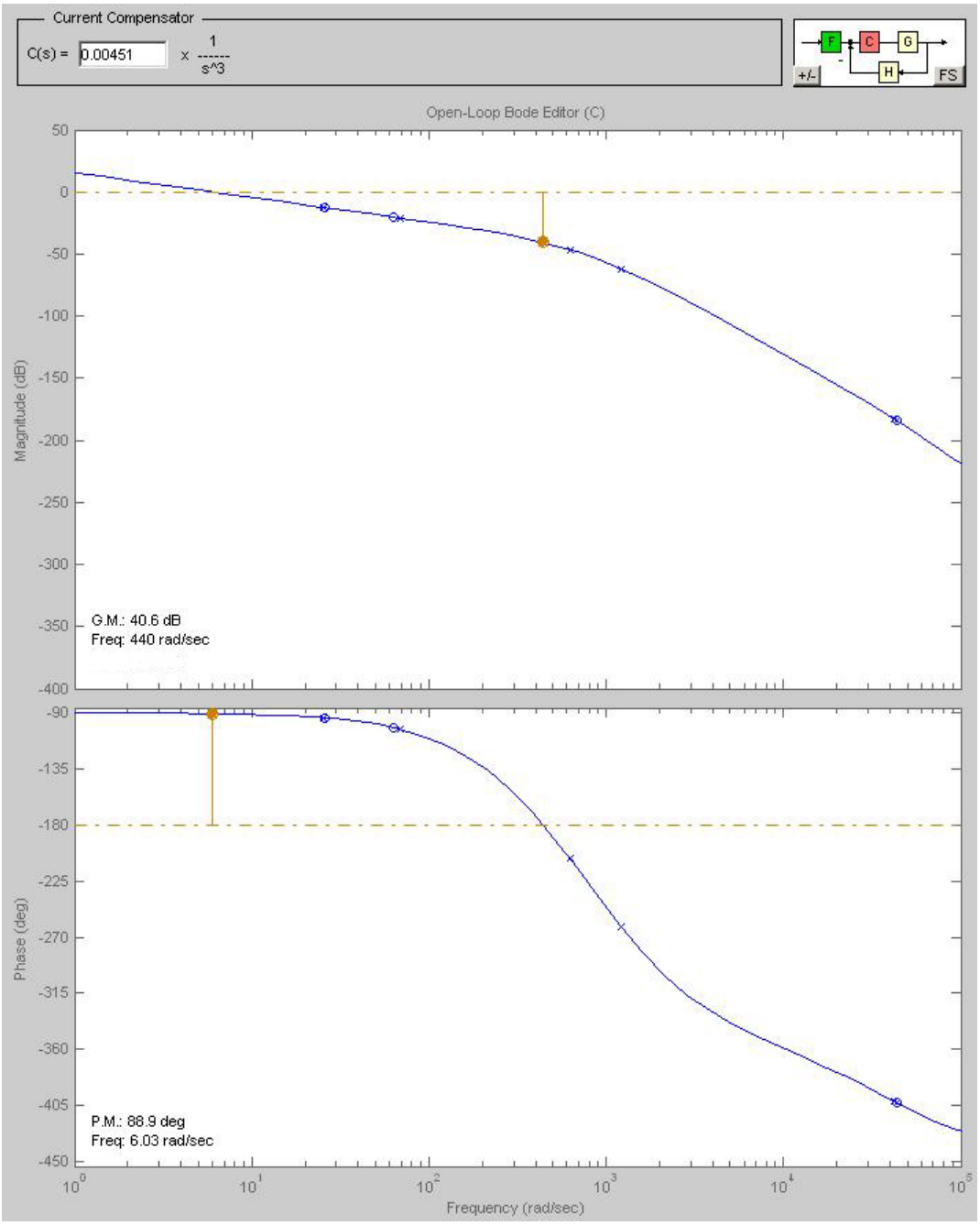

Fig. 5.10 Force Controller Response with Compensation

The force controller's transfer function is shown in Figure 5.10 in the upper left hand corner is shown explicitly in Equation 5.23. The Simulink implementation of this transfer function is simple. Using three integrators and a gain block, the controller transfer function is finalized in Simulink. A call back function in Matlab is used to set the gain of controller and is implemented as a variable, kC, in Simulink. It should be mentioned that this call back m file is used to initialize all variables used in the model. The Simulink implementation is shown below in block diagram form in Figure 5.11. Saturation limits are placed each of the integrators as a type of anti-windup control.

$$C_F(s) = \frac{0.00451}{s^3} \qquad (5.23)$$

Limiting the integrators directly in Simulink is another way to implement anti-windup control without using exterior digital logic. The limits of the integrators are set to the physical limits reasonable for the linear test bed. Since the output of integrator3 is position, the limits are set to reasonable position limits of plus and minus one meter. Likewise, the output of integrator2 is velocity, and the limits are set to the fast mode limits of plus and minus three meters per second. Finally, the output of integrator1 is acceleration, and the limits are set to the acceleration limits calculated dynamically based on the mass of the device under test, generator loading, and motor torque specifications.

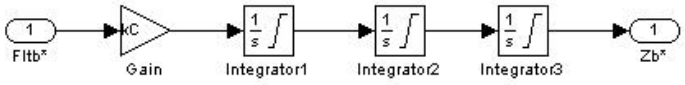

Fig. 5.11 Force Controller Implementation

5.6 Linear Test Bed and Generator Force Modeling

In order to accurately simulate both the position and force controllers to be used on the linear test bed it is vital to have an accurate mathematical model of the test bed. This model will serve as part of the plant function for the design of the force controller along with the transfer functions involved in the modeling of the Delta Tau controller. Another aspect of properly modeling the system is to accurately model the force that will exist due to the electrical load on the device under test. The force controller will be

tested for various loading levels of a sample device under test to ensure the system response to generator loading is correct.

5.6.1 Linear Test Bed Model

Since the Delta Tau plant transfer function captured the relationship between motor torque and device under test position, the output of the position control system is actual position of the device under test. Therefore, to close a force loop controller, it is necessary to understand the relationship between linear position and the force measured by the load cells on the test bed. The relationship is captured by the linear test bed subsystem shown in Figure 5.2 at the beginning of this chapter. The linear test bed model is meant to be a mathematical representation of the actual linear test bed and thus computes the actual values for applied force, carriage position, velocity, and acceleration. The details of this subsystem are shown below in Figure 5.12.

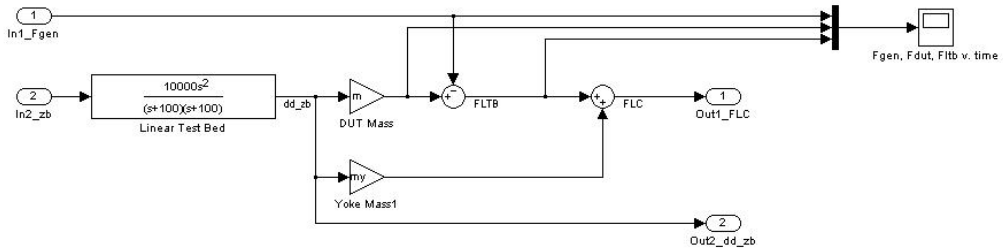

Fig. 5.12 Linear Test Bed Model

This model, again, is very straightforward. The inputs to the model are the actual position of the device under test and the generator force. The outputs are used as feedback quantities, the first is force measured by the load cells, and the second is linear acceleration. A transfer function block is used to take the second derivative to compute linear acceleration. This transfer function block is essentially two Simulink differentiators discussed earlier placed in series, but implemented without integrators. A careful comparison of the associated transfer functions of each block will show this to be true. Once acceleration is known, it is multiplied by the mass of the device under test to

compute the force applied to the device under test. The generator force is then subtracted to compute the total force applied by the linear test bed. Finally, as discussed in chapter three, the yoke mass is multiplied by the linear acceleration and added to the force applied by the linear test bed to compute the total force that is measured by the load cells. The force proportional to the yoke mass is subtracted before it is used as a feedback value in which to compare commanded force generated by the hydrodynamic model.

5.6.2 Generator Force Modeling of the Device under Test

The generator force will be in phase will the velocity of the device under test. One approach to model the generator force is to multiply the velocity of the device under test by a constant. For example, if the peak velocity is near 1 meter per second, multiplying that waveform by 1000 would result in a sinusoidal waveform in phase with velocity. This waveform can be used as the generator loading force. To calculate the amount of power generated with a given generator force, it is possible to use Equation 5.24 below.

$$P = F_{gen} \cdot v \qquad (5.24)$$

Using the example where the generator force is taken to be a sinusoidal waveform in phase with velocity at 1000N, with the velocity peak of 1 meter per second, the generated power would be equal 1000W, or 1kW. Thus, by changing the constant it is possible to vary the generator force simulated and thus the generated power simulated. Since the hydrodynamic coefficients were calculated based on an initial design for a 1kWrms linear generator, generator forces corresponding to loading levels up to 1kWrms will be simulated. Generator loading in Simulink is very simple and is shown below in Figure 5.13. The signal describing the velocity of the device under test can be output from the Delta Tau block since its ultimate output is actual position. Then, the velocity is multiplied by a constant that can be changed using the call back m file. The constant must be negative since the generator force will oppose the velocity, effectively adding more friction to the system. A switch is used in Simulink to quickly switch between the generator being loaded and unloaded.

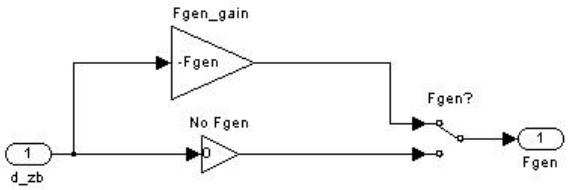

Fig. 5.13 Generator Force Modeling

5.7 Simulation Results

Now that the individual components of the entire system have been understood, simulation results are necessary to show that the model behaves as expected. To show this, a step input is used as the input wave height. This models what would happen if a single wave passed by the OWEC under test and then the water level remained at a higher level. If the hydrodynamic model is working correctly, the linear test bed should provide a force that slowly dies out as time passes. In other words, this simulates a buoy in the water being excited by a single wave and after the wave passes the water level is raised by the amplitude of the single wave. The expected result is that the buoy should oscillate until it reaches steady state and floats at the new water level. Figures 5.14 and 5.15 illustrate how the linear test bed will replicate this behavior when using force control. Figure 5.14 displays commanded wave height (step function) and the actual response of the system under test. Figure 5.15 displays the commanded force and the actual force as controlled by the force controller.

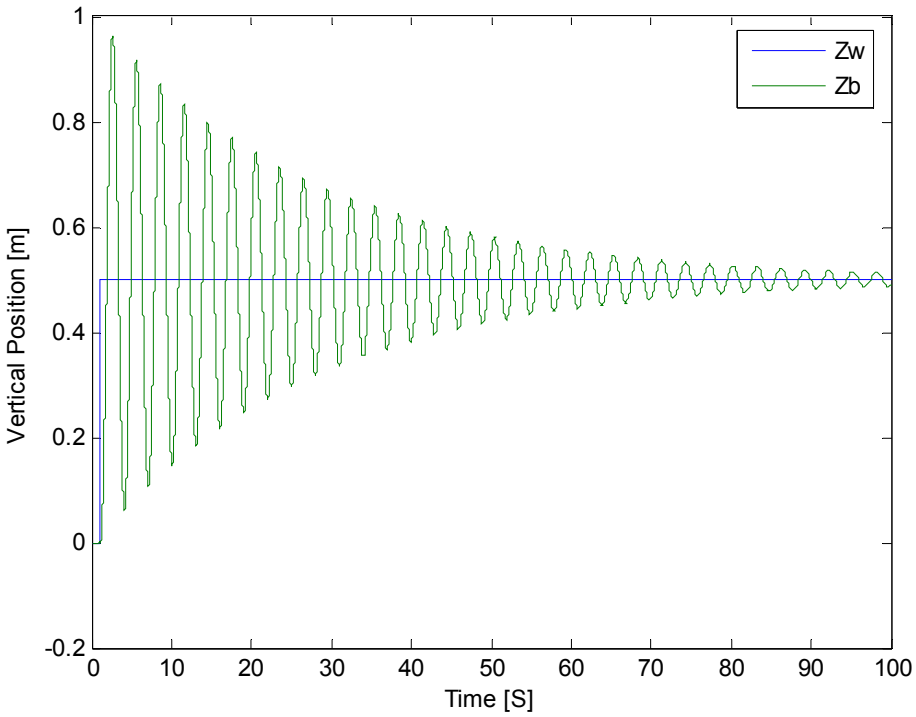

Fig. 5.14 Wave Height and Actual Vertical Position, Step Input

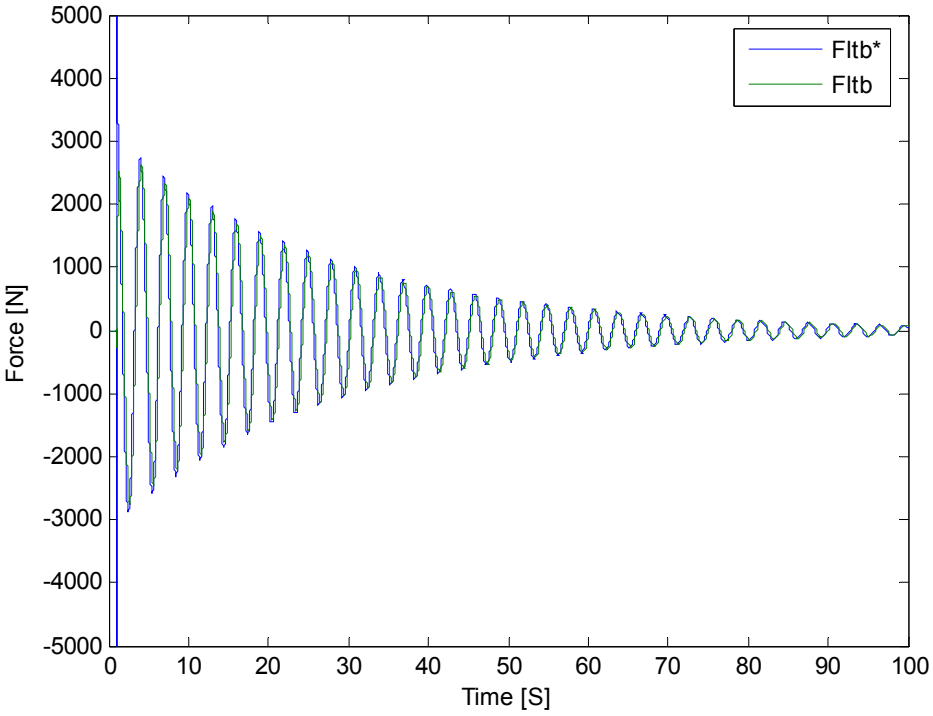

Fig. 5.15 Actual and Commanded Force, Step Input

Figure 5.14 illustrates how the hydrodynamic model will cause the position of the buoy in the linear test bed to oscillate until steady state is reached at the new water level of 0.5 meters. Since the input is a step, the force demanded by the controller initially is very high. The saturation limits placed on the hydrodynamic model discussed earlier limit the force to 5000 Newtons. Figure 5.15 shows the commanded force generated by the hydrodynamic model and the actual force applied to the system under test. These plots indicate that the hydrodynamic model is working correctly and the force controller is tracking commanded force inputs. Since the coefficients for added mass, friction, and water stiffness were only estimated based on an initial buoy design for a 1kW linear generator OWEC, and not calculated through experimentation, the system looks to be under damped. In reality, if the coefficients were calculated correctly through experimentation, it is likely the settling time would be significantly faster.

5.7.1 Sinusoidal Wave Height Input, No Generator Load

In this section the simulation results are presented for a sinusoidal wave height input and with no device under test generator loading. The wave height has a period of 6 seconds and amplitude of 0.75 meters, or 1.5 meters peak to peak. The range of travel for the linear test bed is 2 meters, and with a purely sinusoidal input wave, some resonance will occur. Thus, to ensure that the actual position of the buoy will not exceed the limits of the linear test bed, a 1.5 meter peak to peak sine wave is used. From Figure 5.16, it is possible to see how the device under test resonates slightly with the sinusoidal input wave profile. From Figure 5.17 it is possible to observe that the Delta Tau position loop tracks near perfectly, as the actual and commanded position waveforms are almost identical. This can be explained because the position loop is much faster than the force loop and can easily track the slower position commands generated by the force controller. Figure 5.18 illustrates that the force controller nearly perfectly tracks the force command. Since the coefficients in the hydrodynamic model are not exact it is possible to observe the nature of the under damped system. It takes almost 35 seconds to reach steady state, as noted by the overshoot in Figure 5.18, which would not likely happen of the coefficients were correct.

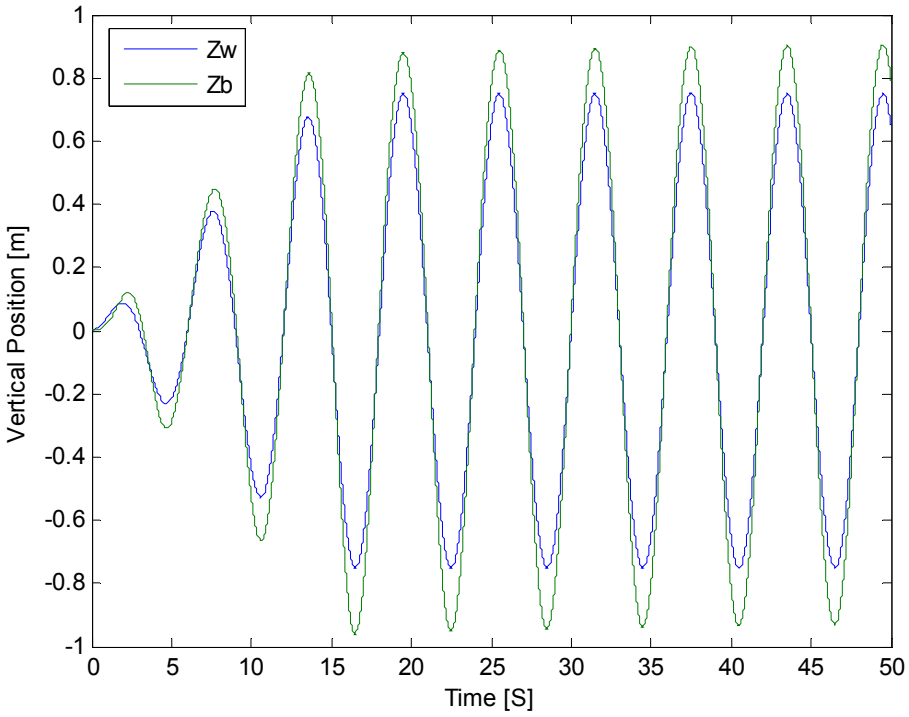

Fig. 5.16 Wave Height and Actual Vertical Position, No Load

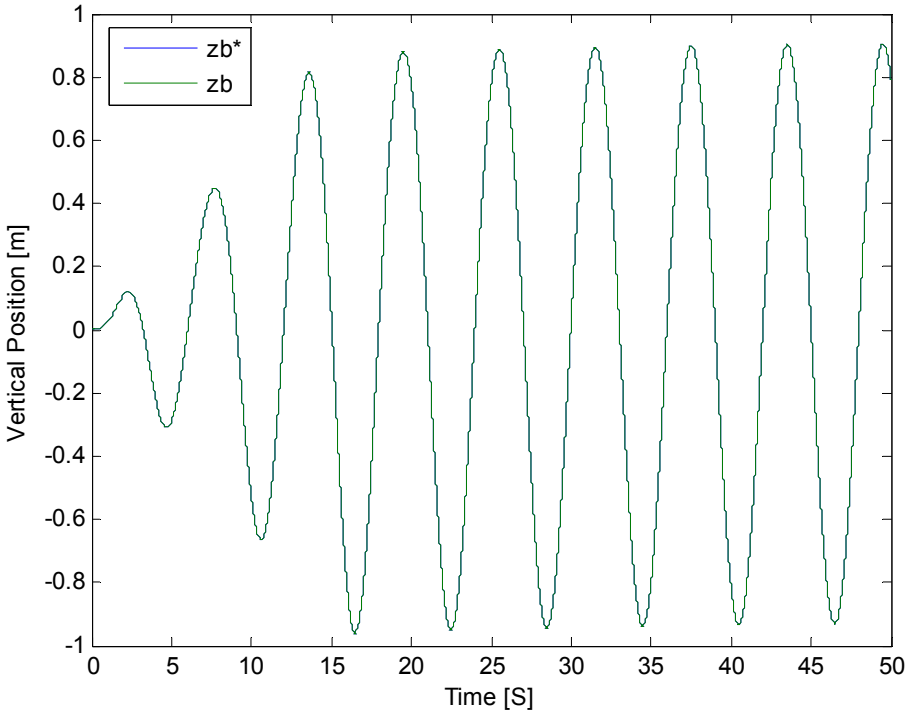

Fig. 5.17 Actual and Commanded Vertical Position, No Load

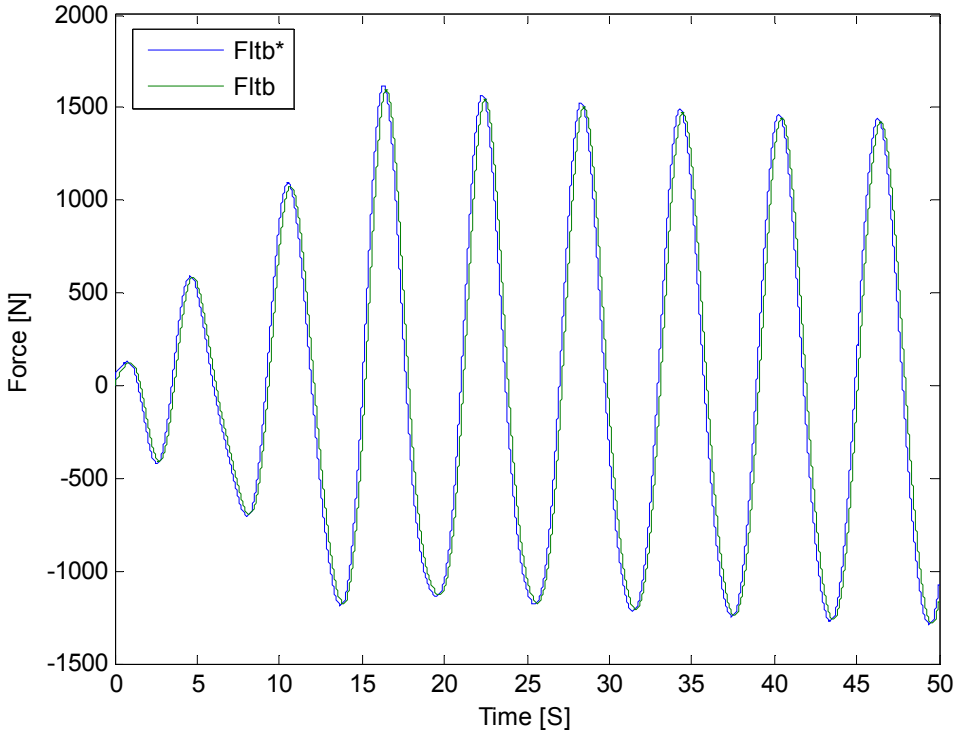

Fig. 5.18 Actual and Commanded Force, No Load

5.7.2 Sinusoidal Wave Height Input, 500W Generator Load

Using the same input wave height parameters of for the unloaded device under test case, a 500Wrms generator load was added and the response of the linear test bed system was considered. Figure 5.19 again show the resonance that occurs when a sinusoidal waveform is used for wave height. Figures 5.20 and 5.21 illustrate the near perfect tracking of position and force commands respectively. The waveforms of interest are shown in Figure 5.22, which shows the forces acting on the linear test bed. Using Equation 5.24, the generator force as a result of the 500Wrms device under test loading is 825N if the linear velocity of the wave is assumed to be 1 meter per second.

This additional force will be supplied by the linear test bed in this application or the wave in a real ocean environment. This occurs because with a generator load, a point absorber buoy does not follow the wave profile exactly because the generator force acts like additional hydrostatic friction in the system. This causes the position of the device under test to lag the wave profile as shown in Figure 5.19. This increases the amount of

driving force exerted by the wave or test bed since there is now more buoyant force available. Comparing Figures 5.22 and 5.18 it is clear the linear test bed provides additional driving force as a result of this additional buoyant force. Figure 5.23 shows the power generated by the device under test by using Equation 5.24. Mathematically, this power is negative as energy is taken out of the system but the power can also be viewed as positive power absorbed by the system as shown in Figure 5.23. The power waveform has a peak value of 707W, which corresponds to 500Wrms.

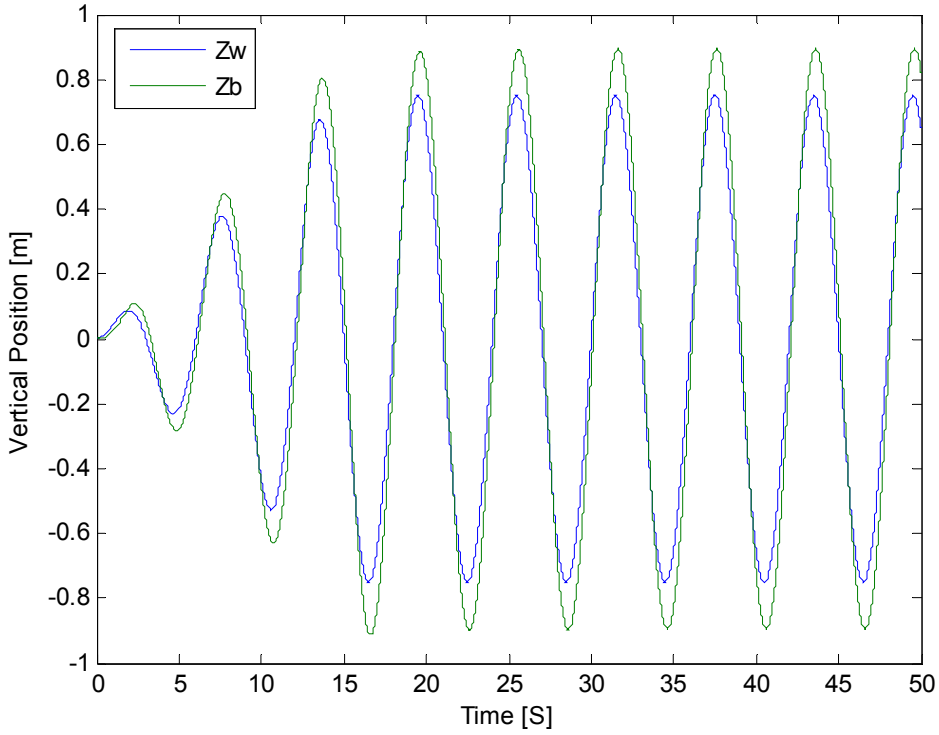

Fig. 5.19 Wave Height and Actual Position, 500W Test

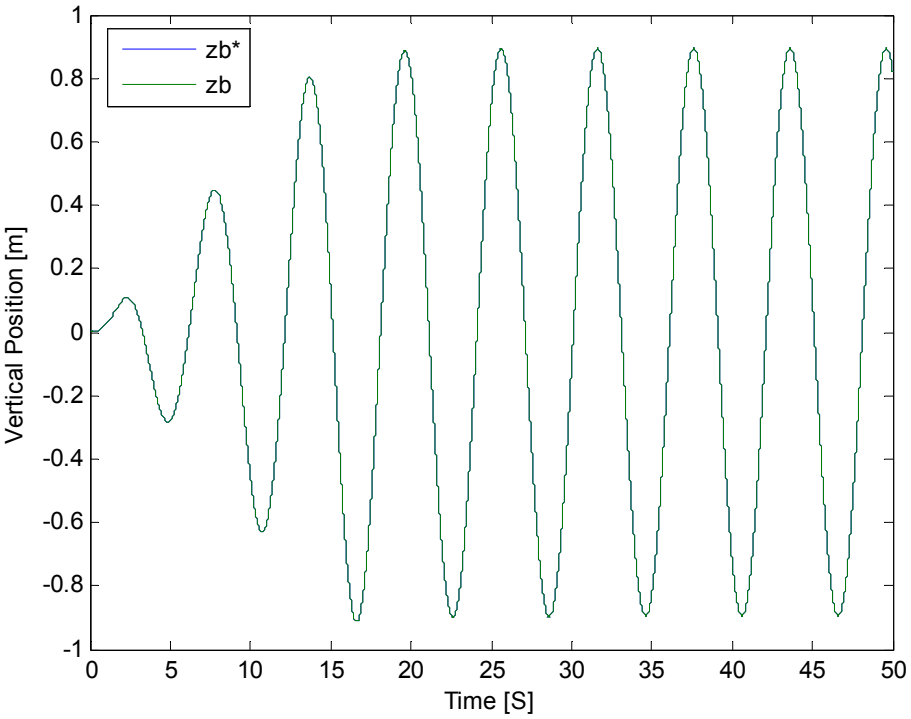

Fig. 5.20 Actual and Commanded Vertical Position, 500W Test

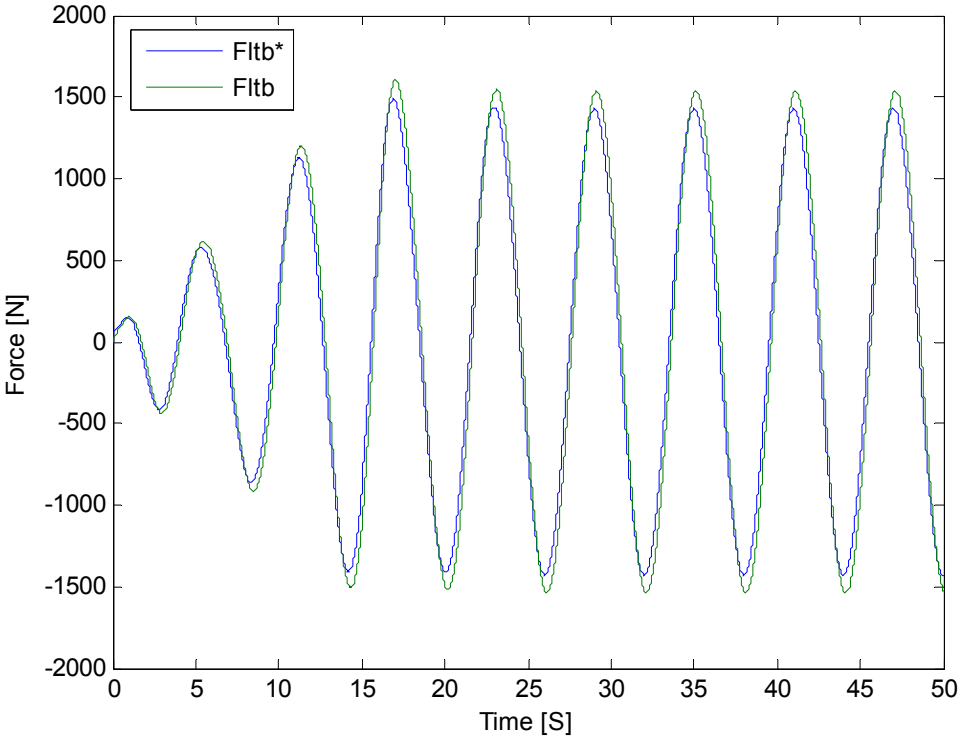

Fig. 5.21 Actual and Commanded Force 500W Test

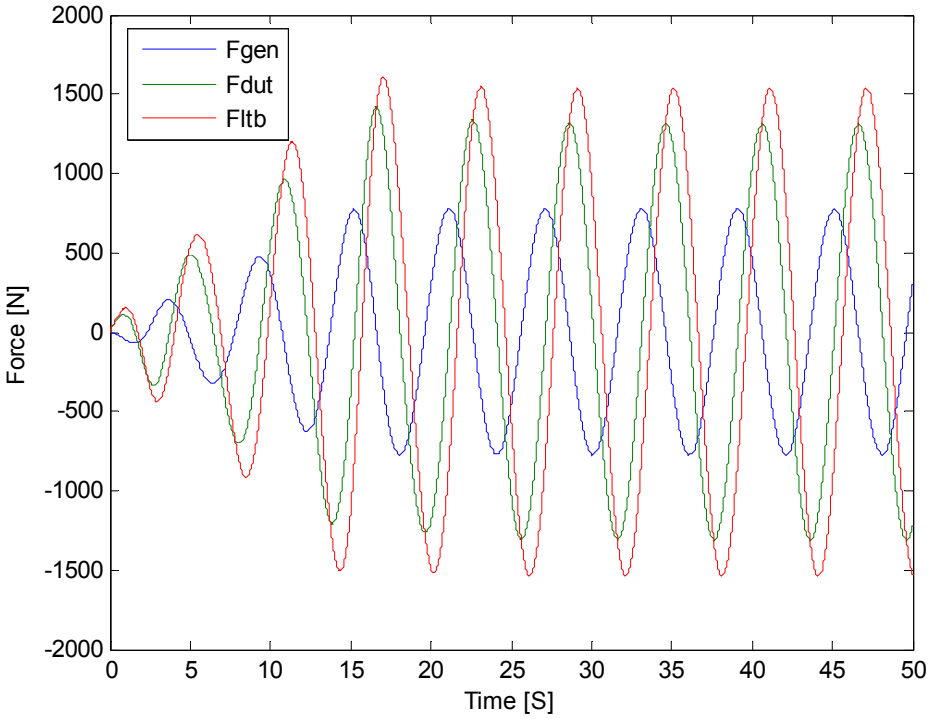

Fig. 5.22 Linear Test Bed Forces, 500W Test

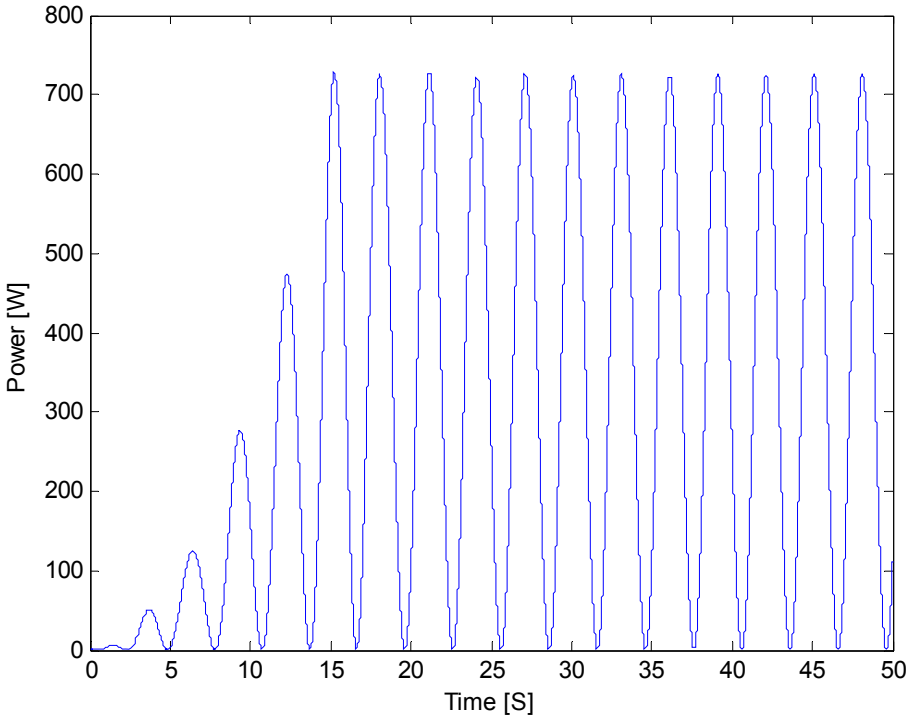

Fig. 5.23 Device under Test Power, 500W Test

5.7.3 Sinusoidal Wave Height Input, 1kW Generator Load

Using the same input wave height parameters of for the unloaded device under test case, a 1kWrms generator load was added and the response of the linear test bed system was considered. A 1kWrms generator load would be considered "full-load" for the 1kW linear generator OWEC, with its geometry used to calculate the hydrodynamic coefficients. This is the reason a 1kWrms electrical load was simulated. With a higher generator load, the generator force is even greater, which effectively adds even more damping to the system. This added "friction" causes the position of the device under test to lag the wave profile even more, resulting in more buoyant force available to drive the system. Thus, the force exerted by the linear test bed should increase. Figure 5.24 illustrates how the buoy position lags the wave profile even compared to Figure 5.19 corresponding to the 500W load. Figure 5.25 and 5.26 illustrate that the position and force controllers are still tracking correctly.

Again, the figure of interest is 5.27 showing the forces acting on the linear test bed system. The force that is used to actually accelerate the device under test, F_{DUT}, remains basically unchanged compared to Figure 5.22. However, the generator force increased because more power is being generated by the device under test. The additional generator force is driven by additional force from the linear test bed, which occurs because more buoyant force would exist in a real ocean environment. The linear test bed exerts more force because of the force command generated by the hydrodynamic model. Finally, Figure 5.28 illustrates the power generated by the device under test. It has a peak of 1.414 kW, which is 1kWrms.

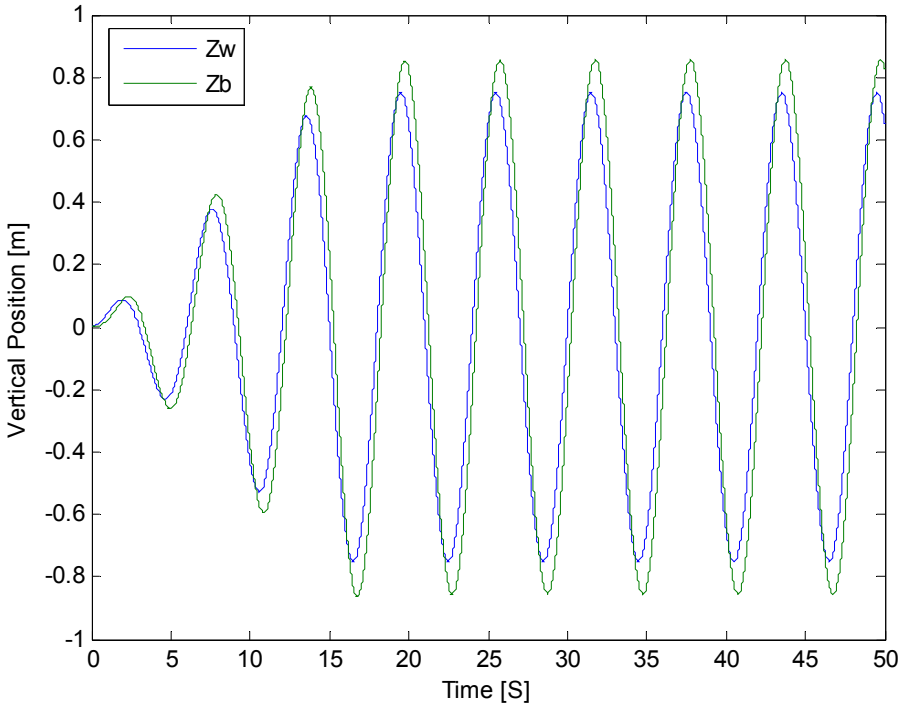

Fig. 5.24 Wave Height and Actual Position, 1kW Test

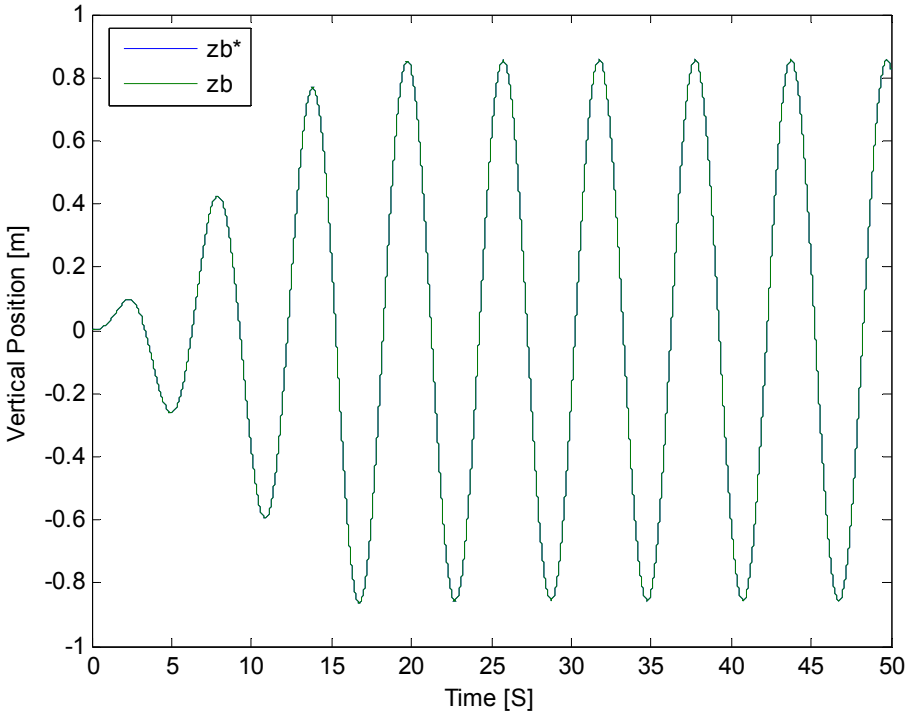

Fig. 5.25 Actual and Commanded Vertical Position, 1kW Test

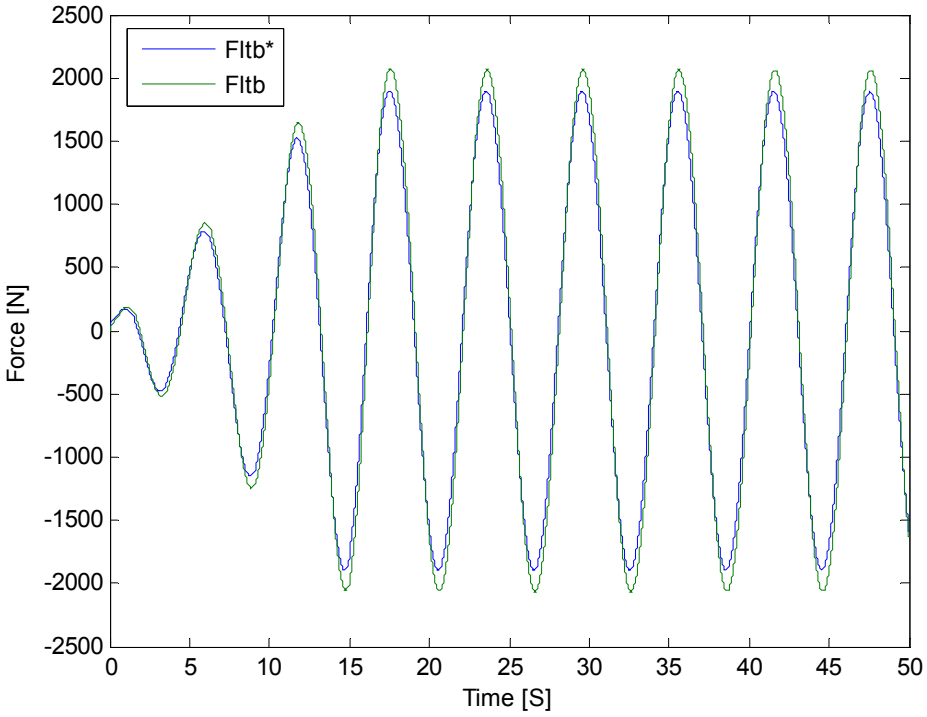

Fig. 5.26 Actual and Commanded Force, 1kW Test

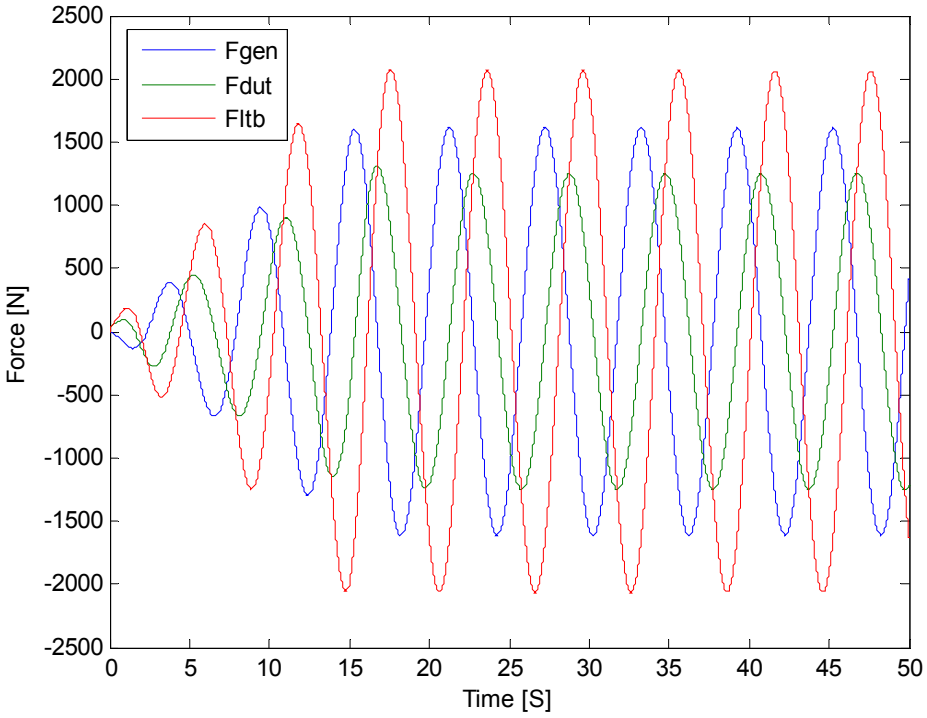

Fig. 5.27 Linear Test Bed Forces, 1kW Test

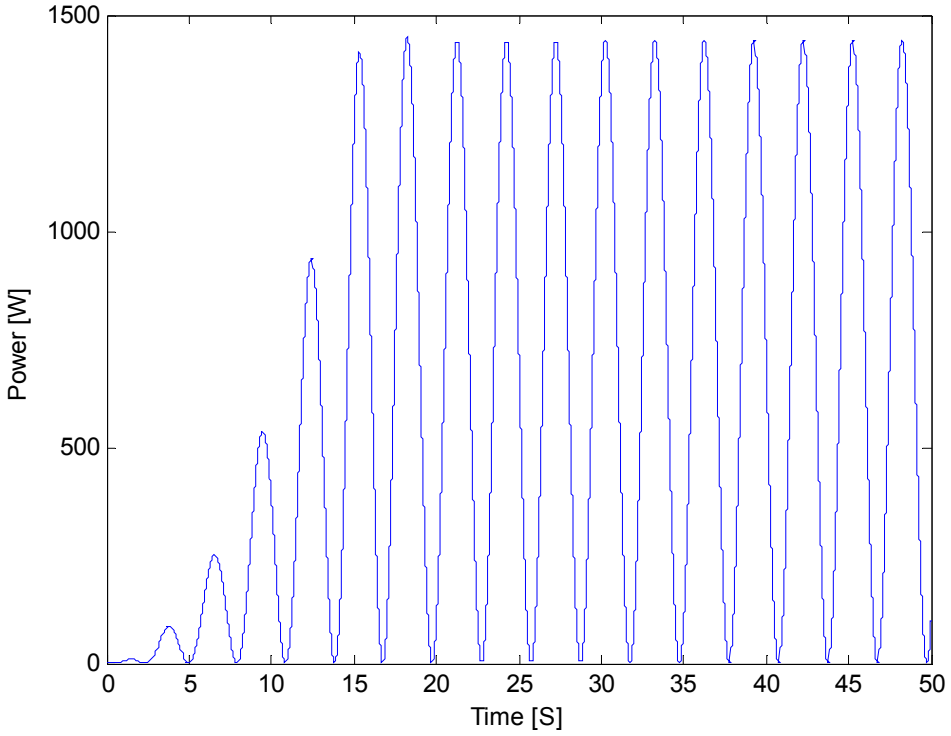

Fig. 5.28 Device under Test Power, 1kW Test

6. CONCLUSION

6.1 Benefits of the Linear Test Bed

The linear test bed will provide many benefits to the research and development of novel, direct-drive OWECs at Oregon State University. The linear test bed will be able to test devices that are rated up to 10kW, as well as testing devices rated for less than 100W. This flexibility allows researchers to test small prototypes to find the optimum topology for a direct-drive OWEC as well as test larger scale prototypes as that optimum topology is discovered. The control system of the linear test bed is also very flexible, allowing for basic position control to advanced force control to simulate the OWECs response to an actual ocean wave. The mechanical design of the linear test bed is very robust and will be able to be used for testing purposes for years to come. Oregon State University believes these benefits will continue to drive wave energy research forward in the future.

When the linear test bed arrives in the MSRF, it will be capable of position control. The Delta Tau controller will be able to read position commands by either reading a data file or low voltage analog input. Right away, researchers will be able to test existing devices on the linear test bed using this mode of control. It will be possible to calculate efficiencies using this mode of control and provide a means for viewing the voltage output of the device under test. Often, just analyzing the voltage output is the first step to verifying a design of a device under test. It will be possible to get an initial idea of how the device performs right away after the linear test bed is installed.

After the initial testing, the implementation of the force control algorithm will allow for much more accurate testing. Using this mode of control, it will be possible to simulate the device under test's actual response to a real ocean wave. Here it will be possible to see how much power the device under test can generate given a certain wave height. The linear test bed will capture the hydrodynamic interaction between the device under test and the wave and will not exert more force on the system than a real wave could produce. This will allow researchers at Oregon State University to test controllers

for various devices under test that will position the device under test such that near maximum power is extracted from the incoming wave front. Much research is currently being done in this field of direct-drive OWEC design at Oregon State University. Also, each of these linear test bed control schemes will allow for a significant amount of flexibility in a linear test bed testing plan.

Furthermore, the linear test bed will have two controllers, which are both very flexible by themselves. It is possible to implement any controller transfer function into the CompactRIO, which is necessary to implement the force control transfer function and the transfer function necessary to implement the hydrodynamics. However, these will be edited and changed in the future as needed. For example, the hydrodynamic model currently used is a linear model based on the Patel equations that is somewhat simple. More complex, nonlinear models may be used in the future and can be implemented on the CompactRIO. Furthermore, if it is determined that closing the force loop using the Delta Tau and associated PID loops would increase performance; steps can be taken to achieve this and are shown later in this chapter.

Finally, the mechanical design of the linear test bed is very robust. The structural components of the machine are nearly all made of steel, with the suspension arms made of aluminum to facilitate moving them by hand. The timing belts used in the linear test bed can support twice the entire weight of the carriage system. This means that if one belt were to fail, the system would not immediately fall to lower range of travel limits or cause the other belt to fail. There are many safety features of the linear test bed that will prevent damage to the linear test bed and its components such as the over travel limit switches, shock absorbers, and the suspension safety link. All of these benefits will continue to drive wave energy research forward at Oregon State University.

6.2 Future Work regarding the CompactRIO Interconnection

The proposed linear test bed will be constructed in OSU's Energy Systems laboratory in the summer of 2007, at which time the CompactRIO will be connected for control and data acquisition purposes. Upon installation and initial operation when actual

PID values for the position control system are known, it may be desired to run additional simulations to verify that the current design of the force controller will work as expected. Additionally, the hydrodynamic coefficients corresponding to the 1 kW linear generator buoy geometry will be verified through wave tank experimentation. After the real coefficients are known, the Simulink model can again re-simulate the performance of the force control algorithm with the correct hydrodynamic coefficients.

Then, the transfer functions for the force controller and the hydrodynamics must be implemented on the CompactRIO. Because the CompactRIO is a digital controller, the hydrodynamic and force controller transfer functions will be implemented in the z-domain and are shown below in Equations 6.1 and 6.2 respectively. These transforms were completed with the "c2d" command in Matlab using the zero order hold discretization method and a sampling time of 0.001 seconds. These transfer functions can now be directly programmed into the CompactRIO either using these discrete transfer functions directly or by using the discrete differentiation and discrete integration methods provided by National Instruments in Labview.

$$F_{LTB}(z)^* = \frac{6.645 \cdot 10^6 z^{-2} - 1.333 \cdot 10^7 z^{-1} + 6.685 \cdot 10^6}{0.8187 z^{-2} - 1.81 z^{-1} + 1} \tag{6.1}$$

$$C_F(z) = \frac{7.517 \cdot 10^{-13} z^{-3} + 3.007 \cdot 10^{-12} z^{-2} + 7.517 \cdot 10^{-13} z^{-1}}{-z^{-3} + 3z^{-2} - 3z^{-1} + 1} \tag{6.2}$$

From a data acquisition standpoint, the CompactRIO analog inputs must be programmed to read the input data correctly to verify that the input signals are within the ranges expected. The analog output must be set up to output the correct voltage range to the Delta Tau to correctly read the position command generated by the force controller. Next, the load cell conditioning necessary to accurately determine the force exerted by the linear test bed to the system under test must be implemented. This will be done using the steps described in chapter 3, and will involve very simple math operations. Finally, the digital I/O discussed in chapter 3 must be implemented using 5V TTL logic on the digital I/O card for the CompactRIO. All wiring diagrams that describe the interconnections that are necessary to connect the CompactRIO are shown in chapter 3.

The physical wiring described must also be completed upon the arrival of the linear test bed.

6.3 Closing the Force Loop with PMAC

As the discussed in chapter 5, the force control algorithm was designed using Matlab Simulink and will be implemented at first with the CompactRIO. However, it is possible to achieve force feedback control using the Delta Tau, using a technique called "cascading servo loops." This is a technique developed by Delta Tau and others based on the extended capabilities of the controller and can be implemented by Oregon State University at a later date if it is determined performance could be boosted using this approach.

The technique involves using an inner loop to control position and an outer loop to control force and joining these loops to implement a closed loop system. To begin, Delta Tau defines a feedback control loop as a servo loop. In this case the inner servo loop is the position feedback loop that will be implemented by the Mundt and Associates. The outer loop will be tuned by Oregon State University and will be a force feedback loop. As discussed, the force applied to the device under test will be measured using dual load cells and input to the Delta Tau using an analog to digital converter and used as reference.

Basically, because of the open structure of the Delta Tau controller, the inputs and outputs of any loop can be changed. Cascading servo loops simply means making the output of an outer servo loop the input of an inner servo loop. Using this technique, the outer loop does not directly drive the linear test bed motor; instead, it modifies the set point of the inner position loop in an effort to drive its own error down to zero. In our case, the outer loop will be this force feedback loop, using dual load cells to measure actual force applied by the linear test bed as shown in Figure 6.1 [15].

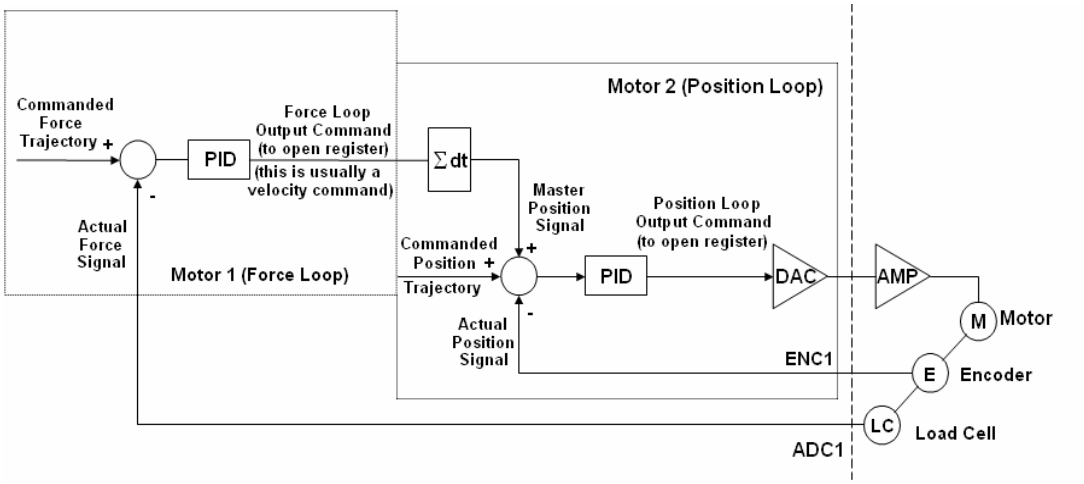

Fig. 6.1 Closing a Force Loop around a Position Loop [15]

To implement this technique it is important to get the position feedback inner loop that will be driving the linear test bed motor tuned. Delta Tau offers several methods to accomplish this inner loop PID tuning. The first is to use a built in "auto tuning" program provided in the Delta Tau software package. Based on the step response, the program computes values for the proportional, derivative, and integral gain terms. The second approach allows the user to compute the gain terms and implement these exact values in the controller. Then, the user can see how the system performs using these values by looking a step response and other applicable responses.

The outer loop in a "cascading servo loop" application uses a feedback sensor measuring whatever quantity if relevant in that system. In our case, the feedback sensor would measure actual force applied to the load. Based on the way the user defines the scale factor of the axis definition statement it is possible to now write motion programs using force commands in engineering units such as Newtons or pounds force. Since it is not possible to tune the outer loop without linking it to the inner loop it is vital to understand how these loops are linked.

To begin, after the outer loop is properly tuned, the Delta Tau controller has the capability of engaging and disengaging the outer loops making switching from force control and position control very smooth. As seen in Figure 6.1, the output from the outer loop can be integrated numerically before being used as a position input to the inner

loop. If it is integrated, the outer loop will effectively output a commanded velocity and if not, it will be a position command. Delta Tau suggests that if the outer loop is engaged and the steady state velocity is nonzero, the value should be integrated. If the steady state velocity is zero, there is no need to integrate. In most cases, the outer loop only needs a proportional gain and possibly an integral gain term according to Delta Tau literature. Delta Tau's software package can be used to tune the outer loop gains as in a standard loop.

In order to implement the cascading servo loop technique, several setup parameters must be changed in the Delta Tau controller. These parameters are changed by editing the values of certain "I-variables." These "I-variables" are defined by Delta Tau and can be changed by the end user to change setup parameters. These variables are used to define parameters ranging from maximum motor speed to limit switch position. In order to understand which I-variables need to be changed in order enable the outer loop please refer to Figure 6.2 below.

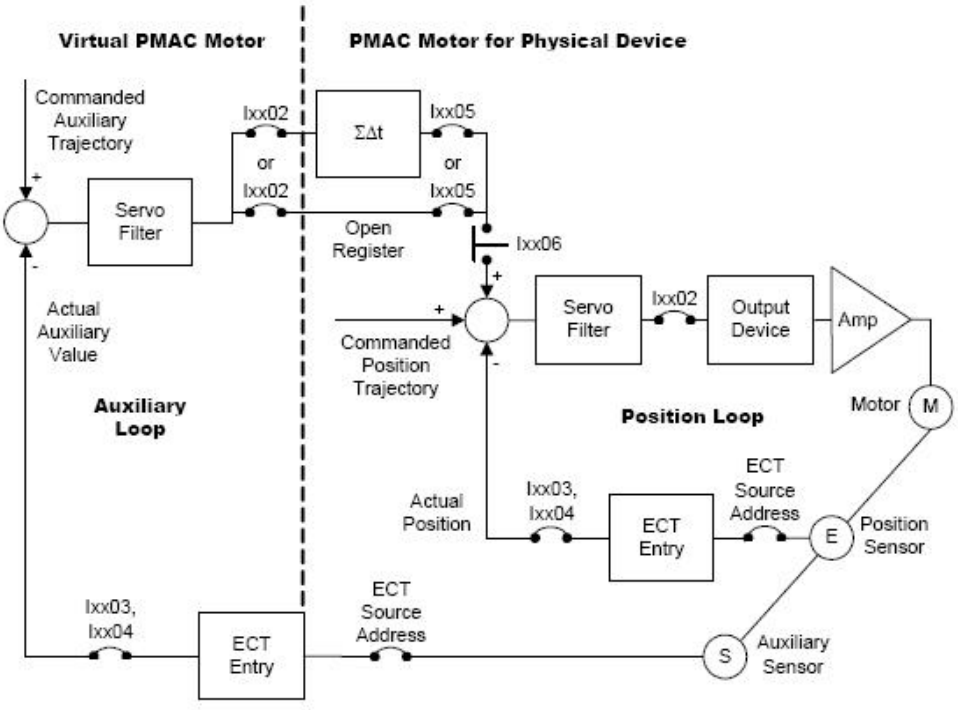

Fig. 6.2 Cascading Servo Loops [15]

From Figure 6.2, it should be noted that the variables that must be changed include Ixx02, Ixx03, Ixx05, Ixx06, and Ixx07. The "xx" is referring to the motor number and the servo loop controlling that motor. Since the output of the servo loops can be changed as discussed above, a motor may not actually be directly driving an actuator or even be a physical motor at all. In the case of cascaded servo loops, the outer loop is actually a "virtual" motor. This "motor" is used to drive the force error to zero using its corresponding servo loop. In order to understand the role of each of the above I-variables, each will be discussed in detail in the following paragraphs.

The Ixx02 variable for the outer loop's motor is used to specify the address of the servo output and can output to any open register. This is the key to cascading servo loops because it links the outer loop to the master position of the inner loop. This register can then be read by either by another servo loop in the case of force control or read by an output device such as a drive through a digital to analog converter (DAC). The Ixx03 tells the Turbo PMAC where to look for its feedback value to close the servo loop for motor xx. Usually this is a result register in the "encoder conversion table" where the raw feedback values have been pre-processed for use in the servo loop. Basically, in force feedback mode, this would be the register where the load cell input from the ADC has been filtered and output to.

Ixx05 specifies the address of the register for master position information of motor xx for the position following function. Usually, this is a register in the encoder conversion table where processed input position data is kept. The Ixx06 variable for the inner loop's servo loop control whether the outer loop is engaged or not. When bit 0 of Ixx06 is set to 0, the outer loop is not engaged and the inner loop will function normally and independently. When bit 0 is set to 1, the outer loop is engaged, and its output will modify the total commanded position of the inner loop. The Ixx07 variable for the inner loop's motor, called the master scale factor, and is a gain term for the outer loop. It should be set to 1 to keep the net outer loop gain as low as possible. A complete description of all I-variables can be found in the Turbo PMAC PCI software manual.

6.4 Final MSRF Interconnection Issues and Future Work

Obviously, since the linear test bed will not yet installed in the MSRF upon the completion of this thesis, there will be several lab installation issues that will need to be addressed. Care has been taken to ensure that the necessary breaker, cabling, and DC bus regulation scheme have been specified and designed in advance. However, once the necessary cabling and breaker arrive at the MSRF, the actual installation of these components must be coordinated with facilities services. The equipment will already be in the lab and ready for Oregon State University facilities electricians to install.

As discussed in chapter 3, float switches will be used to regulate the water in the water rheostats. Testing has been completed that ensures that these float switches will not allow more than two inches of water level fluctuation. However, these float switches have not yet been installed for permanent operation. Recalling Figure 2.19, it will be necessary to locate a rod to use to tether the switch at the appropriate depth. The tether length must also be set using this rod such that only two inches of water fluctuation is allowed. Finally, the wire leads must be used to connect the terminals of the switch to the existing water level controller. To do this, it will be necessary to cut off the plug that comes standard with the float switch and locate the wires that connect to the actual terminals of the switches. Then, using wire leads, the switch terminals will be connected to the existing controller so that pins 4 and 5 on the right terminal block are shorted and opened by the switch as shown in Figure 6.3. This will engage the pump when the float switch is closed and in the “ON” position at minimum water depth allowed.

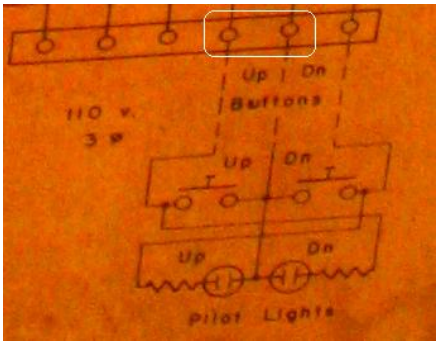

Fig. 6.3 Water Rheostat Controller Connection

Finally, when the linear test bed is installed and testing is ready to begin, it will be necessary to ensure that the water in the four tanks accurately gives a 6 ohm braking resistance. Tests have been done to approximate the water level necessary in each tank to achieve 6 ohms total, but a simple test to check the resistance at these levels should be done. As discussed in chapter 2, it was estimated that 25.43 inches of water depth would give 6 ohms per tank, or 6 ohms total when two sets of two tanks are placed in series, and the sets are placed in parallel. It was assumed that the water rheostat will be used since it is available at no cost and can handle the power dissipation requirements. However, if it is desired to have a more precise braking resistor, a quote for a DC load bank from Mosebach Manufacturing is included as Appendix B.

BIBLIOGRAPHY

[1] S. Ragunathan, "A methodology for Well's turbine design for wave energy conversion," *Proc. IMechE,* vol. 209, pp. 221-232, 1995.

[2] Ocean Power Delivery; http://www.oceanpd.com/

[3] Ocean Power Technology; http://www.oceanpowertechnologies.com/index.htm

[4] AWS Ocean Energy Limited, http://www.awsocean.com/technology.html

[5] K. Rhinefrank, E. B. Agamloh, A. von Jouanne, A. K. Wallace, J. Prudell, K. Kimble, J. Ails, E. Schmidt, P. Chan, B. Sweeny, A. Schacher, "Novel ocean permanent magnet linear generator buoy," *Journal Renewable Energy*, Elsevier 2005, in press.

[6] A. Metzcus, L. Wooderson, A. Heiberg, S. Benton, "Transverse Flux Generator Technical Manual," June 2006.

[7] E.B. Agamloh, A.K. Wallace, A. von Jouanne, "A novel wave energy extraction device with contactless force transmission system," *44th AIAA Aerospace Sciences Meeting*, Reno, Nevada, Jan 2006.

[8] Minoo H. Patel, "Application to Floating Bodies," in *Dynamics of Offshore Structures*, Butterworth & Co. Ltd., pp. 283-286, 1980.

[9] "Operating Instructions CompactRIO cRIO-9012," *National Instruments*, 2006.

[10] "Operating Instructions NI 9205," *National Instruments*, 2005.

[11] "Operating Instructions NI 9203," *National Instruments*, 2006.

[12] "Operating Instructions NI 9263," *National Instruments*, 2004.

[13] "Operating Instructions NI 9401," *National Instruments*, 2005.

[14] P. Clark, "Hardware Reference Manual Turbo PMAC PCI," *Delta Tau Data Systems, Inc.*., 2006.

[15] P. Clark, "User Manual PMAC," *Delta Tau Data Systems, Inc.*., 2006.

[16] J. Brooke, *Wave Energy Conversion*, Elsevier, 2003, eds. R. Bhattacharyya and M.E. McCormick.

[17] K. Budal, "Theory for absorption of wave power by a system of interacting bodies," *Journal of Ship Research*, vol. 21, pp. 248-253, 1977.

[18] K. Budal, J. Falnes, "A resonant point-absorber of ocean wave power," *Nature*, vol. 256, pp. 478-479, 1975.

[19] J. Falnes, *Ocean Waves and Oscillating Systems*, Cambridge University Press, 2002.

[20] K. Budal, J. Falnes. , "Interacting point-absorbers with controlled motion," in *Power from Sea Waves*, ed. B.M. Count, Academic Press, pp. 381-399, 1980.

[21] Energetech; http://www.energetech.com.au/

[22] H. Polinder, M.E.C Damen and F. Gardner , "Linear PM generator system for wave energy conversion in AWS," *IEEE Transactions on Energy Conversion*, vol. 19, No. 3, September 2004.

[23] M.A. Mueller, N.J. Baker and E. Spooner, "Electrical aspects of direct drive wave energy converters," *4th European Conference on Wave Energy*, pp. 235-242, 2000.

[24] M. A. Mueller, "Electrical generators for direct drive wave energy converters," *IEE Proc. Gen. Transm. Distrib*., vol. 149, No. 4, pp. 446-456, 2002.

[25] P. Clark, "Software Reference Manual Turbo PMAC/PMAC2," *Delta Tau Data Systems, Inc*.., 2006.

[26] "Rexroth IndraDrive C Drive Controllers, Power Sections HSC03.1," *Rexroth Bosch Group*, 2007.

[27] Wave Dragon; http://www.wavedragon.net

[28] CSH Incorporated, Float Switches, http://www.cshincorporated.com

[29] Interface, Advanced Force Measurement, http://www.interfaceforce.com

A. ORIGINAL LINEAR TEST BED SPECIFICATION

This machine will be used as a linear test bed that drives various linear power generating devices that will be rated up to at least 10kW of peak power take off (PTO). The physical devices may vary significantly in size and shape. However, some common mechanical trends of the device under test (DUT) will be a vertically oriented center spar and an outer active float that is driven up and down by the test bed (Please see Figure on next page). The center spar will be pivot mounted at the bottom. The outer active float should be attached through a load cell to the driving arm of test bed. The mechanical machine oscillations in the vertical axis will simulate sinusoidal vertical velocity, predetermined velocity profiles, or dynamically controlled force interactions to simulate the real response of a buoy in ocean waves. Therefore the controls need to be programmable for a multiple range of testing activities including the specifications described below:

1. Control Specifications:

a. Control loop output rate = Continuous (preferred), or update freq. >=1kHz

b. Programmable control loop algorithms which send the drive velocity command to the motor driver. Built in capability for end user to program the control loop is essential.

c. Access to PID control parameters. Ability to change PID values during operation, possibly by item 1.b. above.

d. Modes of Control. Listed below are control capabilities which are needed. Control may act on inputs listed in "f." below. Each mode should be demonstrated to operate by tooling company.

i. **Position vs. Time**. ASCII or other means to input position vs. time data points at 1msec intervals for over 10 minutes of data. (10 x 60sec / 0.001sec = 600,000 data points).The control algorithm would then interpolate velocity and output a speed command to the motor driver to provide a continuous velocity command. Some typical examples may be random sea states, sine functions, linear ramps with constant velocities, etc.

ii. **Continuous Programmable Position**. Position is programmable by end user as a function of time using standard Boolean, arithmetic, and trigonometric commands. For example, vertical position as a function of time = Z(t)=Asin(wt)+Bsin(w2t)+Csin(w3t). In this case, time(t) is continuously incrementing in real time.

iii. **Point to Point control with fixed velocity.** This might take the form of a single or continuously operating point to point command using standard PID and a target velocity resulting in typical velocity ramp commands.

iv. **Dynamic Force control**. A basic control loop is described in the attached file "LTBcontrolgeneral_2.pdf". Control loops of this type will be written by the end user. The ability for hardware and software to support this ability is needed. Writing the control algorithms in such a way as to achieve stability will be OSU's responsibility.

v. **Joy Stick Mode**. A simple method to slowly and safely jog the drive for slow controlled positioning of equipment during setup and installation of the DUT.

e. Sensors (payload load cell, position, velocity) > 1kHz Bandwidth. Accuracy within 2 % of full scale. Load cell can be changed for higher resolution when testing lower power (lower force) devices.

f. Anticipated inputs accessible by control algorithm:

i. Position of DUT
ii. Speed of DUT
iii. Force applied to active float of the DUT
iv. Analog 1 (spare)
v. Analog 2 (spare)
vi. Digital 1 (spare)
vii. Digital 2 (spare)

g. Limit stops and switch at both ends of travel to ensure safe limits on the LTB.

h. Adjustable limit stops and switch at both ends of travel to ensure safe limits on the DUT.

i. Emergency brake that locks vertical motion upon loss of power or loss of control.

j. Depending on LTB design and feasibility, a weak link mechanical fuse to prevent LTB damage.

k. **Physical Machine performance**

Mechanical Specification		Largest, 10kW		Smallest, 50w
Mode		Normal	Fast	Normal
Stroke (m)		2	2	0.15
Speed (m/s)		1.0	2.0	0.4
Accel (m/s/s)		1.1	3.0	1.1
Force of PTO (N)		20,000	10,000	150
Force due to PTO cogging (N)		600	300	0
Mass of active buoy (kg)		750	300	10
Mass of active spar (linear distribution) (kg)		1,400	1,400	10
Max Torque about the Z (vertical) axis between the active buoy and the spar (Nm). The torque is caused by a rotating mass inside of the center spar which engages the outer float. The two contributors to the torque are the PTO torque and the inertial effects of the rotating mass.	From PTO	380 Nm	X	x
	Max inertia (1.0kgm^2). Max angular acceleration (40rad/s^2)	40 Nm	X	X

i. Total equivalent Payload = Mass of active float + cogging + Gen load

l. Vertically and horizontally adjustable to accommodate changes in device under test up to maximum dimensions shown in drawing.
m. Continuous cycles of >150 hours will eventually be needed.
n. Long cycle life and MTBF.
o. The Active Spar is mounted at the base on a pivot. The attachment method will be a generic mounting flange between the LTB and the DUT as co-designed by OSU and the Tooling Company.
p. The Active Buoy is mounted with a gimbal mount to tolerate dimensional and alignment variation of the DUT. The attachment point can be located between the top and bottom of the buoy as suggested by the tooling company engineering and design process. The attachment method will be a generic mounting flange between the LTB and the DUT as co-designed by OSU and the Tooling Company.
q. Neither the active spar nor buoy should be allowed to rotate about the Z-axis. A significant relative torque (identified in k above) between the active spar and active buoy may exist depending on the type of DUT.

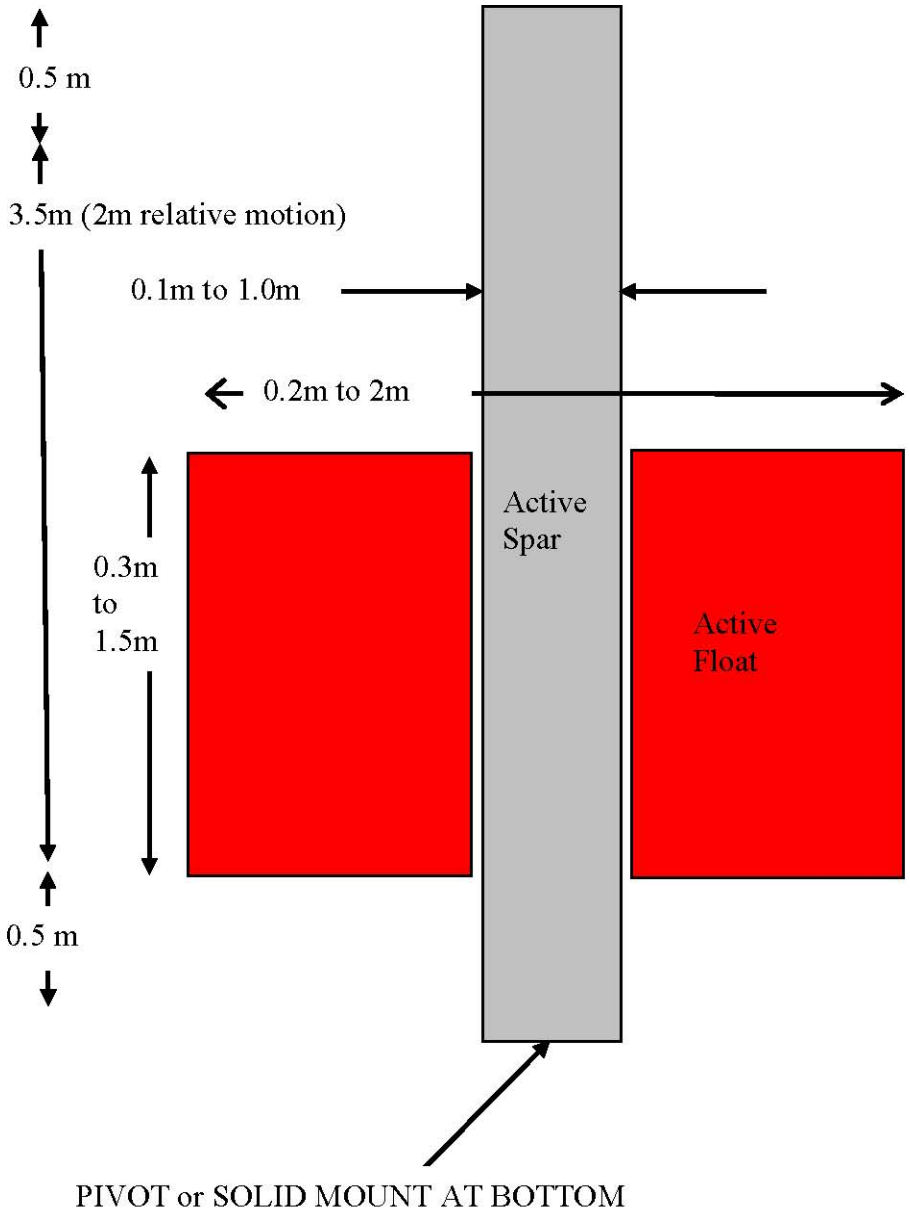

Fig. A.1 Specified System under Test Size and Necessary Displacement

B. DC LOAD BANK QUOTATION

PortaBank™ Quotation Form – DC Resistive Type May 10, 2007

RFQ #: Email Request
Mosebach's Ref# QLB070510-3

Oregon State University
Corvallis OR 97330
Contact #1: Mr. Peter Hogan
P#: 541/737-2630 **F#: N/A** **Email: hogan@eecs.oregonstate.edu**

Qty.	kW	Mosebach's Model #	Approximate Dimensions	Approx. Weight	Price $US	Price $US
			L; W; H		Without branch circuitry fusing	With branch circuitry fusing
1	104.14	**PB105820DC**	50"x29"25"	200 lb	$ N/A	$ 13,095.00

Load Steps and Load Capacity: PB105820DC

	kW Steps	I per step [DC]	Total kW	Max Current
At 820VDC	**1 x 104.14**	**1 x 127A**	**104.14**	**127 ADC**

Voltage: Rated at 820VDC.
Amperage: 1 x 127ADC.
Resistance: 6.46 Ohms.

Enclosure: The PortaBANK™ Portable Load Banks will be placed in electro statically painted light weight metal enclosure, with four casters and four lifting eyes for easy maneuvering. The air inlet and outlet will be protected by 2 screens. The load bank will discharge heat horizontally.
Controls: Mounted on the load bank including 2 digital meters capable of measuring DC volts and amperes. One 104.14kW step controlled by ON/OFF switch using a heavy-duty [1000VDC, 150ADC] rated contactor braking the + side, a master ON/OFF switch, blower ON/OFF switch and positive air flow lamp will be provided.
Control power: 120V, 1Φ, 60Hz taken from the blower power.
Load Elements: Our WeldlessWeave™ and Slimline™ technology utilizes a continuous **Stainless Steel** ribbon to eliminate all welds. By eliminating welds, hot spots are eliminated. To reduce the operating temperature, no thru bolts are used, and a parallel element system reduces the watt density. Finally our resistors are design to withstand vibration, and breakable parts, like ceramics insulators are not used. All this will result in maximum operating life of our resistors. In addition to our WeldlessWeave™ technology, Mosebach uses its recent Slimline™ innovation to provide power resistance in even smaller spaces.
Rating: Continuous duty.
Power Factor: 1.0
Load Connections: CAM-locks.
The Blower Voltage: 120V, 3Φ, 60Hz, 30A must be externally supplied by customer. Please read the "note" section.
Safety Features: The branch circuit fusing, ground lug and the positive air flow sensor. Since our resistors are heavy duty and have been proven on Locomotives and Giant Mining Trucks, we know that there is no risk of resistor failure therefore the Branch Circuit Fusing is Optional!

MOSEBACH MANUFACTURING COMPANY
1417 McLaughlin Run Road • Pittsburgh, PA 15241-3103 USA
T: 412-220-0200 • F: 412-220-0236 • www.mosebachresistors.com

- The additional options available: remote control with 50' cable [N/A], cable set, CAM-locks [included], handle with 2 wheels, handle with 2 wheels and stair climber, fork lift channels [$100.00], weatherproof enclosure with louvers, protective vinyl cover and permanent mount.
- The purchase order must be submitted via fax or email. Please include; the model number, quantity, the cost per item, the total cost, shipping and billing information.
- The list of trade references is required for credit check and for account set up.
- Payment terms: NET 30 days.
- The estimated delivery time would be 6 – 10 weeks from the date the order was placed.
- The shipping must be collect, F.O.B. Pittsburgh, PA. 15241
- Packaging Charges: Each load bank will be fully crated to prevent any shipping damages. $200.00 must be added.
- Warranty: Mosebach Mfg. standard warranty applies. **1 year on parts and workmanship, 2 years on resistors!**
- Quotation is valid for 30 days.
- **NOTE: If some other voltage is more available please specify. In that case 120V, single phase, 60Hz would have to be supplied for the controls.**

  Please keep in mind that this is a custom build load bank based on your specifications! You will be able to test 820V DC voltage at 127ADC maximum!

  If the PO is placed within 30 days I will include CAM-locks free of charge [$300.00 value] and extend the resistors warranty up to 3 years!!!

Mosebach greatly values our clients and we look forward to working with you on this project.

Sincerely,

Damir Saric
Sales Engineer
office: 412 - 220 - 0200 x 40
fax: 412 - 220 - 0236
email: dsaric@mosebachresistors.com
web: www.mosebachresistors.com

MOSEBACH MANUFACTURING COMPANY
1417 McLaughlin Run Road • Pittsburgh, PA 15241-3103 USA
T: 412-220-0200 • F: 412-220-0236 • www.mosebachresistors.com

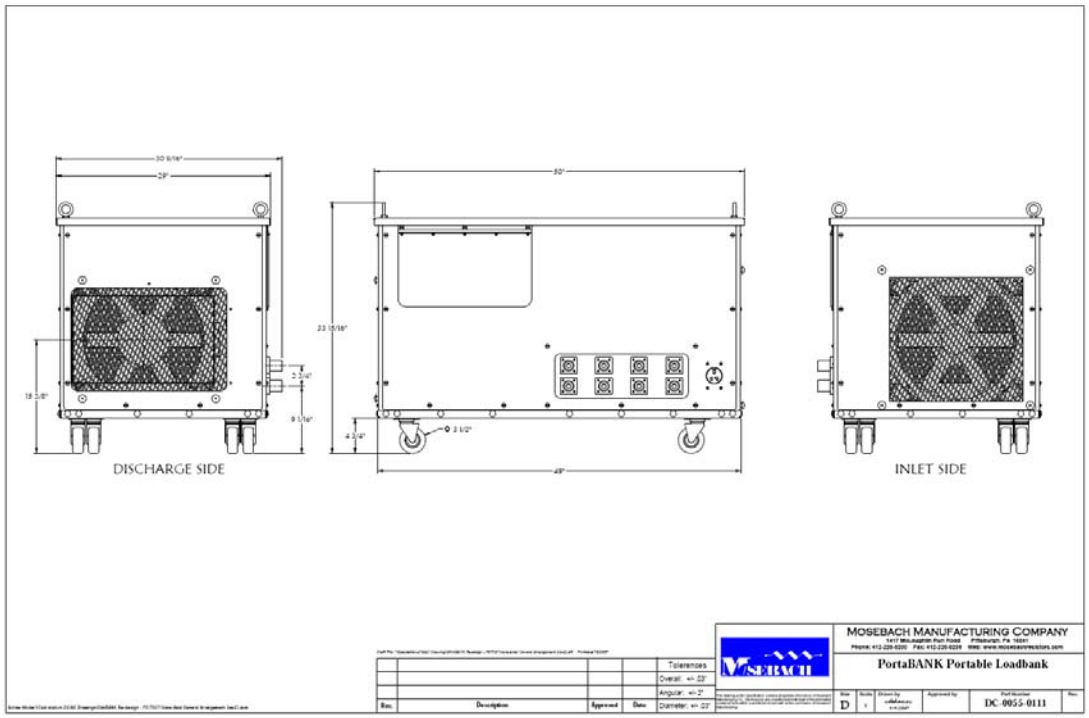

Fig. B.1 Dimensioned Drawing

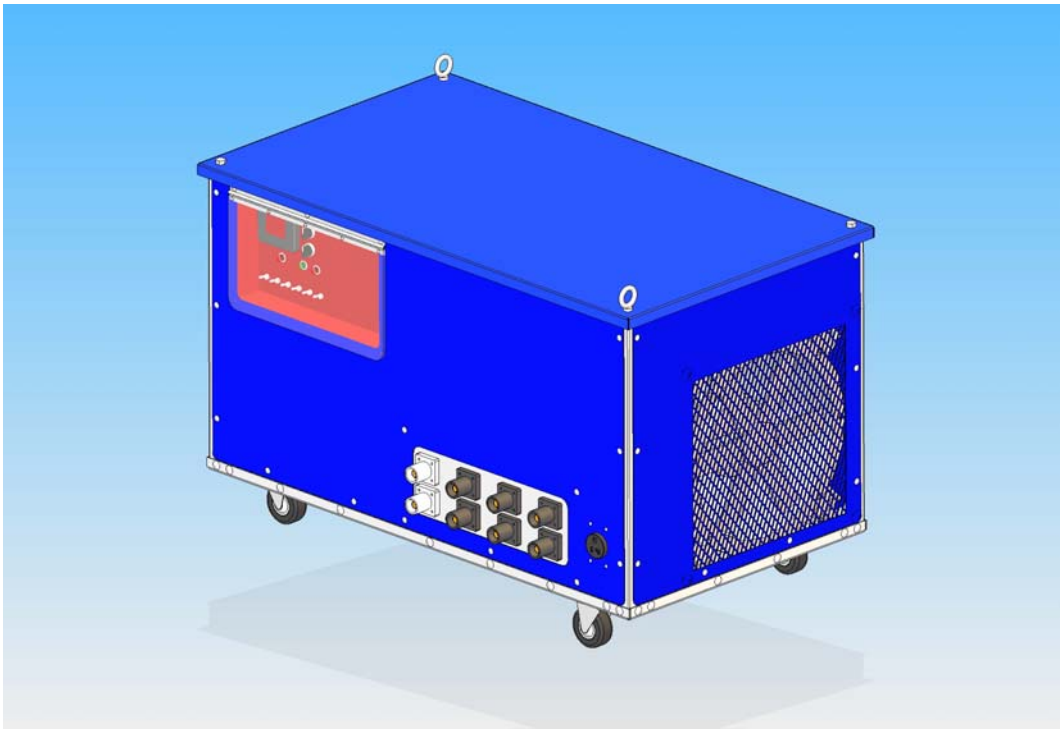

Fig. B.2 Three-Dimensional Drawing